

# NOTE TO USERS

This reproduction is the best copy available.

**UMI**<sup>®</sup>



**University of Alberta**

Investigations of Bacteriocins from *Carnobacterium piscicola*, *Brocothrix campestris* and  
*Bacillus subtilis*

by

*Karen Elizabeth Kawulka*



A thesis submitted to the Faculty of Graduate Studies and Research in partial fulfillment  
of the requirements for the degree of  
Doctor of Philosophy

Department of Chemistry

Edmonton, Alberta

Spring 2004



Library and  
Archives Canada

Bibliothèque et  
Archives Canada

Published Heritage  
Branch

Direction du  
Patrimoine de l'édition

395 Wellington Street  
Ottawa ON K1A 0N4  
Canada

395, rue Wellington  
Ottawa ON K1A 0N4  
Canada

*Your file* *Votre référence*  
*ISBN: 0-612-96285-7*  
*Our file* *Notre référence*  
*ISBN: 0-612-96285-7*

The author has granted a non-exclusive license allowing the Library and Archives Canada to reproduce, loan, distribute or sell copies of this thesis in microform, paper or electronic formats.

L'auteur a accordé une licence non exclusive permettant à la Bibliothèque et Archives Canada de reproduire, prêter, distribuer ou vendre des copies de cette thèse sous la forme de microfiche/film, de reproduction sur papier ou sur format électronique.

The author retains ownership of the copyright in this thesis. Neither the thesis nor substantial extracts from it may be printed or otherwise reproduced without the author's permission.

L'auteur conserve la propriété du droit d'auteur qui protège cette thèse. Ni la thèse ni des extraits substantiels de celle-ci ne doivent être imprimés ou autrement reproduits sans son autorisation.

---

In compliance with the Canadian Privacy Act some supporting forms may have been removed from this thesis.

Conformément à la loi canadienne sur la protection de la vie privée, quelques formulaires secondaires ont été enlevés de cette thèse.

While these forms may be included in the document page count, their removal does not represent any loss of content from the thesis.

Bien que ces formulaires aient inclus dans la pagination, il n'y aura aucun contenu manquant.

# Canada

## ABSTRACT

*Carnobacterium piscicola* LV17B produces precarnobacteriocin B2, CbnB2P, and an immunity protein, CbiB2. CbnB2P is a 66-amino acid peptide (6990.4 Da) comprised of an 18-amino acid leader and the mature carnobacteriocin, CbnB2, a class IIa 48-amino acid peptide containing a conserved YGNGVXC sequence. The immunity protein contains 111 amino acids (12665.5 Da). CbnB2P and CbiB2 were subcloned and overexpressed as maltose binding protein (MBP) fusions in *E. coli* cells. These MBP-fusions were purified on an amylose column and cleaved with Factor Xa, then pure CbnB2P (1-64; a fragment missing 2 C-terminal residues) and CbiB2 were isolated by high-performance liquid chromatography (HPLC). [<sup>15</sup>N] labelled CbnB2P and [<sup>15</sup>N, <sup>13</sup>C] CbiB2 MBP fusions were also produced facilitating investigation of their 3D structures of the corresponding peptides using multi-dimensional NMR techniques. A solution structure [in trifluoroethanol (TFE)] for CbnB2P(1-64) was determined, and in addition to the expected  $\alpha$ -helix for residues 19-39 of the mature peptide, a second  $\alpha$ -helix for the 18-member leader peptide was demonstrated. Initial NMR studies on CbiB2 illustrate good signal dispersion in the nitrogen plane of a <sup>15</sup>N HSQC, implying that elucidation of a solution structure is feasible. *Brocothrix campestris* ATCC 43754 produces a class IIb bacteriocin (i.e. two-peptide), brochocin C (BrcC), comprised of brochocin A (BrcA) and brochocin B (BrcB), both of which contain a double G<sup>-2</sup>G<sup>-1</sup> cleavage site. Separate MBP-fusions of BrcA and BrcB were constructed and overexpressed in Origami™ B BL21(DDE3) *E. coli* cells. MALDI-TOF mass spectrometry shows that multiple fragments are produced suggesting that non-specific cleavage at the several possible double GG positions is occurring. Further studies are currently in progress.

The three dimensional solution structure of subtilisin A (SubA), a bacteriocin produced by *Bacillus subtilis*, was determined by multidimensional NMR techniques using peptide obtained from [U-<sup>13</sup>C, <sup>15</sup>N]-labelled peptone derived from *Anabaena* sp. grown on NaH<sup>13</sup>CO<sub>3</sub> and Na<sup>15</sup>NO<sub>3</sub>. Separate SubA peptides were also produced from [U-<sup>13</sup>C, <sup>15</sup>N]-L-phenylalanine and [U-<sup>13</sup>C, <sup>15</sup>N]-L-threonine in otherwise unlabelled media. SubA is a macrocyclic peptide (covalent link between Asn1 and Gly35) with three unusual crosslinks formed between the sulfurs of Cys13, Cys7, and Cys4 and the  $\alpha$ -carbons of Phe22, Thr28, and Phe31, respectively. SubA underwent complete desulfurization with nickel boride. The resulting desulfurized peptide was subjected to acid hydrolysis to constituent amino acids, which were derivatized to pentafluoropropanamide isopropyl esters. This allowed the stereochemistry of all unmodified residues to be determined as L-amino acids via chiral GC MS. Stereochemistry of the modified residues of SubA was determined by NMR analysis and computer modeling of the eight possible stereoisomers. One stereoisomer with L stereochemistry at Phe22 ( $\alpha$ -R) and D stereochemistry at Thr28 ( $\alpha$ -S) and Phe31 ( $\alpha$ -S) (LDD) fit the NMR data best and gave the lowest energy structures with the best r.m.s.d.. Model amino acid compounds with sulfides at the  $\alpha$ -carbons showed that nickel boride desulfurization proceeds with loss of stereochemistry. Desulfurization of SubA was shown to proceed with inversion of configuration at the  $\alpha$ -carbons of Phe22 and Thr28 and with 4:1 retention at Phe31. This indicates that the reaction proceeds via an N-acyl imine and the geometry of desulfurization is determined by the surrounding peptide structure. This novel post-translational linkage, namely a thiol to the  $\alpha$ -carbon of an amino acid, demonstrates that SubA belongs to a new class of bacteriocins.

## ***Acknowledgements***

***To***

*My mentors, who enabled me*

*Dr. John Vederas, Dr. Peter Mahaffy, Dr. Ken Newman, Dr. Brian Martin*

*Dr. Margaret Ann Armor, Dr. Lois Browne, Dr. Chris Diaper (thesis reader),*

*Dr. Kamaljit Kaur (thesis reader)*

*My husband and children, who were excited and supported me*

*Ivan,*

*Brandy & Paul & Griffyn, Kate, Graham, Abbey & Dave, Nathan, MacLain*

*My friends, who encouraged me*

*Especially Lily & Rick, Sylvie, Jignesh, John & Karen, Doug & Karen, Diana &*

*John, Peter & Deb, and the past and present Vederas group members*

***Thank you***

*To God, for his unfailing love and incredible book....*

*Greater love has no one than this, that he lay down his life for his friends.*

***John 13: 15***

*I lift up my eyes to the hills –*

*where does my help come from?*

*My help comes from the LORD,*

*the maker of heaven and earth.*

*He will not let your foot slip –*

*he who watches over you will not slumber;*

*indeed, he who watches over Israel*

*will neither slumber nor sleep.*

*The LORD watches over you –*

*the LORD is your shade at your right hand;*

*The sun will not harm you by day,*

*nor the moon by night*

*The LORD will keep you from all harm –*

*he will watch over your life;*

*The LORD will watch over your coming and going*

*both now and forevermore.*

***Psalm 121***

*When life gets you down and the quit sign is flashing like a big neon sign in your head,  
try this poem and keep going.*

### ***Don't Quit***

*When things go wrong as they sometimes will,  
When the road you're trudging seems all uphill,  
When the funds are low and the debts are high,  
And you want to smile, but you have to sigh,  
When care is pressing you down a bit -  
Rest if you must, but don't you quit.*

*Success is failure turned inside out,  
The silver tint of the clouds of doubt.  
And you never can tell how close you are,  
It may be near when it seems so far.  
So stick to the fight when you're hardest hit -  
It's when things go wrong that you mustn't quit.*

## TABLE OF CONTENTS

	<b>Page</b>
<b>CHAPTER 1: BACTERIOCINS</b>	
<b>INTRODUCTION</b>	<b>1</b>
1.1: Perspectives	1
1.2: Classification and General Characteristics of Bacteriocins	4
1.2.1 Class II Bacteriocins	9
1.3: Genetics, Synthesis, Regulation, Secretion and Immunity	10
1.3.1: General Genetic Organization	10
1.3.2: Biosynthesis	12
1.3.3: Regulation and Quorum Sensing	16
1.3.4: Secretion, Activation, Processing	18
1.3.5: Immunity	20
1.4: Mode of Action	21
1.4.1: Mechanism	21
1.5: Objective	27

## CHAPTER 2: CLASS II BACTERIOCINS

### RESULTS AND DISCUSSION

#### A: Carnobacteriocin B2 Precursor (CbnB2P) and the Immunity Protein (CbiB2) of *Carnobacterium piscicola* LV17B

2.1	Carnobacteria	29
2.1.1:	<i>Carnobacterium piscicola</i> LV17B: CbnB2 and CbnB2P	29
2.1.2:	<i>Carnobacterium piscicola</i> LV17B: CbiB2	34
2.2:	Subcloning of CbnB2P and CbiB2 in BL21(DE3) <i>E. coli</i>	35
2.2.1:	Isolation of pLQP and pLQ300i Plasmids and Transformation	36
2.3:	Recombinant Proteins Expressed as Maltose Binding Fusion (MBP) Proteins: CbnB2P (1), CbiB2 (5)	38
2.3.1:	How to “Catch” a Protein	38
2.3.2:	The pMAL™ system	39
2.4:	Protein Expression and Purification of CbnB2P and CbiB2	42
2.4.1:	Mass Spectrometry of Labelled and Unlabelled CbnB2P and CbiB2	43
2.4.2:	Circular Dichroism of CbnB2P	44
2.5:	Isotopic Labelling of Proteins	46

2.6:	NMR of CbnB2P and CbiB2	48
------	-------------------------	----

**B: Brochocin C (BrcC) of *Brocothrix campestris***

2.7:	Primary Structure, Production and Regulation of Brochocin C	52
2.8:	Subcloning of BrcA and BrcB in Origami™ B(DE3) <i>E. coli</i>	55
2.9:	Pilot Experiments	56
2.10:	Mass Spectrometry by MALDI-TOF of BrcA and Brc B	59
2.11:	Conclusions for CbnB2P, CbnB2, BrcA, and BrcB	60

**CHAPTER 3: *Bacillus subtilis* & Subtilosin A**

**RESULTS AND DISCUSSION**

3.1:	Overview	62
3.1.1:	The Genus <i>Bacillus</i>	62
3.1.2:	<i>Bacillus Subtilis</i>	62
3.1.3:	An Antimicrobial Peptide Produced by <i>Bacillus subtilis</i> : Subtilosin A (1A)	63
3.2:	Isolation and Purification of Subtilosin A (1A)	68
3.2.1:	<i>Bacillus subtilis</i> JH642	68
3.2.2:	<i>Bacillus subtilis</i> SMY	69

3.2.3:	Antimicrobial Activity	69
3.2.4:	Mass Spectra	70
3.3:	<sup>15</sup> N and <sup>13</sup> C Labelling of Subtilosin A (1B)	70
3.3.1:	Production and Analysis of Labelled Peptone	72
3.3.2:	Production of Universally Labelled Subtilosin A (1B)	76
3.4:	Chemical and Enzymatic Studies of Subtilosin A (1A)	76
3.4.1:	Mild Acid Hydrolysis of Subtilosin A to Uncyclized Subtilosin A	76
3.4.2:	Solubility	76
3.4.3:	Crystallization	77
3.4.4:	Digestion of Sub A with Immobilized Pepsin	78
3.5:	Stereochemical Investigation of Sub A	
3.5.1:	Analysis of the Cysteine-phenylalanine and Cysteine-threonine bonds	78
3.5.2:	Desulfurization and Hydrolysis of Subtilosin A (1A).	82
3.5.3:	Chiral GC MS Analysis of Desulfurized Subtilosin A (1A)	83
3.5.4:	Derivatization and GC MS Analysis of Partial Hydrolysis Fragments from (2)	84

3.5.5: Derivatization and GC MS Analysis of Partial Hydrolysis Fragments from (2)	86
3.5.6: Stereochemical Inferences from Desulfurization Investigations	90
3.6: NMR solution structure	91
3.6.1: NMR Experiments used in the Structure Elucidation of Subtilosin A	94
3.7: Mechanism Possibilities for the Formation of the Sulfur Bridges	95
3.8: Conclusions for Sub A	97

## **CHAPTER 4: EXPERIMENTAL PROCEDURES**

### **GENERAL METHODOLOGIES**

4.1: Bacterial Strains, Plasmids, Culture media	99
4.2: Purchased Strains, Reagents, Solutions	99
4.3: Preparation of Competent Cells	100
4.4: Transformation of Competent Cells	101
4.5: Pilot Experiments	101
4.6: Affinity Chromatography	102
4.6.1 Amylose Resin for the Purification of MBP Cytoplasmic (Soluble) Fusion Proteins	102
4.6.2 Amylose Resin for the Purification of MBP Periplasmic (Insoluble) Fusion Proteins	103

4.6.3: Chitin Beads for the Purification of Cytoplasmic (Soluble) Fusion Proteins	103
4.7: Mass Spectrometry	104
4.8: CD	105

## **BIOLOGICAL EXPERIMENTS**

4.9: CbnB2P and CbiB2	105
4.9.1: Plasmid Isolation and Transformation	105
4.9.2: Production of CbnB2P and CbiB2	106
4.9.2.1: Unlabelled:	106
4.9.2.2: Isotopically Labelled, <sup>15</sup> N	107
4.9.3: Purification of MBP-fusions CbnB2P and CbiB2	107
4.9.4: Cleavage of CbnB2P and CbiB2 Fusion Proteins and Purification	107
4.9.5: HPLC	108
4.9.6: NMR	108
4.10: BrcA and BrcB	109
4.10.1: Subcloning of BrcA and Brc B to Produce Cytoplasmic MBP fusion	109
4.10.1.1: BrcA: Formation of Plasmid pKEK1A	109
4.10.1.2: BrcB: Formation of Plasmid pKEK2B	110
4.10.2: Production of BrcA and BrcB	111

4.10.2.1:	BrcA and BrcB as MBP-fusion Proteins in SOC Media	111
4.10.2.2:	BrcA and BrcB as MBP Cytoplasmic Fusion Proteins, BrcB Intein-fusion in Celtone™-U Complete Medium	112
4.10.2.3:	BrcA as MBP Periplasmic Fusion in <i>E. coli</i> in LB	112
4.10.2.4:	BrcA and BrcB MBP Fusion Proteins in LB and Rich Broth in BL21(DE3) <i>E. coli</i> Cells	112 113
4.10.2.5:	BrcB Intein Fusion ER2566 <i>E. coli</i> in LB	113
4.10.3:	Purification of MBP-fusions BrcA, BrcB (cytoplasmic) BrcA (periplasmic) and BrcB Intein Fusion	114
4.10.4:	Cleavage of the BrcA and BrcB MBP Fusion Proteins and Purification	114
4.11:	SUBTILOSIN A	114
4.11.1:	General.	114
4.11.2:	Production and Purification of Subtilosin A	115
4.11.2.1:	<i>Bacillus subtilis</i> JH642	115
4.11.2.2:	<i>Bacillus subtilis</i> SMY	117
4.11.3:	Mass Spectrometry	117
4.11.4:	Antimicrobial Activity	117

4.11.5:	Mild Acid Hydrolysis of Subtilosin A	118
4.11.6:	Solubility Studies on Subtilosin A	118
4.11.7:	Crystallization Studies on Subtilosin A	118
4.11.8:	Pepsin Digest	119
4.11.9:	Preparation of Labelled Peptone <sup>158</sup>	120
4.11.9.1:	Determination of <sup>13</sup> C and <sup>15</sup> N Enrichment	122
4.11.10:	Production of Labelled Subtilosin A	122
4.11.11:	Labelling with [U- <sup>13</sup> C, <sup>15</sup> N]-Phenylalanine and [U- <sup>13</sup> C, <sup>15</sup> N]-Threonine	123
4.11.12:	Desulfurization of Subtilosin A	124
4.11.12.1:	Hydrolysis of SubA and Formation of N- pentfluoropropanoyl Isopropyl Ester derivatives of Constituent Amino Acids for GCMS Analysis	124
4.11.12.2:	Partial Acid Hydrolysis of Desulfurized Sub A	125
4.11.12.3:	Insulin chain B: Trial Hydrolysis and Derivatization	126
4.11.13:	NMR Spectroscopy	126
	<b>Conclusion</b>	130
	<b>References</b>	135
	<b>Appendix</b>	150

## LIST OF FIGURES

Figure	Page
1.	Schematic arrangement of the genes for class II bacteriocin production. 12
2.	Schematic overview of the suggested machinery for production of class IIa bacteriocins. 15
3.	Primary structure of class I bacteriocins that inhibit peptidoglycan formation. 23
4.	Binding of nisin to lipid II causes pore formation. 23
5.	Proposed model for the mode of action of class IIa bacteriocins. 26
6.	Genetic organization of <i>C. piscicola</i> LV17B. 30
7.	Amino acid sequence of CbnB2. 31
8.	Superimposed ribbon diagrams of CbnB2 and LeuA based on alignment of backbone atoms from Trp18 to Phe22. 32
9.	Schematic representing bacteriocin regulation and production of CbnB2. 33
10.	<p><b>1.</b> Single-strand DNA and amino acid sequences for nucleotides 141-490 of the <i>Hind</i>III fragment from pLQ5.21 containing the structural gene of CbnB2 (red letters). The <i>vertical arrow</i> in the amino acid sequence of the prebacteriocin indicates the G<sup>-2</sup> G<sup>-1</sup> cleavage site.<sup>136</sup></p> <p><b>2.</b> Single-strand DNA and amino acid sequences for nucleotides 441-840 of the <i>Hind</i>III fragment from pLQ5.21 containing the genetic information for CbiB2 (blue letters).<sup>136</sup></p> <p><b>3.</b> Possible promoter sequences, ribosomal binding site (RBS), and the inverted repeat sequence are underlined.</p>

11.	Schematic representation of the pMAL system.	40
12.	Restriction map of pMAL <sup>TM</sup> -c2X (6648 base pairs) and of pMAL <sup>TM</sup> -p2X (6723 base pairs). pMAL-c2 series vectors are identical to the pMAL-p2 series vectors except that the c2X series has an exact deletion of the <i>malE</i> -signal sequence (nt 1531-1605).	41
13.	pMAL-c2X multiple cloning site (polylinker) restriction endonuclease enzyme sites.	41
14.	<b>A.</b> CD spectrum of CbnB2P (0-60% TFE). <b>B.</b> Characteristic shape and magnitude of protein secondary structural motifs by circular dichroism.	45-46
15.	Dispersion of signals in <sup>15</sup> N HSQC.	48
16.	<sup>15</sup> N HSQC of CbnB2P (with and without the amino acid labels).	50
17.	Graphical representation of 3D structure of CbnB2P.	51
18.	<sup>15</sup> N HSQC of CbiB2 (initial data only).	52
19.	Genetic organization of the brochocin-C operon.	53
20.	Single-strand DNA and amino acid sequences for nucleotides 1201-1900 of the <i>EcoRI</i> fragment of pAP7 containing the structural ( <i>brcA</i> and <i>brcB</i> ) and immunity ( <i>brcI</i> ) genes of brochocin C.	54
21.	Schematic representation of the IMPACT-CN system with N-terminus cleavable intein tag.	58
22.	Amino acid sequence of presubtilosin A and the cleavage position.	65
23.	Cyclic and bridging connectivity proposed by Babasaki.	66

24. Genetic locus for production of subtilisin A (**1A**). 67
25. Amino acid sequence of subtilisin A (**1A**) The positions of 68  
the post-translationally formed linkages are indicated by solid lines.
26. MALDI-TOF mass spectrometry of unlabelled Sub A. **A:** The average 71  
mass of pure Sub A  $[M+H]^+$  ion. **B:** Expansion of the molecular ion region  
showing the isotope pattern for the molecular ion.
27. Apparatus for *Anabaena* sp. fermentation. **A.** Sterile filters for inlets of 73  
solutions and gases; **B.** pH probe; **C.** Filament light tubes to provide light for  
photosynthesis in addition to banks of fluorescent lights surrounding the  
vessel (not shown); **D.** 2 N HCl addition by a peristaltic pump.
28. The twelve days of *Anabaena*. 75
29. NMR spectra of Sub A U- $[^{13}\text{C}, ^{15}\text{N}]$ Phe A: **A.**  $^{13}\text{C}$ -COSY at 125 MHz 80  
showing Phe C $\beta$  (y-axis) correlations to aromatic carbon (x-axis)  
correlations; **B.**  $^{13}\text{C}$ -COSY of the Phe C $\beta$  (y-axis) to C $\alpha$  (x-axis) correlations;  
**C.**  $^1\text{H}^{13}\text{C}$ -plane from HNCA displaying intraresidue Phe C $\alpha$  (y-axis) to  
 $^1\text{H}$  (x-axis),  $^{15}\text{N}$  correlations.  $^1\text{H}, ^{13}\text{C}$ -HSQC demonstrating that only the C $\beta$   
(y-axis) have protons (x-axis) directly attached protons. The C $\alpha$  and  
C $\beta$  resonances of Phe22 and Phe31 are nearly overlapped (indistinguishable  
in panes 1 A and B), but the two C $\alpha$  to NH correlations are clearly separated  
in panel C.

30.	Structure of cyclothiazomycin, a <i>nonribosomal</i> peptide from <i>Streptomyces</i> .	81
31.	Examples of fungal diketopiperazines. <b>A.</b> Gliotoxin; <b>B.</b> Aranotin; <b>C.</b> Sporidesmin; <b>D.</b> Sporidesmin C.	82
32.	GC MS of crude derivatization mixture from desulfurized subtilisin A ( <b>2</b> ).	84
33.	GC MS analysis of partial hydrolysis fragments from:	85
	Fragment 1: Residues 17-26. D-Phe detected. L-Phe was absent from the mixture; 27a	
	Fragment 2: Residues 29-34. Both D-Phe and L-Phe detected; 27b	
	Fragment 3: Residues 30-34. Both D-Phe and L-Phe detected; 27c	
34.	<b>A.</b> Reductive cleavage of thioether bridges of subtilisin A ( <b>1A</b> ) to form <b>2</b> followed by complete hydrolysis and derivatization to determine residue stereochemistry. <b>B.</b> Proposed sequence of reductive desulfurizations.	87
35.	<b>A:</b> Superposition on the backbone of residues 4-13 and 22-31 of the eight lowest energy structures of subtilisin A; <b>B:</b> Representative conformer of subtilisin A in the same orientation, illustrating the outward pointing sidechains. The positions and stereochemistry of the crosslinks are indicated <b>C:</b> Backbone representation of <b>1</b>	93

## Appendix:

A.1.	NOE Data for subtilisin A ( <b>1B</b> )	150
A.2.	MALDI-TOF of <sup>15</sup> N and <sup>13</sup> C labelled subtilisin A ( <b>1B</b> )	158
A.3.	Nonspecific cleavage of BrcB on the intein column	159

## LIST OF ABBREVIATIONS

<b>AA</b>	Amino Acid
<b>Abu</b>	$\alpha$ -Aminobutyric acid
<b>AMP</b>	Antimicrobial peptide
<b>Arg</b>	Arginine
<b>Asn</b>	Asparagine
<b>Asp</b>	Aspartic acid
<b>ATCC</b>	American Type Collection Centre
<b>ATP</b>	Adenosine triphosphate
<b>Ala</b>	Alanine
<b>BHI</b>	Brain Heart Infusion broth
<b>CMM</b>	Complete minimal media
<b>Cys</b>	Cysteine
<b>Cyt C</b>	Cytochrome C
<b>Da</b>	Daltons
<b>DMSO</b>	Dimethylsulfoxide
<b>DSM</b>	Difco sporulation media
<b>DSS</b>	3-(Trimethylsilyl)-1-propanesulfonic acid
<b>DTT</b>	Dithiothreitol
<b>EDTA</b>	Ethylenediaminetetraacetic acid
<b>Gln</b>	Glutamine
<b>Glu</b>	Glutamic acid

<b>Gly</b>	Glycine
<b>GRAS</b>	Generally regarded as safe
<b>GSP</b>	General secretion pathway
<b>His</b>	Histidine
<b>Ile</b>	Isoleucine
<b>Ins Ch B</b>	Insulin chain B
<b>IPTG</b>	Isopropyl-1-thio- $\beta$ -D-galactopyranoside
<b>IR</b>	Infrared spectroscopy
<b>LAB</b>	Lactic acid bacteria
<b>LB</b>	Lauria Bertani broth
<b>Leu</b>	Leucine
<b>Lys</b>	Lysine
<b>MALDI-TOF</b>	Matrix assisted laser desorbtion ionization – time of flight
<b>Met</b>	Methionine
<b>NMR</b>	Nuclear magnetic resonance
<b>NSM</b>	Nutrient sporulation media
<b>Phe</b>	Phenylalanine
<b>PFPA</b>	Pentafluoropropionic anhydride
<b>PMF</b>	Proton motive force
<b>Pro</b>	Proline
<b>RBS</b>	Ribosome binding sites
<b>RP-HPLC</b>	Reversed phase high performance liquid chromatography

<b>rpm</b>	Revolutions per minute
<b>Ser</b>	Serine
<b>Sub A</b>	Subtilosin A
<b>TAE</b>	TRIS acetate buffer
<b>TFA</b>	Trifluoroacetic acid
<b>Thr</b>	Threonine
<b>Trp</b>	Tryptophan
<b>TSBY</b>	Tryptic soy broth yeast extract
<b>Tyr</b>	Tyrosine
<b>UV</b>	Ultraviolet
<b>Val</b>	Valine
<b>YT</b>	Yeast extract

## CHAPTER 1: BACTERIOCINS

### INTRODUCTION

#### 1.1: Perspectives

Various preservation techniques are used to avoid different forms of spoilage and food poisoning, including reduction of temperature, water activity, and pH, as well as addition of preservatives such as antimycotic (*e.g.* natamycin), inorganic (sulfite, nitrite) and organic compounds (propionate, sorbate, benzoate). Other technologies for food preservation include pasteurization and sterilization by heating, as well as packaging and aseptic processing to restrict access of microorganisms to products. With the increasing demand for more natural and microbiologically safe food products, there is a need for new preservation techniques. Among the emerging conservation technologies is the use of natural additives such as egg white lysozyme and bacteriocins of lactic acid bacteria (*e.g.* nisin) to control the growth and survival of undesirable microorganisms.<sup>1,2</sup> Bacteriocins are antimicrobial peptides that have been identified as key molecules in natural early defense mechanisms against infection<sup>3</sup> and are seeing growing use to aid in food preservation.<sup>3</sup>

The production of gene-encoded antimicrobial peptides is widespread among animal and plant<sup>4</sup> species and is one of an extraordinary array of microbial defense strategies that also include classical antibiotics, metabolic by-products, lytic agents, and protein exotoxins. Bacteriocins, produced by lactic acid bacteria (LAB) form an abundant and diverse family of microbial defense systems,<sup>5</sup> as evidenced by the high frequency of

journal articles concerning these antibacterial peptides.<sup>6</sup> LAB (frequently termed “the lactics”) are associated with plants (cabbage, corn, barley, mashes, kale and silage), sourdough bread, meat, and dairy products as well as sewage and the gastrointestinal, respiratory and urogenital tracts of humans and animals.<sup>7</sup> LAB’s have been used for centuries (more than 10,000 years)<sup>5</sup> in fermented food and hence are given GRAS (generally regarded as safe) status and are approved by the FDA.<sup>5</sup> As a result, only LAB bacteriocins are currently used in food preservation without further regulatory approval.<sup>5</sup>

In 1928, nisin A, a potent antimicrobial peptide (AMP) produced by the LAB *Lactococcus lactis*, was the first bacteriocin to be discovered and approved for use in foods, specifically, to prevent the outgrowth of *Clostridium botulinum* spores in cheese spreads in England.<sup>8</sup> Subsequently characterized in 1971, it is presently the commercial bacteriocin most widely used as a biopreservative in dairy products. It is accepted by the World Health Organization as a safe food preservative in over 80 countries.<sup>9</sup> Nisin A possesses excellent properties, such as thermostability, nontoxicity, and a broad activity spectrum against vegetative cells and spores of Gram-positive bacteria,<sup>3,10-12</sup>

Manufacture of dairy products such as acidophilus milk, yogurt, buttermilk, and cheeses (cottage, soft and hard), utilizes starter cultures containing LAB. These bacteria are also commercially significant in meat, alcoholic beverages and vegetable processing.<sup>13</sup> Even prior to knowledge of fermentation chemistry, the food and dairy industries valued LAB for their ability to produce aromatic and flavor-enhancing compounds with acceptable product texture (organoleptic and rheological properties).<sup>14</sup> However, LAB can also be a nuisance by producing off-flavors.<sup>13</sup> LAB have also been

implicated in patients with impaired immune systems as etiologic agents of endocarditis, bacteremia and septicemia.<sup>13</sup> Recent research suggests that the use of LAB to provide transient intestinal flora may be helpful for the prevention of disease development by competitive inhibition of harmful organisms.<sup>13</sup> However, such LAB need to be soluble, stable at physiological pH and resistant to inactivation by intestinal proteases.<sup>3</sup>

The rapid rise and spread of bacterial pathogens resistant to broad-spectrum antibiotics requires alternative therapeutic approaches.<sup>15,16</sup> Indiscriminant use of antibiotics results in selection pressure for the evolution of antibiotic resistance mechanisms in bacteria, including human pathogens.<sup>17,18</sup> An improved approach may be use of bacteriocins as “designer drugs” with a relatively narrow spectrum of antimicrobial activity to target specific bacterial pathogens. Their innate diversity and higher activity allow targeting of a particular infection thereby expanding the pharmaceutical arsenal and reducing selection pressure for resistance on a broad range of bacteria.

The pathogen, *Listeria monocytogenes*,<sup>19</sup> a Gram-positive bacterium, has been found to possess some natural resistance to traditional food preservation, most notably its ability to grow at near-freezing temperatures (-0.4 – 50 °C).<sup>20</sup> Recurring and serious outbreaks of Listeriosis has focused research attention on class IIa bacteriocins due to their excellent listericidal activity in the pico- and nano-molar range.<sup>21</sup> In normal adults, Listeriosis causes "flu-like" symptoms although serious complications such as convulsions, confusion and coma can occur. People at risk include the immunocompromised, pregnant mothers and newborns. Newborns may experience more serious complications such as meningitis and septicemia.

Luchansky and coworkers, developed a class IIa bacteriocin pediocin gel that protects hotdogs from *Listeria* contamination.<sup>22</sup> Pediocin-producing bacteria were also added to sausage resulting in a reduction of *Listeria* numbers to less than one ten-thousandth of the original. Active pediocin was found after two months of refrigeration demonstrating the longevity of this treatment.<sup>5</sup> Davidson has patented piscicolin, another listericidal bacteriocin, for use in meat products and as a rinse agent for salad greens and chicken parts.<sup>5</sup>

Investigations of bacteriocins, with respect to antimicrobial activity in food preservation (especially in minimally processed foods) and pharmaceutical applications, has provided insight into bacteriocin processing and secretion, mechanisms of cell immunity and structure-function relationships.

## **1.2: Classification and General Characteristics of Bacteriocins**

LAB are a phylogenetically diverse group of Gram-positive, anaerobic, nonsporulating coccus- or rod-shaped bacteria with less than 50 mol% G+C (guanine and cytosine) in their DNA. They ferment carbohydrates to lactic acid as the sole (homofermentative) or a major (heterofermentative) end product.<sup>3</sup> This is partly responsible for their preservative effect in foods due to a concomitant lowering of pH.<sup>23</sup> Other common features include a cationic nature and demonstration of nearly identical net charges at various pH values.<sup>6,24</sup>

Bacteriocins produced by gram-positive LAB are a heterogeneous group of ribosomally synthesized antimicrobial cationic peptides ranging in molecular size from a

few thousand Daltons to large proteins (> 50 kDa) possibly containing carbohydrate or lipid moieties.<sup>3</sup> The smaller bacteriocins are synthesized as prepeptides that undergo post-translational modifications to form the mature biologically active peptides that are active against a range of other, often closely related, bacteria.<sup>25</sup> These modifications expand the chemical properties and activities that can be achieved with a repertoire of only 20 proteinogenic amino acids.<sup>26</sup> The competitive environments in which many Gram-positive bacteria find themselves has probably driven their diversity: an ability to generate novel bacteriocins results in peptides having unique modes of action. In addition, many bacteria are capable of producing more than one bacteriocin. As any given peptide is unlikely to have an antimicrobial spectrum that encompasses all pathogens encountered by the producer species, it is beneficial to have multiple bacteriocins with overlapping activities.<sup>3</sup> Resistance is also less likely to develop. These proteinaceous molecules first attracted attention because of their physiological capability of interfering with the growth on agar media of certain other, closely related, bacteria.<sup>6</sup> The antagonistic interaction between competing bacteria was first described in 1877, when Pasteur and Joubert recorded that some *Escherichia coli* strains interfered with the growth of *Bacillus anthracis*.<sup>4</sup>

Although there is a classification of bacteriocins (Table 1), categorization continues to evolve in conjunction with the discovery of new and unusual peptides. Bacteriocins have been divided into four main categories with the emergence of two distinct families; lantibiotics and nonlantibiotics. Classification<sup>3,4,23,27-29</sup> is based upon a number of criteria, namely molecular mass, thermostability, enzymatic sensitivity,

presence of post-translationally modified amino acids, mode of action and structure-function similarities.

Lantibiotics (class I),<sup>30-34</sup> such as nisin and mersacidin, undergo extensive post-translational modifications and are characterized by the presence of:

- unusual dehydro amino acids, dehydroalanine (Dha) and dehydrobutyrine (Dhb)
- monosulfide bridges that form intramolecular rings, lanthionine and 3-methylanthionine
- possible keto amide residues at the N-terminus
- a variety of other modified nonprotein amino acids, including 2,3-dehydroalanine (Dha) and 2,3-dehydrobutyrine (Dhb), *S*-aminovinyl-D-cysteine, *S*-aminovinyl-D-methyl-cysteine, lysinealanine, hydroxyaspartic acid, D-alanine, 2-oxobutyrate and hydroxypyruvate<sup>35</sup>

Post-translational modifications are rare among the nonlantibiotic bacteriocins, except for disulfide bridge formation, and amino acid sequencing is usually facile *via* automated Edman degradation technology. Sequential end group analysis is accomplished using phenylisothiocyanate (PITC), which reacts with the N-terminal amino groups of proteins.

Most bacteriocins that have been studied belong to classes I and II, because they are both the most abundant ones and the most prominent candidates for industrial application. Class II receives more attention due to their activity against *Listeria* species. Investigations of a wide range of class II bacteriocins (Table 2) has led to the division of

this class into two subgroups: IIa, *Listeria*-active singly expressed peptides with a consensus sequence in the N-terminus of YGNGVXC<sup>A</sup> and IIb, systems of two different complementary peptides.<sup>24,36</sup>

---

<sup>A</sup> Some authors extend the “pediocin-box” motif: YGNGVX<sub>1</sub>CX<sub>2</sub>K/NX<sub>3</sub>X<sub>4</sub>C, where X<sub>1-4</sub> represents polar uncharged or charged residues<sup>21,28</sup>

**Table 1:** Classification and characteristics of bacteriocins.

<i>Class</i>	<i>Characteristics</i>	<i>Subclasses</i>
<b>I. Lantibiotics</b>	<ul style="list-style-type: none"> <li>-Ribosomally synthesized precursor peptides that undergo unusual extensive post-translational modifications of amino acids</li> <li>-Small (20-25 amino acids, &lt; 5 kDa) peptides containing intramolecular thioether rings formed by lanthionine and <math>\beta</math>-methylanthionine</li> </ul>	<ul style="list-style-type: none"> <li><b>Ia.</b> Elongated, amphiphilic with pore-forming activity</li> <li><b>Ib.</b> Globular, consisting of anionic or neutral peptides, no net charge, enzyme-inhibitory</li> </ul>
<b>II. Nonlantibiotics<sup>a</sup></b>	<ul style="list-style-type: none"> <li>-Ribosomally synthesized inactive prepeptides that undergo minimal post-translational modification of cysteine and by cleavage at a double glycine (-2, -1) releasing a mature cationic peptide</li> <li>-Diverse chemical and genetic characteristics</li> <li>-Small (30-70 amino acids, &lt;10 kDa), thermostable (100°C to 121°C), amphipathic peptides</li> </ul>	<ul style="list-style-type: none"> <li><b>IIa.<sup>b</sup></b> Conserved amino acid motif, YGNGVXC, near the N-terminus</li> <li>-Referred to as “pediocin-like” or “<i>Listeria</i>-active” (i.e. listericidal)</li> <li>-Share ~ 40-60% sequence similarity in the N-terminal half 37-48 residues</li> <li><b>IIb.</b> Complementary two-peptide bacteriocins; display low or no activity alone but can increase five-fold for combined activity</li> <li><b>IIc.</b> Other unmodified bacteriocins<sup>29</sup></li> </ul>
<b>III. Nonlantibiotics</b>	<ul style="list-style-type: none"> <li>-High-molecular-weight (&gt;30 kDa), heat labile proteins</li> </ul>	
<b>IV.<sup>c</sup></b>	<ul style="list-style-type: none"> <li>-Complex bacteriocins carrying lipid or carbohydrate moieties</li> </ul>	

<sup>a</sup> one or two pairs of cysteine residues that form disulfide bridges are referred to as “cystibiotics”; a single cysteine residue that must be in the reduced thiol form for activity is referred to as a “thiolbiotic”<sup>6</sup>

<sup>b</sup>van Belkum and Stiles divide Class II Bacteriocins into six groups: IIa – cystibiotics containing four cysteine residues that form two disulfide bridges, one each in the C- and N- termini; IIb – cystibiotics with one disulfide bridge in the N-terminal half; IIc – cystibiotics lacking the YGNGVXC motif with the disulfide bridge spanning the N- and C-sections of the molecule; IId – only one or no cysteine residues, lacking the YGNGVXC motif; IIe – two separate complementary peptides (E = enhancing or S= synergistic); II f – Atypical Bacteriocins: cyclic or leaderless peptides

<sup>c</sup>Previous definition of IIc: Bacteriocins dependent upon export using the translocase general secretory (sec) pathway (GSP)

<sup>d</sup>This category has been excluded from Nes’ classification because these compounds have not been purified and evidence for them is based upon loss of activity.<sup>23</sup>

### 1.2.1: Class II Bacteriocins

Class IIa bacteriocins have a high content of amino acid residues with ionizable side chain groups (i.e. basic amino acids), nonpolar residues and small amino acids such as glycine, which confer a high degree of conformational freedom to the bacteriocins.<sup>37</sup> Cysteine content is an important characteristic of IIa's and they are often referred to as cystibiotics, i.e. they have at least two cysteines participating in disulfide bridging. These disulfide bridges appear to be crucial for their activity.<sup>38</sup> The intramolecular pattern of monosulfide and disulfide bonds assists in secondary structure stabilization by reducing the number of possible unfolded structures. This is an additive effect with respect to structure, and more disulfide bonds can result in greater antimicrobial activity of the peptide.<sup>4</sup> Class IIa N-termini often contain  $\beta$ -sheets, maintained in a  $\beta$ -hairpin conformation that are stabilized by the N-terminal disulfide bridge conferring amphiphilicity to the N-terminus. An amphiphilic  $\alpha$ -helix spanning similar regions in different molecules is predicted for most of the C-terminal region thereby leaving only a short nonhelical portion at that terminus. It is interesting to note that class IIa bacteriocins described thus far are produced by food-associated LAB predominantly from meat and dairy (some vegetables) such as: *Lactobacillus*, *Enterococcus*, *Pediococcus*, *Leuconostoc*, and *Carnobacterium*.

Class IIb bacteriocins consist of two separate peptides that are either type E (enhancing) where antibacterial activity of one of the peptides is enhanced by the other, e.g. thermophilin 13, or type S (synergistic) in which the peptides have little or no activity alone, e.g. brochocin-C, which consists of brochocin A (BrcA) and brochocin B

(BrcB) (Table 2). To date more than 15 two-peptide bacteriocins have been identified within both class I and II.<sup>36</sup> Their sequences and structures are varied although sequence homology is occasionally seen between two-peptide systems. Analogous to class IIa, the class IIb two-peptide bacteriocins are formed as biologically inactive precursors that undergo enzymatic removal of a N-terminal leader during export; either by a *sec*-dependent pathway, or more commonly, by cleavage at a double-GG position by a dedicated ABC transporter. The mature biologically active bacteriocins are generally cationic, amphiphilic species with little or no cysteine content.

**Table 2:** Examples of class IIa and IIb bacteriocins

Class IIa: (YGNGVXC motif)		Class IIb
Leucocin A	Pediocin PA-1	Lacticin F
Mesentericin Y105	Divercin V41	Thermophilin 13
Mundticin	Enterocin A	Lactococcin G
Piscicolin 126	Enterocin P	Lactococcin M
Bavaricin A	Carnobacteriocin BM1	Plantaricin EF
Sakacin P	Carnobacteriocin B2	Plantaricin JK
Sakacin A		Plantaricin S
		Brochocin-C

### 1.3: Genetics, Synthesis, Regulation, Secretion and Immunity

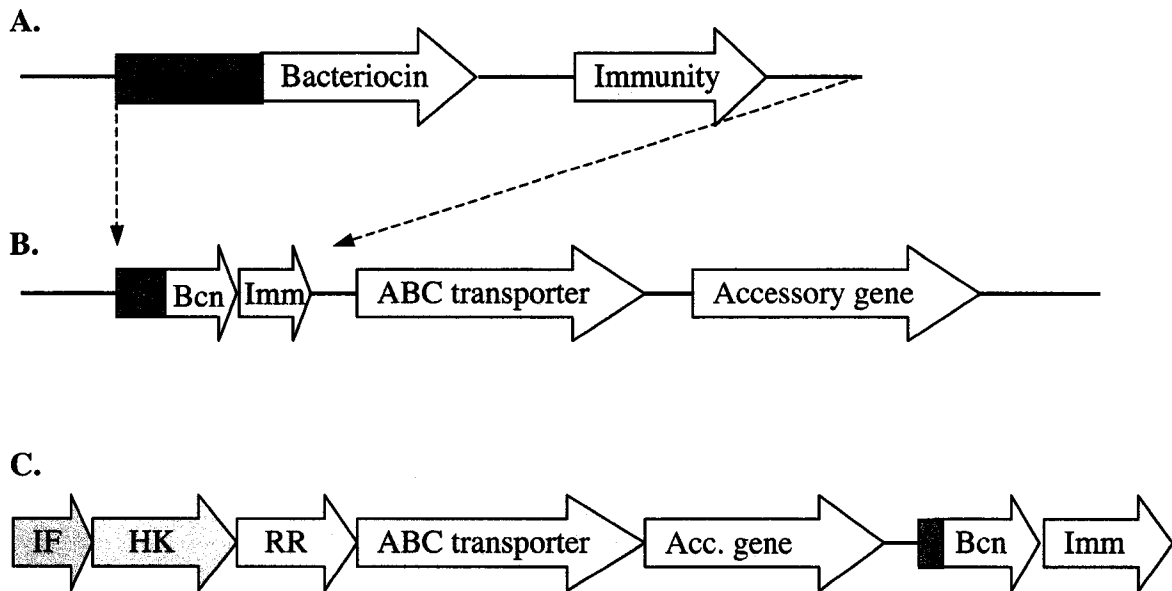
#### 1.3.1: General Genetic Organization

Considerable genetic diversity exists among bacteriocins (Figure 1).<sup>29</sup> Genes are generally clustered and may be encoded on plasmids and/or on the chromosome<sup>39</sup> with minimum genetic machinery consisting of the structural and cognate immunity genes.<sup>3</sup> Typically the minimal requirement for class II bacteriocins is four genes (five for two-

peptide bacteriocins), organized into one or more operons, including genes that encode for<sup>3</sup> (Figure 1):

- the bacteriocin prepeptide (two for the two-peptide bacteriocins),
- the cognate immunity protein,
- a dedicated cell-membrane-associated, ATP-binding cassette (ABC) transport protein, often designated with a “T”, and,
- a membrane-bound accessory protein, often designated with an “E”.

Regulatory genes<sup>24</sup> may be required for synthesis of some bacteriocins and will encode for three groups of proteins including: a secreted induction peptide [induction factor (IF)], proteins that are homologous to histidine kinases (HK), and response regulators (RR). Transcription can be activated by an induction peptide and/or be auto-induced by the pure or synthesized bacteriocin.<sup>29</sup> Nisin is an example of a bacteriocin that is autoregulated and therefore does not require an IF gene.<sup>31</sup> Operons within the clusters are differentially regulated to ensure an appropriate balance between synthesis, modification, and export.<sup>3,40-43</sup> It is uncertain whether published genetic loci are complete as many LAB produce several bacteriocins and contain a variety of bacteriocin genes that are scattered over the chromosome and plasmids.<sup>29</sup> For example, *Carnobacterium piscicola* LV17B produces at least three bacteriocins, involving genes at three locations (two on plasmids, one on the chromosome).<sup>29,37,40,44</sup> Genome sequencing should assist in elucidating the full bacteriocin producing potential of LAB.

**Figure 1:** Schematic arrangement of the genes for class II bacteriocin production.

- A. For a class II bacteriocin produced by the *sec* pathway, this is all the DNA required *e.g.* divergicin A<sup>45</sup>
- A. Pediocin PA-1/AcH; an unregulated class II bacteriocin with a double-GG leader
- C. Regulated class II bacteriocin, *e.g.* carnobacteriocin B2

### 1.3.2: Biosynthesis

Bacteriocins are ribosomally synthesized as prebacteriocins containing an N-terminal extension or leader sequence that, for class II, is cleaved at a specific processing site by a protease that can be part of the N-terminal domain of the ABC transport protein (Figure 2). The leader sequence contains a double glycine, G<sup>-2</sup>G<sup>-1</sup>, for the majority of class IIa bacteriocins, *or* an N-terminal signal peptide, depending on the chosen secretion pathway: 1. a dedicated transport system consisting of two distinct proteins, an ABC-type translocator and accessory protein, or 2. the translocase general secretion pathway, GSP (*sec*-type).<sup>45-48</sup>

Class IIa GG-type bacteriocin leader sequences vary in length from 14-30 residues. For leader peptides of the same size, similarity in sequence consensus elements is particularly high. Charge and hydrophobicity of the individual amino acids is consistently conserved. A consensus sequence, LSXKEL/MXXI/VXGG,<sup>3,24</sup> occurs at positions -12 to -1, and the primary structure has hydrophobic residues at positions -4, -7, -12 -15, and hydrophilic ones at -8, -9 and -11. Secondary structure predictions of the double-glycine leader peptides indicate an  $\alpha$ -helical structure.<sup>3</sup> Usually lysine or asparagine is found after the N-terminal methionine. Prepeptide cleavage occurs on the C-terminal side of the double G<sup>-2</sup>G<sup>-1</sup> position with export to outside of the cell.<sup>49</sup> The same ABC transporter protein is likely responsible for both transmembrane translocation and bacteriocin transport. The double glycine type leader peptide is required for secretion and may also function to deactivate the peptide since the prepeptides typically exhibit greatly reduced activity. The similarities present in the leader peptides described above suggest that the corresponding ABC transporters and associated proteins may also be similar as they tolerate some sequence variation.<sup>50-55</sup> This permits heterologous expression of class II bacteriocins using secretory machinery of another bacteriocin, which could be advantageous if more than one bacteriocin is desired for broader activity for applications in the food or pharmaceutical industries. Particularly, this would assist the development of LAB producing multiple bacteriocins, each one having its specific range of target bacteria, in order to attack a broad range of undesirable organisms.<sup>24</sup>

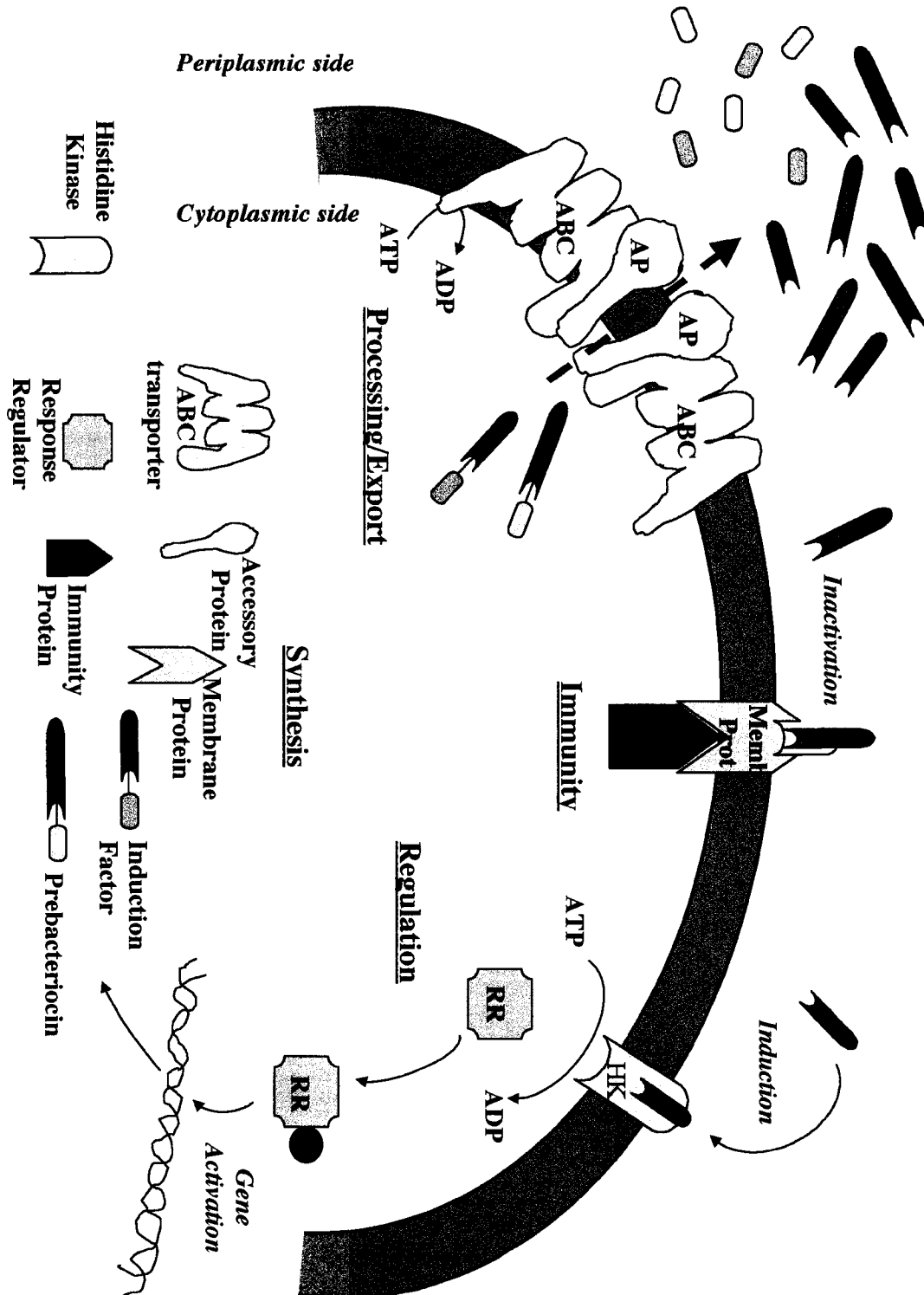
Many bacteriocins are synthesized during post-logarithmic growth when both nutrients and space for bacterial multiplication are exhausted.<sup>26</sup> Microbial “warfare”

ensues, since further growth only occurs at the expense of bacterial competitors, employing exquisitely designed compounds that are toxic for specific competing target cells.<sup>26</sup> The yield of peptide per unit biomass is affected by several factors, including the producing strain, media (carbohydrate and nitrogen sources and types, cations, anions, etc.) and fermentation conditions (pH, temperature, agitation, and aeration). LAB are nutritionally fastidious microorganisms; their growth and bacteriocin production are often limited by organic nitrogen sources and the carbon substrate. Due to the heterogeneous nature of bacteriocins, growth conditions need to be determined empirically for each producer organism. Cessation of growth usually correlates with the conclusion of the exponential phase and may be followed by a decrease in peptide titre.<sup>B</sup> This can result from adsorption of bacteriocins on producer cells or may involve cleavage by proteases.<sup>4</sup>

---

<sup>B</sup> Since adsorption of bacteriocins to cells is maximal at pH 5.5-6.5 and decreases at low pH, it is not surprising that fermentations without pH control that become acidic often see no reduction of bacteriocin titre.

**Figure 2:** Schematic overview of the suggested machinery for production of class IIa bacteriocins: three component regulatory system, synthesis, processing, secretion, and immunity.



### 1.3.3: Regulation and Quorum Sensing

In many strains, bacteriocin production is controlled in a cell-density dependent manner by a genetic and functional triad referred to as a “three component regulatory system”.<sup>56,57</sup> Three co-transcribed genes encode for: a secreted bacteriocin-like peptide pheromone (or induction factor),<sup>23,41</sup> a histidine kinase (HK) sensor protein, and a response regulator (RR) (a DNA-binding effector protein) (Figure 2).<sup>58</sup> The quorum sensing mechanism is a cascade of events initiated by the peptide pheromone (PP). Cells constitutively produce a low basal amount of induction peptide. At a certain threshold level (dependent upon transcriptional activity in the producing cell and the number of cells present) the concentration of the PP will be sufficient to induce bacteriocin biosynthesis. The secreted pheromone binds to the histidine kinase resulting in autophosphorylation (at a conserved histidine residue) followed by phosphoryl group transfer to the response regulator (at an aspartic acid residue). The response regulator activates transcription by binding to tightly regulated promoters, which, in turn regulates the operons.<sup>59-62</sup> Massive production of pheromone and bacteriocins ensues.

This regulatory mechanism was first discovered when Saucier,<sup>63</sup> Diep,<sup>59</sup> and Eijsink<sup>64</sup> *et al* observed that LAB strains lost their bacteriocin phenotype (Bac<sup>+</sup>) when cells in the growth medium were diluted below a certain threshold level. Subsequent return to full population density could not reactivate bacteriocin production. However, bacteriocin production could be restored by the addition of cell-free supernatant from a bacteriocin-producing organism.<sup>59,63</sup> Analysis of the supernatant

revealed a small bacteriocin-like peptide. Biochemical and genetic analysis revealed the nature of this peptide pheromone.<sup>59,64</sup>

The peptide pheromones (PP) are unmodified small peptides synthesized as precursors with N-terminal double-glycine cleavage sites, but are shorter than bacteriocins (19-26 amino acids) and generally display no antagonistic activity. These pheromones are gene encoded and are transcriptionally linked to genes encoding the HK and RR. They are highly strain specific and only activate the cognate histidine kinase, so that the pheromone “talks” to the cells of its own strain but does not “talk” to cells belonging to other strains.<sup>61</sup> The concentration of induction peptide required for expression to occur is approximately  $10^{-10}$  M. CbnS, for example, is the peptide pheromone required for carnobacteriocin B2 (CbnB2) production. (Additionally, at sufficiently high concentrations CbnB2 is involved in regulation as an autoregulator.)<sup>43</sup> However growth conditions and environmental factors<sup>C</sup> have also been found to influence the expression of these induction peptides.<sup>29,65-67</sup>

Histidine kinases contain a hydrophobic domain at the N-terminus and are membrane associated (Figure 2). These hydrophobic domains presumably function as the sensor and for those that are involved in regulation of bacteriocin synthesis, 5-7 transmembrane sequences are postulated.<sup>3</sup>

The sensing of its own growth, which is likely to be comparable to that of competing bacteria, enables the producing organism to switch on bacteriocin production at times when competition for nutrients is likely to become more severe. It

---

<sup>C</sup> Media composition, oxygen access, temperature, pH, and [salt] etc. may effect competence development, basal expression of genes involved in pheromone production and sensing, pheromone secretion and processing effectiveness, or the affinity of the HK for the pheromone

also ensures synchronization of bacteriocin production by cells of the same strain through cell-cell communication. Additionally, the requirement of a quorum ensures that the considerable investment of energy in bacteriocin synthesis only occurs if there are sufficient other producers, so that the effort expended to combat competitors is shared and the potential impact is maximal.<sup>29</sup>

#### **1.3.4: Secretion, Activation, Processing**

Bacteriocins having double-GG leader peptides, which function as transport signals for the precursor.<sup>52</sup> Bacteriocins use a dedicated bacteriocin transport apparatus consisting of two different membrane-bound proteins: an ABC transporter and an accessory protein (Figure 2).<sup>23</sup> ABC transporters consist of a hydrophobic integral membrane domain and a cytoplasmic ATP-binding domain that are usually expressed together and probably associate to be functional. Deletion mutations in either of the genes encoding for these proteins results in complete loss of bacteriocin production.<sup>40,43,68-71</sup> The transport of substrates, such as sugars, peptides, amino acids, and inorganic ions<sup>72</sup> requires hydrolysis of ATP as the energy source. The ABC transporter appears to have a dual function, as the maturation protease and exporter. The proteolytic domain may bind a bacteriocin precursor and ATP hydrolysis may induce conformational changes in the transporter resulting in concomitant leader peptide removal and transmembrane transport.<sup>26,73</sup> Many ABC-transporters lack distinctive structural characteristics<sup>73</sup> and, as a result, the transport machinery normally tolerates some sequence variation in the leader peptides.<sup>29</sup> Thus, one set of transport proteins can transport several precursor peptides.<sup>29</sup> This has been exploited

for heterologous expression<sup>49,74</sup> of class IIa bacteriocins but secretion efficiency can depend upon the bacteriocin and bacterial host.<sup>51,75</sup>

ABC transport proteins are produced as single polypeptide chains of approximately 720 residues with the ATP-binding domain at the C-terminus and the hydrophobic domain with six putative membrane-spanning sequences at the N-terminus (Figure 2).<sup>76</sup> Topology analysis indicates that the proteolytic domain in the N-terminus is probably located in the cytoplasm.<sup>73</sup> Alignment of several double-GG transporters reveals a 150 amino acid N-terminal domain with two conserved motifs: 1. a cysteine motif (QX<sub>4</sub>D/ECX<sub>2</sub>AX<sub>3</sub>MX<sub>4</sub>Y/FGX<sub>4</sub>I/L) and, 2. a histidine motif (HY/FY/VVX<sub>10</sub>I/LXDP). The C-terminal portion consists of approximately 200 amino acids and contains a highly conserved ATP-binding domain, which is unique to ABC-transporters.<sup>70,77</sup> Both the N- and C- terminal regions are believed to be crucial for ABC-transporter activity.

The accessory proteins (Figure 2) have an average length of 470 AA's. These proteins exhibit significant homology, and are essential for bacteriocin production, but have unknown function.<sup>40,43,50,70,71</sup> Hydropathy plots suggest that a short stretch of the hydrophobic N-terminal portion is on the intracellular side of the membrane, followed by a transmembrane domain and the major hydrophilic C-terminus exposed to the extracellular side of the membrane.<sup>28,68,69,76,78</sup> The accessory proteins are required for externalization of class IIa bacteriocins with postulated activities related to membrane translocation and/or processing of the leader peptide.<sup>70,79</sup>

### 1.3.5: Immunity

Bacteria that produce antimicrobial peptides could potentially be susceptible to their own peptides. Generally bacteriocin-producers obtain protection from their own bacteriocin by the concomitant expression of a cognate immunity protein (Figure 2).<sup>6,80</sup> Immunity proteins appear to be highly specific and normally confer immunity to the cognate bacteria.<sup>3</sup> The bacteriocin operon usually has the bacteriocin structural gene adjacent and downstream of the immunity gene.<sup>D</sup>

Immunity proteins consist of 50-150 amino acids, are cationic and are principally hydrophilic molecules. However, amino acid sequence analysis indicates some hydrophobic segments.<sup>38,81,82</sup> Comparative studies has shown that sequence similarities between two immunity proteins may be low even though corresponding bacteriocins are quite similar, and vice versa.<sup>38,80,83</sup> They are located (Figure 2) intracellularly<sup>38,81,82</sup> and divided into a minor membrane-associated fraction plus a major cytoplasmic fraction.<sup>81,82,84-86</sup> They do not appear to interact directly with bacteriocins in aqueous solution,<sup>82,84,85</sup> nor is known whether the intracellular immunity protein acts directly to prevent binding of the extracellular-bacteriocin to the membrane.<sup>82</sup> The mechanism of action is unclear, but it is postulated that immunity proteins act by disturbing either the process of bacteriocin aggregation and pore formation, or alternately, the interaction between the bacteriocin and a putative membrane-located receptor.<sup>24,80</sup> Cytoplasmic membranes of bacteria have anionic

---

<sup>D</sup> The co-transcription is readily illustrated in regulated bacteriocin production systems where the sensitivity of the bacteriocin producer varies according to the bacteriocin production state.<sup>37,40,80</sup>

groups exposed to the exterior, and immunity proteins have cationic character and may bind to the cytoplasmic membrane through electrostatic interactions and hydrophilic domains. Presumably the immunity protein functions by interfering with the ability of the bacteriocin to disrupt normal membrane structure and function.<sup>28,82</sup>

## **1.4: Mode of Action**

### **1.4.1: Mechanism**

Bacteriocins of lactic acid bacteria (LAB) and their mode of action is a major topic of research.<sup>87</sup> Their positive charge presumably facilitates interactions with the negatively charged bacterial phospholipid-containing membranes and/or acidic bacterial cell walls, whereas their amphiphilic character enables membrane permeabilization.<sup>87</sup> These small cationic peptides direct their activity primarily against sensitive Gram-positive bacterial species. Although precise mechanistic descriptions are unknown, investigations have demonstrated that generalized membrane disruption models (barrel stave or carpet) are too simplistic to adequately describe the bactericidal action.<sup>88</sup> Subtle structural differences in peptides may lead to marked differences in specificity, and small differences in target cells may lead to marked variations in their susceptibility to a peptide. Construction of hybrid bacteriocins has shown that an important determinant of target-cell specificity for pediocin-like (type IIa) bacteriocins is the C-terminal region.<sup>89</sup> Although there are C-terminal similarities that may allow subgroup classification, CbnB2 and Leu A are non-conformists and bear distinctive regions.<sup>89</sup>

Bactericidal activity by class I and II bacteriocins is proposed to occur by permeabilizing the cell membrane of target organisms, or in certain cases, by targeting intermediates of cell wall biosynthesis, specifically the inhibition of peptidoglycan formation.<sup>90-92,90</sup> Recent investigations indicate that action for pediocin-like (type IIa) bacteriocins may depend on membrane proteins involved in sugar transport.<sup>93,88,94-98</sup> It has been shown that three class I lantibiotics, (Figure 3), nisin<sup>9,90,92,99-101</sup> mersacidin,<sup>100,102,103</sup> and actagardine<sup>33</sup> require lipid II as a cell membrane receptor prior to pore formation.<sup>91</sup>

Type Ia lantibiotics such as nisin, epidermin and Pep5 are flexible, elongated, amphipathic molecules whose primary mode of action is the formation of pores in the bacterial cytoplasmic membrane (Figure 4).<sup>92,104</sup> It is proposed that nisin initially binds to the outwardly oriented (with respect to the cell membrane) carbohydrate moiety of lipid II in a 1:1 ratio. A negatively charged surface is not essential for binding, but the N-terminal region of nisin is essential for lipid II recognition and preventing peptidoglycan biosynthesis. Both the C-terminal and flexible “hinge” regions of nisin may then translocate across the cytoplasmic membrane to allow highly specific pore formation, resulting in the release of monovalent cations and ATP.

Type Ib lantibiotics such as mersacidin and actagardine possess a rigid globular shape and inhibit glycosyl transferases by forming a tight complex with their membrane-bound substrates.<sup>102</sup> The action of mersacidin on transglycosylation by



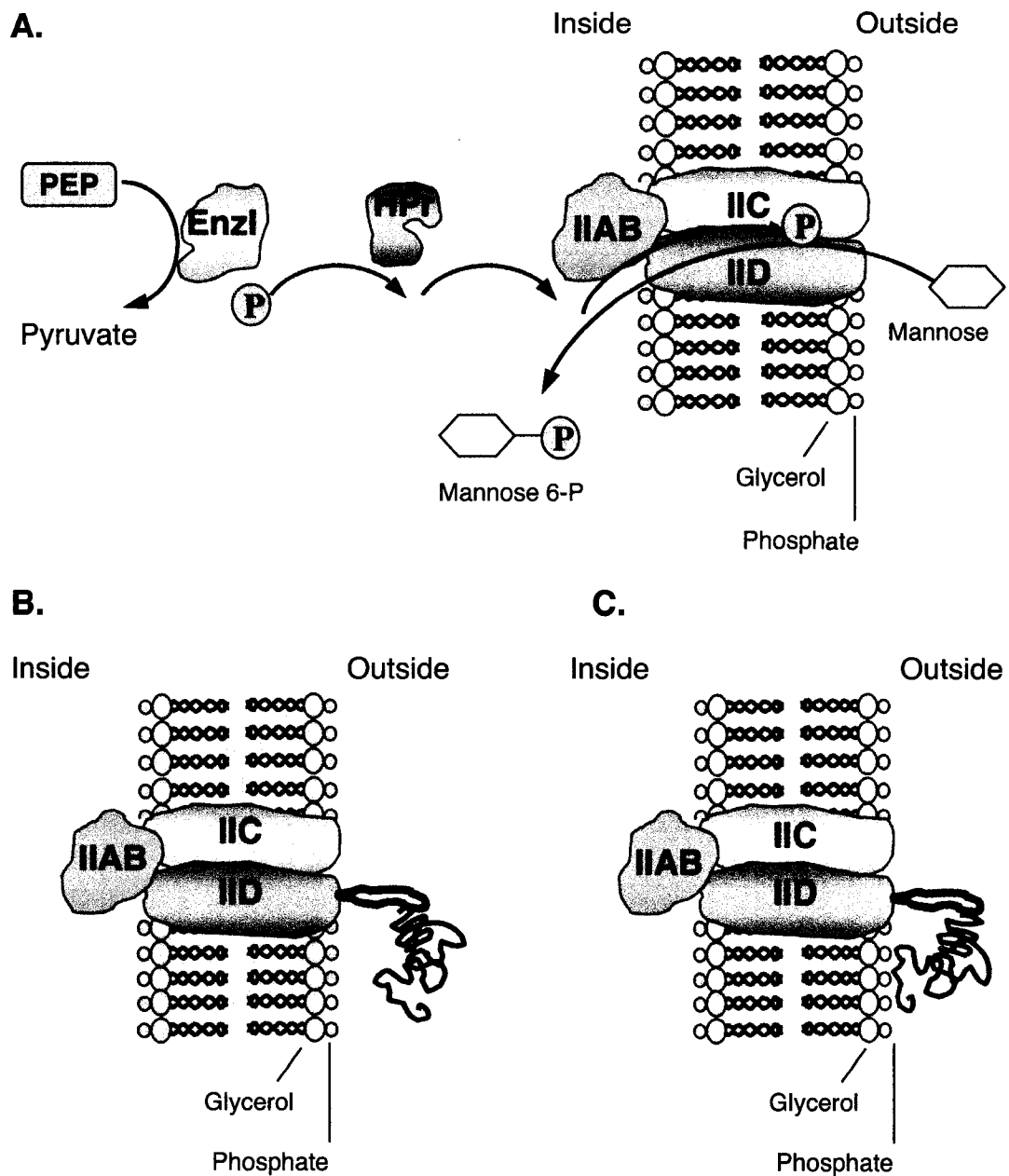
interaction with lipid II occurs *via* a binding site that is not targeted by any currently used antibiotic.

For class IIa bacteriocins, recent findings support the proposal of a putative receptor on the surface of sensitive cells.<sup>88,96</sup> A surface protein membrane receptor can account for the narrow and strain specific-spectrum of activity. Minor differences in phospholipid composition between strains of the same species or related strains are unlikely to be responsible for specificity. The enantiomer of leucocin A, which contains all D amino acids, is inactive, thereby showing that a chiral interaction is required at the bacterial surface.<sup>83,96,97</sup> Also, some *Listeria* strains show cross-resistance to class IIa bacteriocins but are still sensitive to nisin.<sup>105</sup> Recently, Hechard proposed a mannose PTS permease ( $EII_t^{MAN}$ ) as a target molecule for class IIa bacteriocins on the surface of *L. monocytogenes* and *E. faecalis*. (Figure 5).<sup>88</sup> Most bacteria import specific sugars via the phosphotransferase system (PTS) to support a host of bacterial processes.<sup>106</sup> The PTS system involves phosphoenolpyruvate (PEP) as the high-energy molecule to drive both transport and chemical modification of sugars.<sup>106</sup> The PTS is a multi-component complex consisting of EI (enzyme I), Hpr (Histidine-containing phosphocarrier), and a specific carbohydrate transport protein EII. PEP phosphorylates EI, followed by transfer to Hpr and then to EII.  $EII_t^{MAN}$  (MAN is for mannose) is composed of four subunits (Figure 5):<sup>95</sup> IIAB and IIB are cytoplasmic subunits involved in phosphorylation, and IIC is a membrane bound protein responsible for sugar transport. Additionally, an integral membrane subunit, IID is specifically found within the PTS permease of the mannose family (Figure 5).<sup>95</sup>

Within IID, from sensitive *Listeria* strains, there is an unusual motif, not present in other IID subunits. This is a putative external loop (represented by the sequence: SQVKLDKGAYIEWDKLPAGGEMHKAFEQVNQG). It has been suggested that this loop is a receptor for various class IIa bacteriocins and that they may interact (probably via the non-conserved C-terminal portion) by a direct protein-protein contact<sup>95</sup> with the IID subunit EII<sub>t</sub><sup>MAN</sup>. This could act as an anchor to provide pore formation in the cytoplasmic membrane, possibly with recruitment of additional bacteriocin molecules. It may also result in a conformational change of the PTS system to an open state that could assist in permeabilization of a target cell.

Bacterial sugar transport is genetically controlled,<sup>95</sup> and Hechard and coworkers have proposed that an *mptR* operon regulates a  $\sigma^{54}$ -dependent<sup>94</sup> PTS system in *L. monocytogenes* and *E. faecalis*. Knockouts within this operon, *mptA* and *mptD*, have led to resistance, thereby supporting the proposal that EII<sub>t</sub><sup>MAN</sup> permease plays an essential role in sensitivity to IIa's.<sup>95</sup> Also, since expression of PTS permease is specifically induced by the transported sugar,<sup>107</sup> it has been suggested that glucose and mannose activate the expression of a protein involved in sensitivity, probably the EII<sub>t</sub><sup>MAN</sup> PTS permease, thereby leading to an increase in the number of potential protein receptors.<sup>95</sup>

**Figure 5:** Proposed model for the mode of action of class IIa bacteriocins. The subunits of  $EII_{MAN}$  are represented by IIAB, IIC, and IID. **A.** The phosphorylation and uptake of mannose. **B.** The bacteriocin recognizes the extracellular loop. **C.** The bacteriocin interacts with the cytoplasmic membrane.



## 1.5: Objective

Understanding the relationships between structure and function of bacteriocins is of significant importance and a great challenge in antimicrobial research. Knowledge of the three-dimensional structure of bacteriocins can provide a basis for detailed studies on structure-activity relationships<sup>96,108</sup> and mechanism of action. Sequence and structural comparisons between precursor, mature, and immunity proteins, within and among classes, are useful in evaluating conservation of, N-termini, C-termini and secondary structural features (helical regions, unstructured portions, and  $\beta$ -sheets). Within our group nuclear magnetic resonance (NMR) spectroscopy was employed to elucidate structures of single-peptide type IIa bacteriocins such as leucocin A (LeuA)<sup>109</sup> and carnobacteriocin B2.<sup>110</sup> Molecular biology tools are invaluable in these investigations since cloning, isolation, and fermentation techniques produce the proteins of interest.

This thesis project involved the purification and structural investigation of bacteriocins from three Gram-positive bacteria, *Carnobacterium piscicola* LV17B (class IIa), [precarnobacteriocin (CbnB2P) and the immunity protein (CbiB2)] and *Brocothrix campestris* (class IIb), [brochocins A and B (BrcA, BrcA) which form brochocin C (BrcC)], and *Bacillus subtilis* (unclassified) (subtilosin A). Maltose-binding protein fusions were utilized for growth (<sup>15</sup>N and <sup>13</sup>C labelled and unlabelled) and purification of precarnobacteriocin B2 (CbnB2P), the immunity protein (CbiB2), and brochocins A and B (BrcA, BrcB). Additionally an intein protein fusion of BrcB has also been evaluated. Subtilosin A was produced directly by *B. subtilis*

fermentation in both unlabelled (for chemical investigations) and labelled (for NMR studies) forms. The peptone media required to label subtilisin A was made by fermenting blue-green algae, *Anabaena sp.* on sodium [ $^{15}\text{N}$ ] nitrate and sodium [ $^{13}\text{C}$ ] bicarbonate. The three-dimensional structure of subtilisin A was determined to reveal highly unusual post-translational modifications.

## CHAPTER 2: CLASS II BACTERIOCINS

### RESULTS AND DISCUSSION

#### A: Carnobacteriocin B2 Precursor (CbnB2P) and the Immunity Protein (CbiB2) of *Carnobacterium piscicola* LV17B

##### 2.1 Carnobacteria

Bacteriocin production in the genus *Carnobacterium* was originally noted by Schillinger<sup>111</sup> and Holzapfel.<sup>112</sup> Bacteria belonging to this genus are recognized as non-aciduric lactobacilli. Differentiation of these bacteria from *Lactobacillus* is demonstrated by their inability to grow on acetate agar at pH 5.6, their ability to grow at high pH (8.5-9.5) and their ability to produce L(+)-lactate and oleic acid.<sup>113</sup> *Carnobacterium piscicola* LV17 is a *Lactobacillus*-type organism originally isolated from chill-stored vacuum-packaged meat and produces carnobacteriocins A, B2 (CbnB2) and BM1.<sup>114</sup> Production of bacteriocins from *C. piscicola* was first reported by Ahn and Stiles, who also genetically engineered plasmids to generate *C. piscicola* LV17A and LV17B strains.<sup>115</sup>

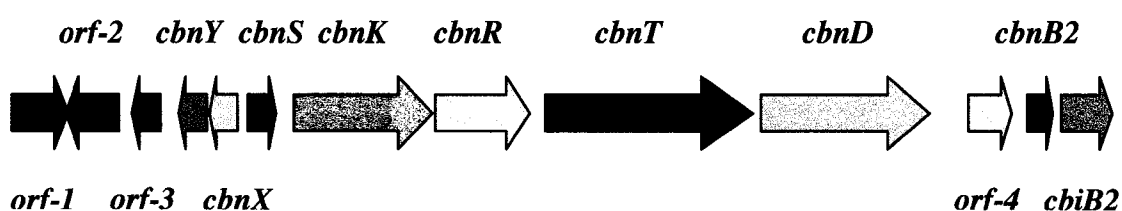
##### 2.1.1: *Carnobacterium piscicola* LV17B: CbnB2 and CbnB2P

CbnB2 is a class IIa cationic, heat stable, pore-forming bacteriocin that has a YGNGVXC sequence motif near the N-terminus (Figure 10). It is active against many lactic acid bacteria in addition to strains of *Enterococcus* species and *Listeria monocytogenes*.<sup>114,116</sup>

Genetic characterization of the *cbnB2* gene cluster revealed the presence of four ORF's (open reading frames).<sup>114</sup> The genetic determinants (Figure 6)<sup>42</sup> of CbnB2 are

located on a 61-kb plasmid (pCP40) and include an immunity gene, found downstream of *cbnB2*, as well as several ORF's involved in regulation, found upstream of *cbnB2* (Figure 6).

**Figure 6:** Genetic organization of *C. piscicola* LV17B.



- cbnB2*:** structural CbnB2 precursor
- cbiB2*:** immunity; *cbnT*-ABC transporter (716 AA)
- cbnD*:** accessory protein (455 AA)
- cbnS*:** induction factor, IF (41 AA)
- cbnK*:** histidine kinase, HK (442 AA)
- cbnR*:** response regulator, RR (245 AA)

CbnB2 (48-amino acid peptide,  $4569.9 \pm 0.7$  Da) is initially synthesized as the precursor, CbnB2P, and undergoes post-translational cleavage at a Gly<sup>2</sup>Gly<sup>-1</sup> site to remove an 18-member leader peptide to afford the mature bacteriocin (Figure 7). CbnB2P has a calculated molecular mass of 6991.8 Da and a theoretical pI of 9.70 (EXPasy). Our group has elucidated the three-dimensional solution structure of CbnB2 using nuclear magnetic resonance (NMR) techniques.<sup>110</sup> Since CbnB2 has approximately 60% sequence homology to Leu A,<sup>109</sup> it can be compared to Leu A by superposition of three-dimensional structures in order to evaluate structural motifs. (Figure 8).<sup>110</sup>

Understanding the relationships between structure and function a great challenge in bacteriocin research.<sup>24</sup> Comparisons involving the activity spectrum, amino acid sequences and structures of bacteriocins help in identifying regions that have a critical role in cell recognition and/or their bactericidal action.<sup>24</sup> Significant similarities in amino acid sequence do not necessarily coincide with analogous structural motifs and vice versa (Figure 8). Equivalent  $\alpha$ -helical regions, comprising the more variable amino acid sequences, are postulated to be involved in receptor recognition.<sup>110</sup> Solution of the structures of CbnB2P is of interest because it is much less active than the mature bacteriocin, CbnB2.

**Figure 7:** Amino acid sequence of CbnB2<sup>42</sup> The consensus motif and double-GG are represented by red and green lettering, respectively.

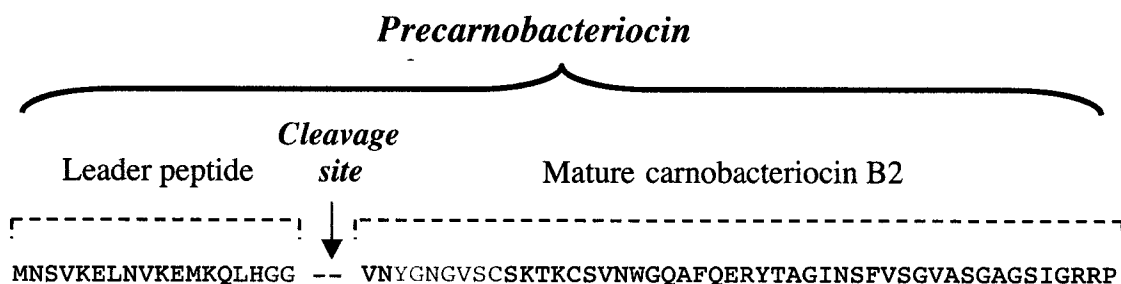
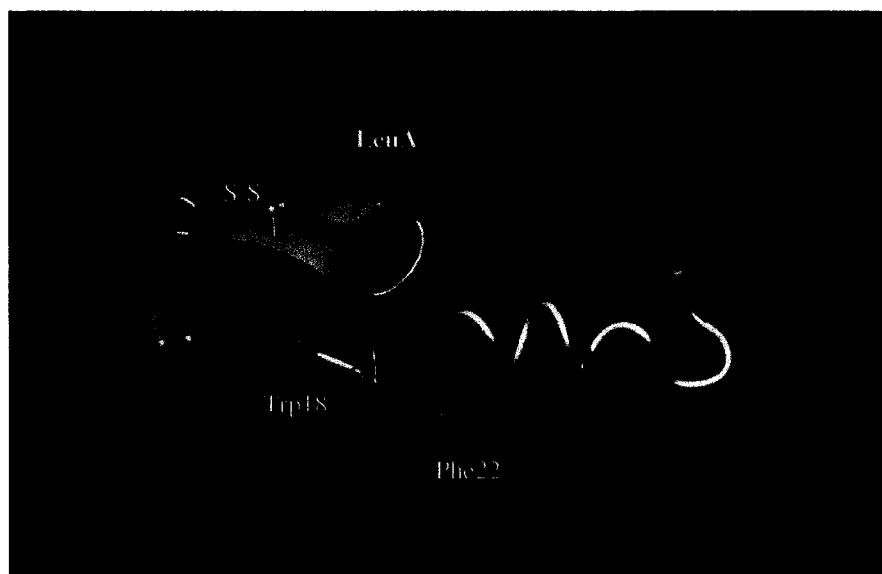


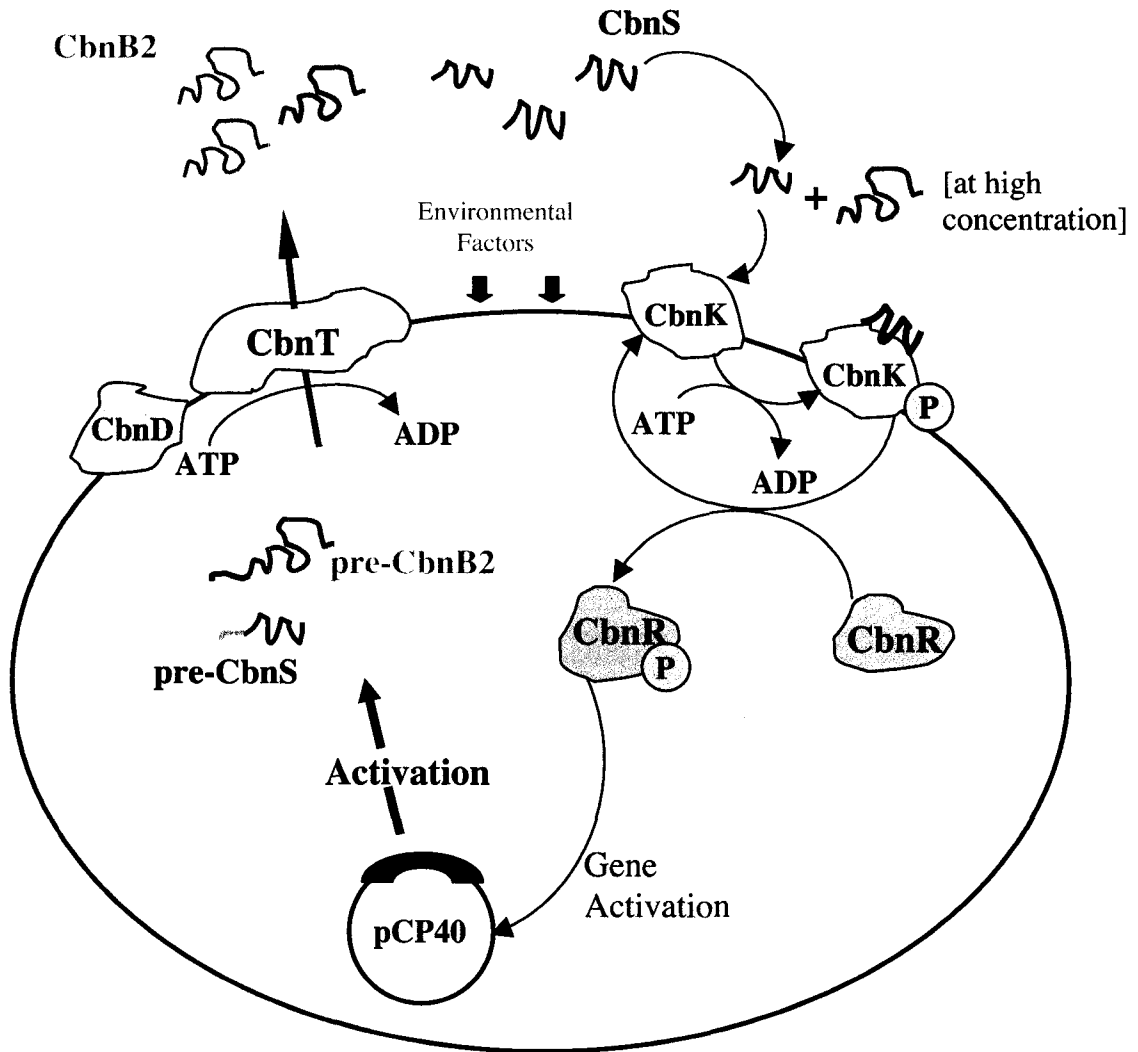
**Figure 8:** Superimposed ribbon diagrams of CbnB2 and LeuA based on alignment of backbone atoms from Trp18 to Phe22<sup>110</sup>



Regulation<sup>E</sup> of CbnB2 production entails peptide-pheromone dependent quorum sensing via the induction peptide CbnS, and at high concentrations, the bacteriocin itself acts as an inducer, resulting in autoinduction.<sup>42,63</sup> The *cbnS* gene encodes for a 41 amino acid product (MKIKTITKKQLIQIKGG--SKNSQIGKSTSSISKCVFSFFKKC) that is cleaved at the G<sup>-2</sup>G<sup>-1</sup> position resulting in a 24-member peptide. A schematic representing the overall production and regulation of CbnB2 is depicted in Figure 9.

<sup>E</sup> For *C. piscicola* LV17B four different transcripts appear to be co-regulated in a cell-density dependent manner, encompassing *cbnBM1* & *cbiBM1*, *cbnB2* & *cbiB2*, *cbnX* & *cbnY*, and *cbnS*, respectively. Homologues for Cbn's -K, -R, -T, -D have also been discerned in LV17A. It has been shown that concerted regulation of expression is supported by the presence of homologous direct repeat motifs within their promoter regions.

**Figure 9:** Schematic representing bacteriocin regulation and production of CbnB2.



- |  |                                     |
|--|-------------------------------------|
| <b>CbnR:</b> Response Regulator; RR  | <b>CbnD:</b> Accessory Protein      |
| <b>CbnK:</b> Histidine Kinase; HK  | <b>CbnT:</b> ABC-transporter system |
| <b>CbnS:</b> Peptide Pheromone   | <b>P:</b> Phosphate                 |
| <b>pCP40:</b> Plasmid containing genetic information for the production of CbnB2 |                                     |

**2.1.2: Carnobacterium piscicola LV17B: CbiB2**

The immunity protein for carnobacteriocin B2, denoted as CbiB2, contains 111 amino acids with a mass of  $12,662.2 \pm 3.4$  (calculated 12,665.6)<sup>195</sup> and has a theoretical pI of 8.93. The gene locus, *cbiB2*, is located downstream of the structural gene, *cbnB2* (Figure 6). The mechanism of immunity that protects the producer organism against its own bacteriocin is not understood, however immunoblot analysis denotes that the majority of the intracellular pool of CbiB2 is in the cytoplasm with a small proportion membrane-associated.<sup>82</sup> Since investigations of bacteriocins from LAB indicate that their antimicrobial effects are exercised through action at the outer cell membrane, it is possible that immunity mechanisms are also activated at the membrane, but from inside the cell. Proposals for the action of CbiB2 suggest interference with functional pore complex *formation* in the membrane, *or blocking* the functional cytoplasmic pore to prevent the efflux of intracellular components. This may interact with a receptor protein that binds *both* the bacteriocin and its immunity protein, and could prove to be a key feature of the mode of action.<sup>82</sup> The immunity protein is specific; no immunity to carnobacteriocin BM1 is conferred by CbiB2 when it is expressed in homologous or heterologous hosts.<sup>82</sup> A protective effect is not discerned when the immunity protein is added to a growing culture of sensitive cells. Furthermore, no significant binding of CbiB2 to microtiter plates coated with CbnB2 is observed, nor does it or possess the ability to inactivate CbnB2 in solution.<sup>82</sup>

**2.2: Subcloning of CbnB2P and CbiB2 in BL21(DE3) *E. coli***

Elucidation of tertiary structures for CbnB2P and CbiB2 is of prime importance in identifying structural consensus elements and the role they may play in regulation and modes of action with respect to the mature bacteriocins and immunity proteins. CbnB2P and CbiB2 from bacterial strain *C. piscicola* LV17B have been previously isolated and characterized.<sup>82,114</sup> However, elucidation of their 3D structure employing two- and three-dimensional NMR methodologies requires adequate quantities (1 to 2 mM; 10–20 mg) of homogeneous protein.<sup>113</sup> Additionally, since multi-dimensional NMR of complex peptides necessitates <sup>13</sup>C and/or <sup>15</sup>N labelling, media selection, protein yield, optimal fermentation conditions and expense must be carefully evaluated. Identification of these peptides was originally achieved using the wild type *C. piscicola* LV17.<sup>116</sup> Subsequent investigations utilized cloning methodologies for overexpression in *E. coli* JM107 cells of a maltose binding fusion protein employing the plasmids pLQP for CbnB2P and pLQ300i for CbiB2.<sup>82,114</sup> Unfortunately, JM107 *E. coli* cells tend to expel the clones, especially as they age. Furthermore, they are not protease deficient, which results in significantly decreased yields or, in some cases, no yield. Therefore transformation of the plasmids into competent protease deficient *E. coli* BL21(DE3) cells was undertaken.

### 2.2.1: Isolation of pLQP and pLQ300i Plasmids and Transformation

Both plasmids, pLQP and pLQ300i, were isolated according to standard molecular microbiology techniques<sup>117,118</sup> utilizing QIAGEN plasmid kit instructions. Purification protocols were based on a modified alkaline lysis procedure, followed by binding of DNA to an anion-exchange resin. Since RNA, proteins, dyes and low molecular weight impurities do not bind they are flushed through the column at moderate salt concentration. Then plasmid DNA is eluted in a high-salt buffer with subsequent concentration and desalting to generate the purified plasmids (small scale). The purification procedure is monitored by agarose gel electrophoresis and once plasmid purity is confirmed, the pure DNA is added to subcloning efficiency DH5 $\alpha$  *E. coli* cells for amplification. The alkaline lysis methodology is used again for the large-scale isolation of plasmid DNA. Once it is purified and dried, DNA sequencing ascertains that there are no errors in the nucleotide sequences. The DNA and amino acid sequences for the structural genes *cbnB2* and *cbiB2* are depicted in Figure 10.<sup>114</sup>

Transformation methodologies abound with respect to variations in incubation temperatures and time. Competent BL21(DE3) *E. coli* cells, chosen because they are deficient in proteases *lon* and *ompT*, are mixed with pure DNA and are incubated on ice followed by heat-shock treatment. Only cells that are transformed produce isolated colonies on LB agar with added ampicillin because plasmid insertion confers ampicillin resistance to the cell. The bacterial strain and plasmids and their properties are listed in Table 3.

- Figure 13:** 1. Single-strand DNA and amino acid sequences for nucleotides 141-490 of the *Hind*III fragment from pLQ5.21 containing the structural gene of CbnB2 (red letters). The *vertical arrow* in the amino acid sequence of the prebacteriocin indicates the G<sup>-2</sup>G<sup>-1</sup> cleavage site.<sup>114</sup>
2. Single-strand DNA and amino acid sequences for nucleotides 441-840 of the *Hind*III fragment from pLQ5.21 containing the genetic information for CbiB2 (blue letters).<sup>114</sup>
3. Possible promoter sequences (RBS), and the inverted repeat sequence with the greatest negative free energy are underlined.

```

AAATACCCTGGTTCAAGATGTATTTTCCAAAAAATGTTTCAGATATGATATAGTTTTTTT 200
                               -35                               -10
                               M N S V K E L N
GAAATACAAATATAAAATAAAGGAGTTTGATTTAGATGAATAGCGTAAAAGAATTAACG 260
                               RBS                               ↓
V K E M K Q L H G G V N Y G N G V S C S
TGAAAGAAATGAAACAATTACACGGTGGAGTAAATTATGGTAATGGTGTTCCTTGCAGTA 320

K T K C S V N W G Q A F Q E R Y T A G I
AAACAAAATGTTTCAGTTAACTGGGGACAAGCCTTTCAAGAAAGATACACAGCTGGAATTA 380

N S F V S G V A S G A G S I G R R P
ACTCATTGTAAAGTGGAGTCGCTTCTGGGGCAGGATCCATTGGTAGGAGACCGTAAATAT 440

                               M D I K S Q T L Y
ATAAAATACAATATAGAGCAAGGTGGTGATACAATGGATATAAAGTCTCAAACATTATAT 500
                               RBS

L N L S E A Y K D P E V K A N E F L S K
TTGAATCTAAGCGAGGCATATAAAGACCCTGAAGTAAAAGCTAATGAATTCTTATCAAAA 560

L V V Q C A G K L T A S N S E N S Y I E
TTAGTTGTACAATGTGCTGGGAAATTAACAGCTTTCAAACAGTGAGAACAGTTATATTGA 620

V I S L L S R G I S S Y Y L S H K R I I
AGTAATATCATTTGCTATCTAGGGGTATTTCTAGTTATTATTTATCCATAAACGTATAATT 680

P S S M L T I Y T Q I Q K D I K N G N I
TCCTTCAAGTATGTAACTATATATACTCAAATACAAAAGGATATAAAAAACGGGAATAT 740

D T E K L R K Y E I A K G L M S V P Y I
TGACACCGAAAAATTAAGGAAATATGAGATAGCAAAAAGGATTAATGTCCGTTTCCTTATAT 800

Y F
ATATTTCTAATTTTTTTCAATGATGTTAGTTGACTTCAAAAAG 840

```

**Table 3:** Plasmids and producer strains for CbnB2P and CbiB2

<i>Plasmid and producer strain</i>	<i>Relevant properties<sup>a</sup></i>	<i>Reference or source</i>
Plasmids		
pMAL <sup>TM</sup> -c2X	Amp <sup>r</sup> , 6648-bp, lacI, lacZ $\alpha$ and malE expression vector	[143-147]
pLQP	pMAL-c containing malE-cbnB2 fusion	[136]
PLQ300i	pMAL-c containing malE-cbiB2 fusion	[82]
Strains		
E. coli BL21(DE3)	F <sup>+</sup> ompT hsdS <sub>B</sub> (r <sub>B</sub> m <sub>B</sub> ) gal dcm (DE3); bacteriophage DE3 lysogen carrying the T7 RNA polymerase gene controlled by the lacUV5 promoter	[148]

<sup>a</sup> Amp<sup>r</sup>, ampicillin resistant

## 2.3: Recombinant Proteins Expressed as Maltose Binding Fusion (MBP) Proteins:<sup>119-123</sup> CbnB2P, CbiB2

### 2.3.1: How to “Catch” a Protein

Wild type bacteria do not preferentially overproduce the ‘proteins of interest’. Since *E. coli* normally produce approximately 1900 different kinds of proteins and a total of about 2.4 million individual protein molecules,<sup>124</sup> detecting just one is a monumental task without a specific assay or known biological activity that can serve as an isolation technique, which would enable the researcher to “fish out” the protein of interest. The Protein and Purification (pMAL<sup>TM</sup>) System meets the requisite criteria by utilizing affinity chromatography. Isolated and purified CbnB2P and CbiB2 plasmids, *cbnB2P* and *cbiB2*, were used without further manipulation and are described below. Following

transformation into the requisite *E. coli* cells pilot experiments were conducted to optimize fermentation, induction, cleavage and purification conditions.

### 2.3.2: The pMAL™ system

In this system the cloned gene is inserted into the multiple cloning site (MCS), or polylinker, of a pMAL vector down-stream from the *malE* gene, which encodes the MBP (Maltose Binding Protein, ~42,000 Da) (Figure 11). The MCS contains a cluster of unique restriction endonuclease sites (Figures 12 and 13) allowing for insertion of the desired gene into the vector. The MCS cluster is comprised of different restriction enzyme recognition sites very close to each other, thereby offering several choices with regard to enzyme choice in preparation of the plasmid and insert for cloning. A strong P<sub>tac</sub> promoter is used in conjunction with the *malE* translation initiation signals to express large quantities of the fusion protein. There are several advantages to the pMAL system: 1. reliable expression with good yields (up to 100 mg/L in more than 75% of the cases tested; typical yields are 10-40 mg/L), 2. enhanced solubility<sup>119</sup> of fusion proteins expressed in *E. coli*, and 3. a gentle one-step purification technique utilizing maltose as an eluent. The pMAL vectors also include a sequence encoding for the recognition site of a specific protease (Factor Xa) thereby allowing for cleavage of the protein of interest from MBP *without* adding any vector-driven residues to the protein. Additionally, the pMAL system contains a *lacZα* (truncated *lacZ*) gene (downstream from the MCS) providing a simple  $\alpha$ -complementation method to determine if the desired DNA fragment has been inserted into the vector. The truncated *lacZα* can be complemented by the remaining portion of the *lacZ* encoded by the host *lacZβ* gene to produce an active

enzyme capable of converting the substrate Xgal (5-bromo-4-chloro-3-indolyl- $\beta$ -D-galactoside) to a blue product. However, disruption by the inserted gene causes non-complementation of *lacZ $\alpha$*  and the active enzyme is not produced causing desired colonies to remain white on plates containing Xgal. The pMAL™ restriction map shown in Figures 12 and 13 delineates the organization and relationship of these key features.

**Figure 11:** Schematic representation of the pMAL system.

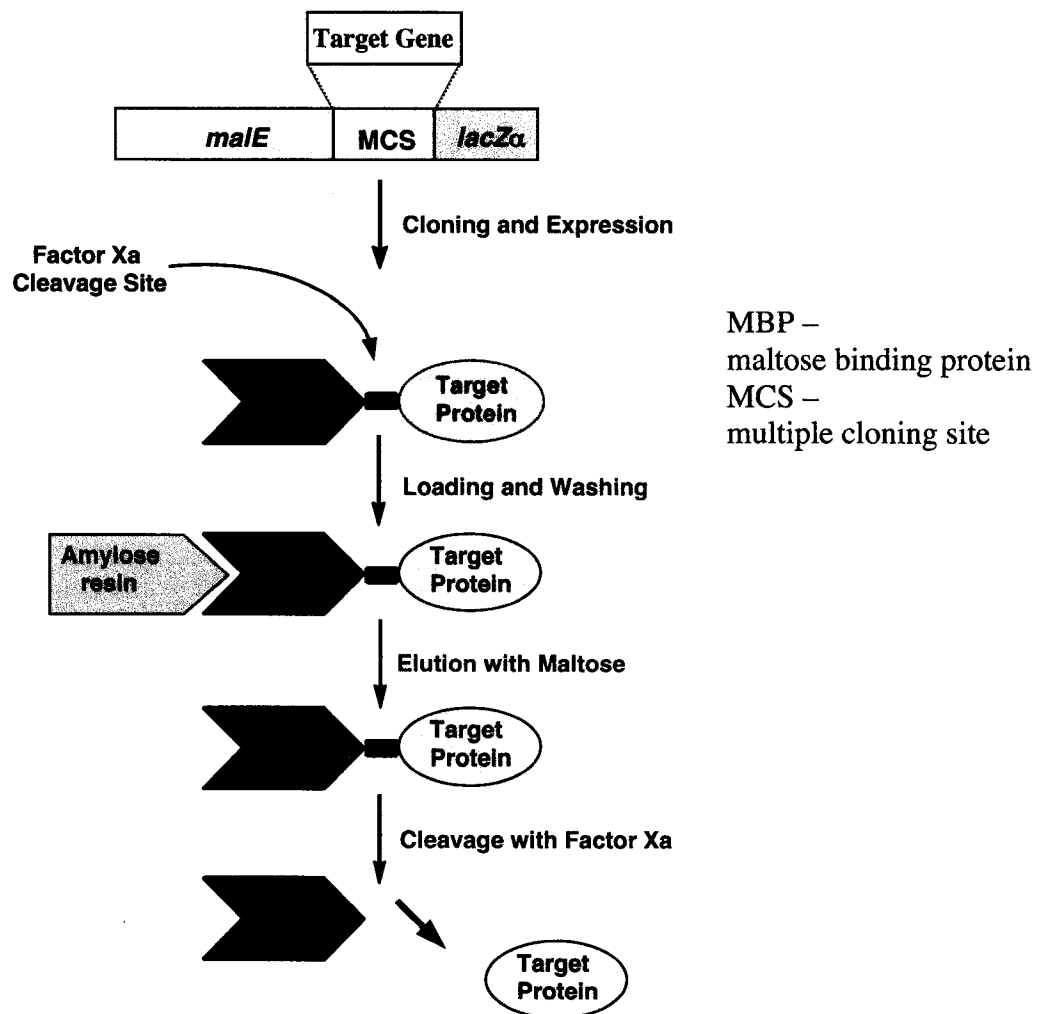


**Figure 12:** Restriction map of pMAL<sup>TM</sup>-c2X (6648 base pairs) and of pMAL<sup>TM</sup>-p2X (6723 base pairs). pMAL-c2 series vectors are identical to the pMAL-p2 series vectors except that the c2X series has an exact deletion of the *malE*-signal sequence (nt 1531-1605).

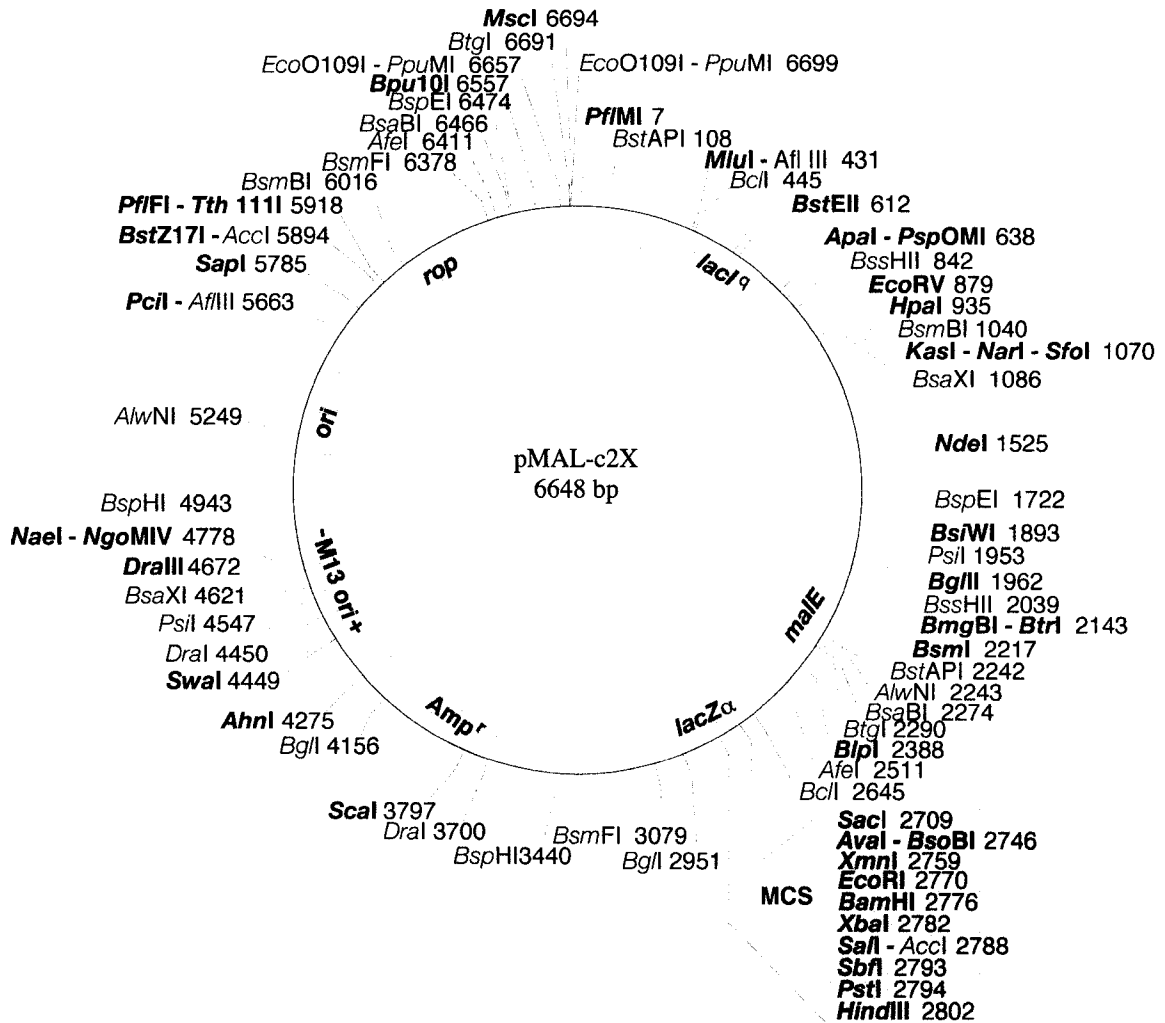
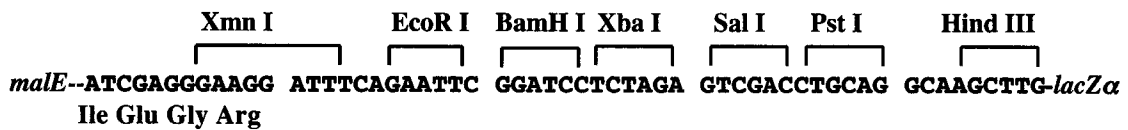


**Figure 13:** pMAL-c2X multiple cloning site (polylinker) restriction endonuclease enzyme sites



## 2.4: Protein Expression and Purification of CbnB2P and CbiB2

CbnB2P and CbiB2 are expressed in *E. coli* as recombinant protein fusions composed of the maltose-binding protein encoded on pMAL-c2X and the 66 and 111 amino acids of CbnB2P and CbiB2, respectively. The fusion proteins of both are expressed in, and purified from, the cytoplasm of BL21(DE3) *E. coli* cells. After purification on an amylose column, between 70-100 mg of the fusion proteins were recovered per litre of fermentation culture. The presence of a recognition sequence for Factor Xa<sup>F</sup> allows for specific cleavage<sup>125,126</sup> of the recombinant proteins without any extra amino acids at the N terminus. Excellent results are achieved during this reaction as more than 90% of the substrates were cleaved as indicated by the peak areas in HPLC separation and molar calculations of lyophilized materials, *i.e.* substrate versus the desired cleaved protein. After the cleavage reaction, CbnB2P and CbiB2 are purified to homogeneity by reversed-phase HPLC. The approximate amounts of proteins isolated are: CbnB2P, 5-6 mg/L and CbiB2, 6-7 mg/L. The overexpressed fusion proteins containing the precarnobacteriocin (CbnB2P) and the immunity protein (CbiB2) are analyzed by SDS-PAGE gel electrophoresis (12%), indicating that all of the clones produced proteins of the expected sizes. Expression in and purification from complete minimal media (CMM) for isotopic labelling of the proteins is accomplished as above except for the use of isotopically <sup>15</sup>N-labelled ammonium sulfate.

---

<sup>F</sup> Restriction Protease Factor Xa (blood coagulation factor Xa) is a serine protease with an extended substrate binding region matching the IEGR tetrapeptide segment and can be used as a “restriction protease” to cleave fusion proteins specifically after the Arg residue at an inserted -Ile-Glu-Gly-Arg-junction.

### 2.4.1: Mass Spectrometry of Labelled and Unlabelled CbnB2P and CbiB2

MBP-fusion proteins and cleavage products are detected by MALDI-TOF mass spectrometry utilizing sinapinic acid as a matrix. The masses of unlabelled CbnB2P-MBP-fusion and CbnB2P are 48,300 and 6739.2, respectively, whereas the  $^{15}\text{N}$  labelled CbnB2P-MBP-fusion, and CbnB2P are 48,380 and 6825.8 Da, respectively. The CbnB2P mass is lower than the calculated value of 6991.8 (disulfide bridge intact) for the unlabelled peptide. Two possibilities exist as an explanation for this anomaly. The first possibility is that *E. coli* enzymes may cause proteolytic cleavage at the C-terminus during expression.<sup>127,128</sup> In CbnB2P residues Arg-Arg-Pro (numbered 64 to 66) are represented by the codons, AGA CCG TAA. The codon AGA is rare with respect to other codons for arginine and, additionally, the AGA codon is rarely used in *E. coli* (the frequency is 2.1 per 1000 codons).<sup>129</sup> It has been proposed that the ribosomes become stalled at rare arginine codons<sup>127</sup> and nascent polypeptides are then targeted for proteolytic degradation in BL21(DE3) cells. This may result in protein heterogeneity<sup>128</sup> since one to three residues become targets for proteolytic removal, which results in variable mass values within the same sample. The second possibility is that factor Xa, considered to be a very specific proteolytic enzyme,<sup>126</sup> has been reported to cleave at arginine sites other than the tetra amino acid sequence, Ile-Glu-Gly-Arg.<sup>130</sup> Therefore, if one assumes that any of the residues Arg-Arg-Pro (64 to 66) are proteolytically removed by either method, the calculated masses (disulfide bridge intact) would be 6894.7 (-Pro), 6738.5 (-Pro and Arg) or 6582.3 Da (-Pro, Arg and Arg). The mass value determined by MALDI-TOF of 6739.2 Da is in agreement with the calculated value of 6738.5 Da,

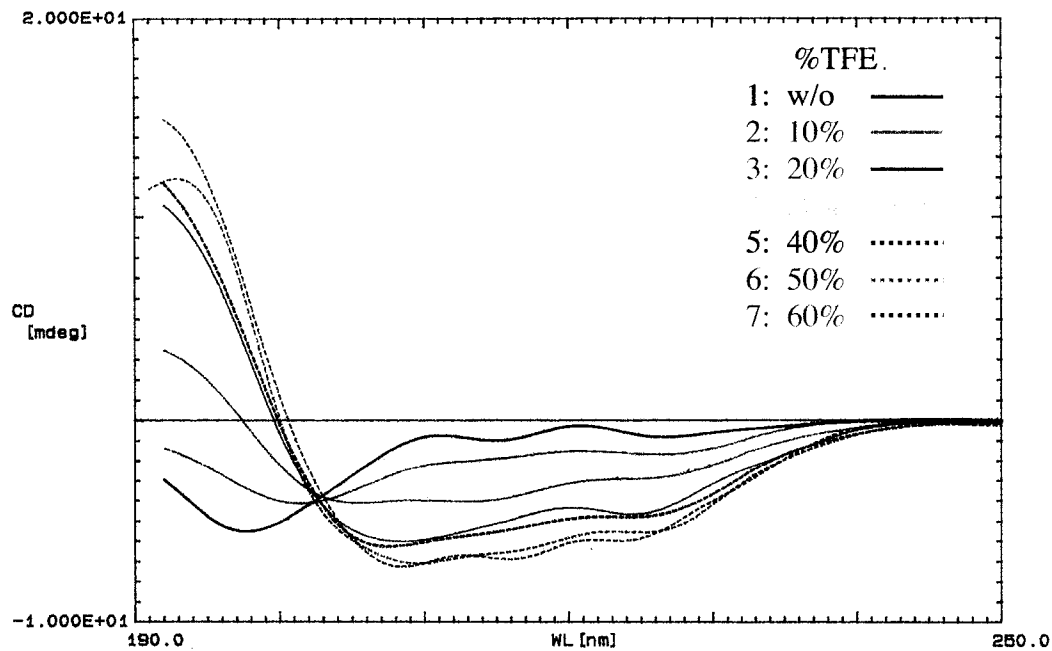
which represents cleavage of Arg65 and Pro66. This is also confirmed upon  $^{15}\text{N}$  labelling. The  $^{15}\text{N}$  labelled CbnB2P mass is 6825.8 Da and represents the addition of 87 mass units, corresponding to the presence of 87 nitrogens, which is representative of complete  $^{15}\text{N}$  labelling. Based on the masses of the fusion protein, it appears that enzymatic cleavage by *E. coli* is the more plausible explanation.

Mass spectra show that the unlabelled CbiB2-MBP-fusion is 54 360 Da and the immunity protein is 12666.0, which is in agreement with the calculated mass of 12665.6. Within the nucleotide sequence for the immunity protein are three arginines, at positions 56, 67, and 95 represented by the codons, CGT, AGG and AGG, none of which are rare. In contrast to CbnB2P, this peptide is produced in its entirety without proteolytic removal of any residues. This further suggests that enzymatic activity at the rare codon AGA is a likely possibility for the truncation of CbnB2P-MBP by *E. coli* proteases.

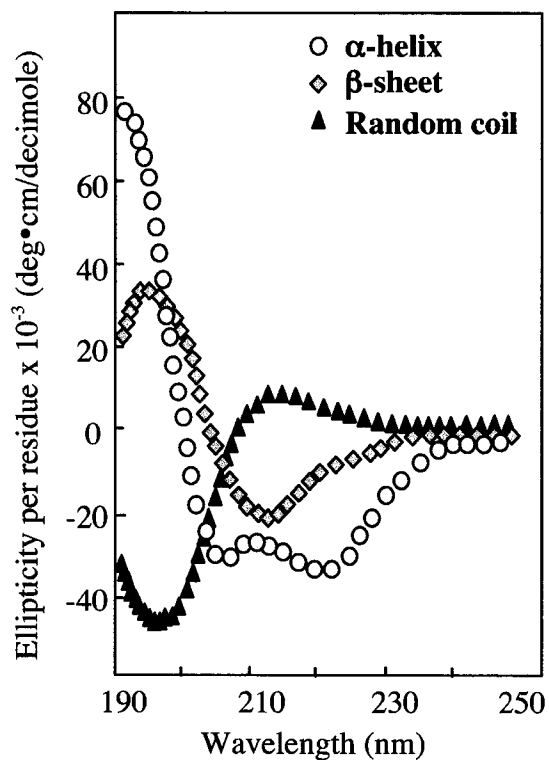
#### **2.4.2: Circular Dichroism of CbnB2P**

To date, structural investigations of class II nonlantibiotic bacteriocins (one- or two-component) having 48 amino acids or fewer by circular dichroism (CD) studies,<sup>131</sup> computer simulations and NMR solution structure elucidation<sup>43,109,110,132,133</sup> indicate that they generally lack a defined structure in aqueous environments.

However, partly helical structures are adopted in more hydrophobic environments such as trifluoroethanol (TFE), dodecyl phosphocholine micelles (DPC) and liposomes.<sup>29</sup> CD studies of CbnB2P in the absence of organic solvent and in the presence of varying concentrations of MeOH and TFE suggest the peptide's compliance with this statement (Figure 14). The best inducement of structure occurs with 60% TFE.

**Figure 14: A.** CD spectrum of CbnB2P (0-60% TFE)

**B.** Characteristic shape and magnitude of protein secondary structural motifs by circular dichroism.



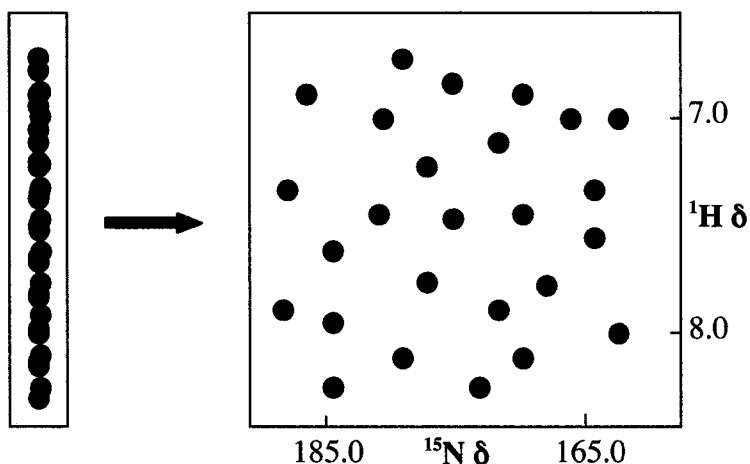
## 2.5: Isotopic Labelling of Proteins

Homonuclear  $^1\text{H}$  NMR spectra of small rigid proteins (<10 kDa, ~ 80 amino acids) can sometimes allow most NOE's and  $^3\text{J}$  couplings to be measured and the residues identified. However, for larger proteins the number of protons present scales approximately linearly with molecular mass, as do the rotational correlation times and thus the linewidths of the NMR resonances.<sup>134</sup> This results in extensive chemical shift overlap and degeneracy. Smaller peptides can also present resonance assignment difficulties if they are flexible and contain identical residues at multiple sites. Heteronuclear NMR spectroscopy can circumvent these problems by accessing multi-dimensional NMR experiments that utilize  $^{13}\text{C}$  and  $^{15}\text{N}$  uniformly labelled proteins. Spectral resolution is improved by increasing the dimensionality of the NMR spectrum so that the highly overlapped  $^1\text{H}$  resonances are separated in 3D and 4D spectra according to the better-resolved heteronuclear resonances. The efficiency<sup>134</sup> of coherence transfer is increased by utilizing relatively large one- and two-bond ( $^1J$  and  $^2J$ ) scalar coupling interactions between pairs of heteronuclei and between heteronuclei and their directly attached protons, instead of the relatively small  $^1\text{H}$  homonuclear three-bond scalar coupling interactions.

Many multi-dimensional heteronuclear NMR experiments correlate a heteronuclear resonance with a proton resonance by transfer of polarization between the heteronuclear ( $S$ ) and proton ( $I$ ) spins.<sup>134</sup> The NMR experiment can start with excitation of either  $I$  or  $S$  spin polarization and ends with detection of either  $I$  or  $S$  spin magnetization. The overall sensitivity of heteronuclear correlation NMR experiments is

proportional to the gyromagnetic ratios of each nucleus. Therefore indirect or proton detection is used whenever possible in order to maximize sensitivity. The gain in sensitivity for  $^1\text{H}$ - $^{13}\text{C}$  correlations is approximately 24 for methyl protons, 16 for methylene protons, and 8 for methine protons, whereas for  $^1\text{H}$ - $^{15}\text{N}$  correlations of backbone amides the gain is about 30.<sup>134</sup>

One of the most common experiments performed in  $^{15}\text{N}$ - $^1\text{H}$  hetero-correlation is an HSQC<sup>135-138</sup> (heteronuclear single quantum coherence), which uses  $^1\text{H}$  for detection. The HSQC experiment, based on the INEPT (insensitive nuclei enhanced by polarization transfer) pulse sequence, is an integral component of virtually all heteronuclear 3D and 4D experiments. The experiment starts with excitation of the proton, then polarization transfer to nitrogen and spin manipulation, followed by magnetization transfer back to the proton for detection. This experiment spreads out the signals using the chemical shift range of  $^{15}\text{N}$  (Figure 15) and is ideal for measuring amide exchange rates or assisting in spin system identification. Good dispersion of signal in the nitrogen plane usually indicates that a three-dimensional structural solution of a protein is feasible. Identification of the peaks within the  $^{15}\text{N}$ -HSQC can act as a reference (book-keeping device) by providing a way to correlate residues in other experiments. This is very helpful for facile identification of spin systems when the correlations are spread into a 3<sup>rd</sup> dimension, e.g.  $^{13}\text{C}$ , wherein only a few signals may be present at a particular carbon chemical shift.

**Figure 15:** Dispersion of signals in  $^{15}\text{N}$  HSQC.

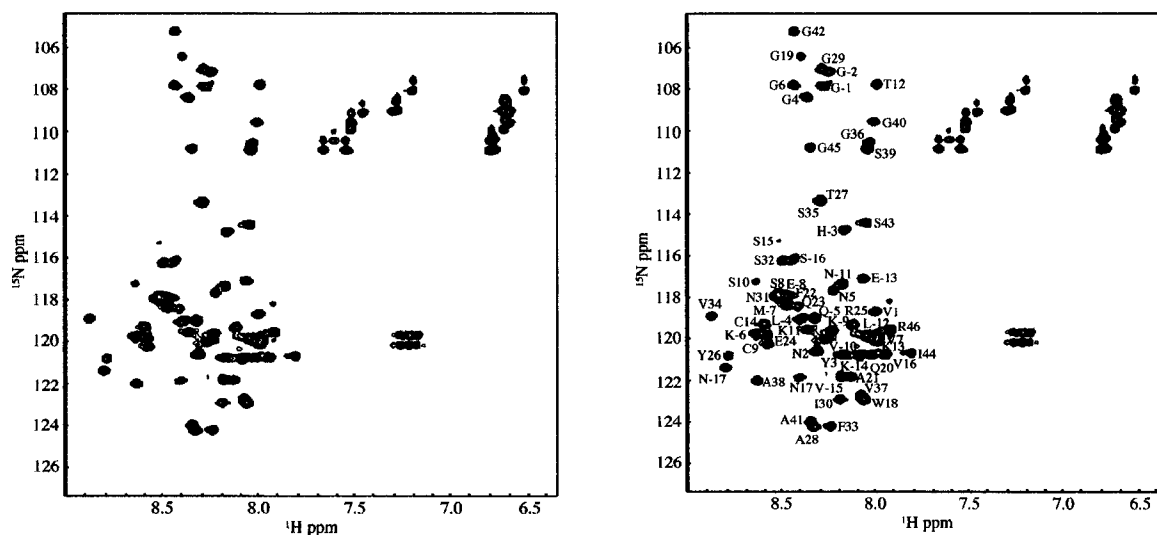
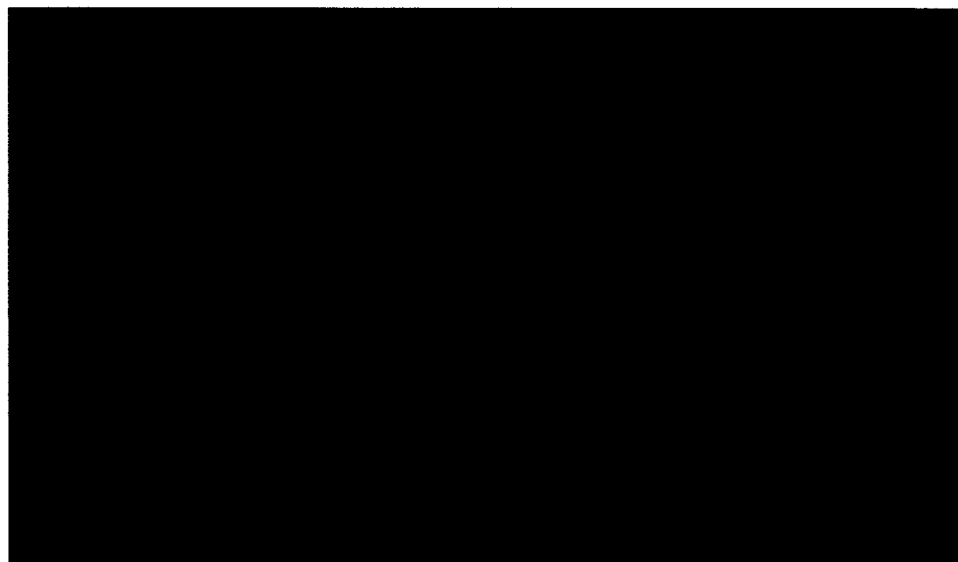
## 2.6: NMR of CbnB2P and CbiB2

Nitrogen and proton assignments for the CbnB2P(1-64) amino acid precursor peptide, CbnB2P, and the 111 amino acid immunity protein, CbiB2, were performed by Dr. Tara Sprules of our group using standard NMR experiments (see 3.6, Table 6). Shown below (Figures 16 and 18) are the  $^{15}\text{N}$  HSQC spectra delineating good dispersion of signals in the nitrogen plane. It has been shown that  $^1\text{H}$  NMR shifts are strongly correlated to the character and nature of the secondary structure in proteins.<sup>139</sup> Particularly,  $\alpha$ - $^1\text{H}$  chemical shifts experience an upfield shift when corresponding amino acids are in a helical configuration and a comparable downfield shift when the residues are in a  $\beta$ -strand or extended configuration with respect to the random coil value.<sup>110,139-141</sup> The solution structure of mature CbnB2 (48 amino acids) was previously determined<sup>110</sup> and shown to have a well-defined central helical structure (residues 18-39, mature

peptide) possessing amphipathic character, while the C- and N-termini exhibit random coil structure. Figure 17 is a backbone rendering of the three-dimensional structure of CbnB2P(1-64), based on NMR data, which shows the mature and leader portions of the precursor peptide. As expected, structural elements found in the mature CbnB2 are also present in the corresponding CbnB2P(1-64). There is an  $\alpha$ -helix in the leader peptide from -14 to -4 in the leader portion and no contacts can be detected between the leader peptide and the C-terminal helix. As noted by Ennahar *et al*, sequence similarity is particularly high for leaders of the same size, and charges and hydrophobicity of individual amino acid residues have been conserved in the corresponding positions (Table 4).<sup>24</sup> Further studies elucidating the structural elements of bacteriocin leader peptides will determine if an  $\alpha$ -helical element is conserved and essential for recognition by ABC-transporter and accessory proteins.

**Table 4:** Sequence alignment of leader peptides (containing 18 amino acids) for class IIa bacteriocins based on the C-terminal double-glycine motif.

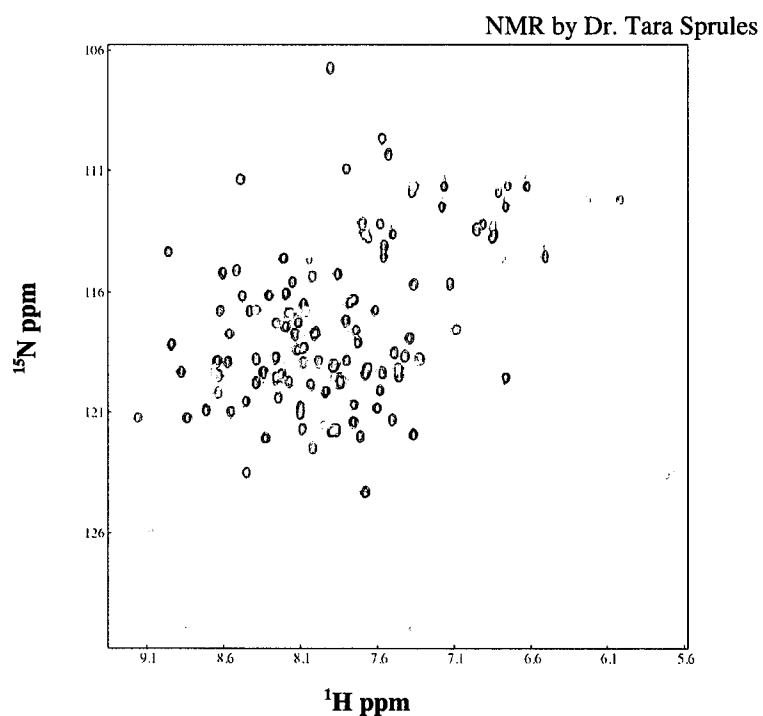
Bacteriocin	Leader Sequence	Reference
Sakacin A/curvacin A	<b>MNNVKELSMTELQTITGG</b>	[83]
Carnobacteriocin BM1	<b>MKSVKELNKKEMQQIIGG</b>	[200]
Carnobacteriocin B2	<b>MNSVKELNVKEMKQLHGG</b>	[200]
Sakacin	<b>MEFIELSLKEVTAITGG</b>	[49]
Enterocin A	<b>MKHLKILSIKETQLIYGG</b>	[85]
Pediocin AcH/PA-1	<b>MKKIEKLTEKEMANIIGG</b>	[79,80]

**Figure 16:**  $^{15}\text{N}$  HSQC of CbnB2P(1-64) (with and without the amino acid labels)**Figure 17:** Graphical representation of 3D structure of CbnB2P(1-64)

NMR, Structure Calculation and Graphical Representation by Dr. Tara Sprules

Studies on CbiB2 are at the initial stages of investigation. The immunity protein has proven to be intractable with respect to solubilization, thereby resulting in a very low concentration of sample (<0.1 mM) for possible NMR studies. The purification procedures following factor Xa cleavage may require revision. Currently lyophilization of the cleaved peptide causes the peptide to become insoluble and further investigation is ongoing as to whether the difficulty is intrinsic.

**Figure 18:**  $^{15}\text{N}$  HSQC of CbiB2 (initial data only)

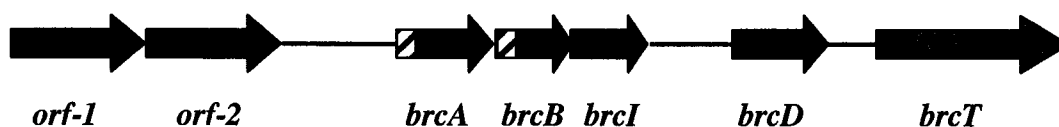


## **B: Brochocin C (BrcC) of *Brochothrix campestris***

### **2.7: Primary Structure, Production and Regulation of Brochocin C**

Brochocin C (BrcC) is a chromosomally encoded, heat-stable, two-peptide nonlantibiotic class IIb bacteriocin produced by *Brochothrix campestris* ATCC 43754. It was originally discovered by Siragusa and Cutter<sup>142</sup> with subsequent biochemical and genetic characterization by McCormick *et al.*<sup>75</sup> The BrcC operon is comprised of five ORFs (Figure 19). There are two structural genes, *brcA* and *brcB*; an immunity gene, *brcI*; and genes that encode proteins possessing homology to ATP-transporter and accessory proteins, *brcT* and *brcD* (Figure19). The *brcI* gene, which is found downstream and overlaps the *brcB* gene, encodes for a 53-amino acid peptide *sans* a double glycine leader peptide. In *Brochothrix campestris* both peptides are ribosomally synthesized as prepeptides, and the mature peptides BrcA (59-amino acid peptide, 5245 Da) and BrcB (43-amino acid peptide, 3945 Da) are revealed following cleavage of the N-terminal leader peptide after the Gly-Gly cleavage site. The DNA nucleotide and amino acid sequence is shown in Figure 20.

**Figure 19:** Genetic organization of the Brochocin-C operon

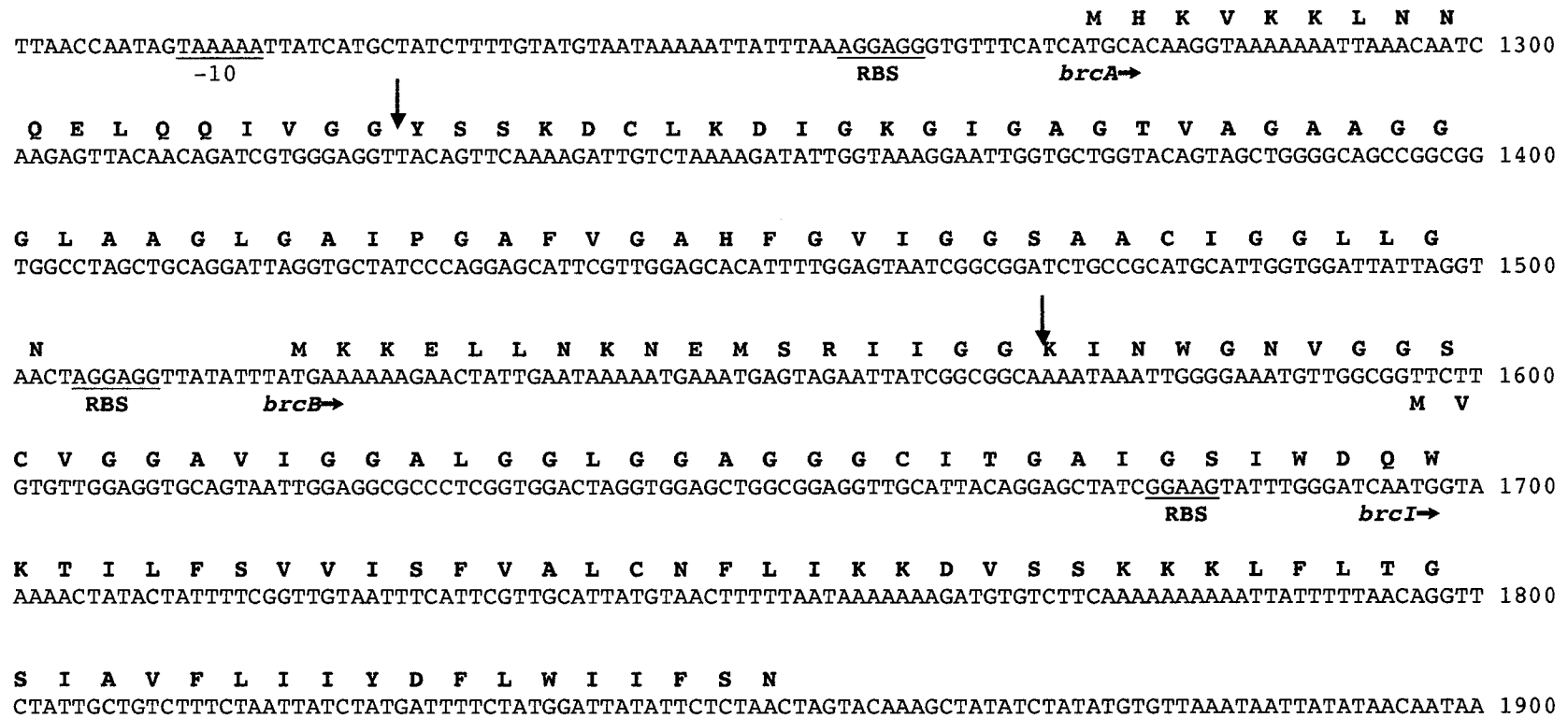


Interestingly brochocin-C possesses a broad activity spectrum<sup>M</sup> that compares favorably to that of nisin, including action against bacterial endospores and Gram-negative bacteria when the outer membrane of the cells is compromised.<sup>75,116</sup> Usually the outer membrane of Gram-negative bacteria acts as a barrier and is impenetrable to these antibiotic peptides, thereby typically preventing antimicrobial activity.<sup>143</sup> Although it is generally proposed that the two-peptide bacteriocins form poration complexes, the molecular recognition responsible for the observed synergy is not understood.<sup>36</sup> Related studies on other two-peptide bacteriocins, lactacin F<sup>9</sup> and thermophilin 13,<sup>115</sup> suggest membrane fluidity may influence the action of these antimicrobial peptides.

---

<sup>M</sup> It has been reported to be active versus 35 strains of *B. thermosphacta*, 10 strains of *Listeria monocytogenes*, many strains of *Carnobacterium*, *Enterococcus*, *Kurhtia*, *Lactobacillus*, and *Pediococcus* and spores of *Clostridium* and *Bacillus* species.

**Figure 20.** Single-strand DNA and amino acid sequences for nucleotides 1201-1900 of the *EcoRI* fragment of pAP7.4 containing the structural (*brcA* and *brcB*) and immunity (*brcI*) genes of brochocin C



## 2.8: Subcloning of BrcA and BrcB in Origami™ B(DE3) *E. coli*

Subcloning of BrcA and BrcB was undertaken employing the maltose binding protein system that was described for CbnB2P and CbiB2. Previous cloning experiments were performed for BrcA using the pMAL™-p2X vector (Figure 12).<sup>144</sup> Full expression of the *maltE* gene directs peptides to the periplasm of the host cell. The 'p2X' denotes periplasmic, which means that the fusion protein is directed to the periplasm. For those proteins that can be successfully exported, this allows folding and disulfide bond formation to take place in the periplasm of *E. coli*. Initially, a periplasmic construct was chosen to provide an environment that would facilitate disulfide bond formation with concomitant protein folding.<sup>144</sup> Structure elucidation by multi-dimensional NMR techniques would ideally be done on a mature and conformationally correct peptide so that an accurate representation of its native structure can be determined. However, periplasmic production is typically one-tenth that of cytoplasmic production and purification can be problematic due to larger volumes (400 mL of sucrose solution is needed for a 1 L fermentation). With inherently small yields of protein, the procedure becomes unmanageable and expensive for <sup>13</sup>C and <sup>15</sup>N labelled material required for structural studies. The pMAL™-p2X and pMAL™-c2X vectors are identical except that the -c2X series has an exact deletion of the *maltE*-signal sequence (nt 1531-1605). The 'c2X' denotes that the fusion protein is directed toward the cytoplasm. This allows for increased yields in conjunction with simpler and more productive purification techniques. Both are characterized by a four amino acid recognition sequence [Ile-(Glu or Asp)-Gly-

Arg] for cleavage by factor Xa, thereby allowing separation of the desired peptide from the MBP, without additional vector residues being attached.

A survey of various *E. coli* host strains identified an Origami™ B(DE3) *E. coli* host that permits disulfide bond formation utilizing cytoplasmic constructs. Origami™ B(DE3) *E. coli* host strains are derived from Tuner™ strains, which are *lacZY* mutants of BL21, and possess a unique combination of mutations that facilitate the expression of intact soluble proteins in *E. coli* with 10-fold more antimicrobial activity.<sup>145,146</sup> Mutations in the thioredoxin reductase (*trxB*) and glutathione reductase (*gor*) genes significantly enhance disulfide bond formation in the cytoplasm. Deletion of the *lacY* permease gene allows for adjustments of IPTG induction and consistent expression of target protein throughout all cells in a culture. Therefore construction and transformation of the plasmids pKEK1A and pKEK2B (containing the *brcA* and *brcA* genes, respectively) into competent Origami™ B(DE3) *E. coli* cells was undertaken. The bacterial strain and plasmids and their properties are listed in Table 5. DNA sequencing confirmed that the nucleotide sequences are correct for pKEK1A and pKEK2B. The DNA nucleotide and amino acid sequences for the structural genes *brcA* and *brcB* are depicted in Figure 20.

## 2.9: Pilot Experiments

Pilot experiments were performed using the *E. coli* hosts TB1, BL21(DE3), and Origami B(DE3) for the MBP-fusions plus TB1 and Origami B(DE3) for the Intein fusion. The purpose of these studies is to determine growth patterns and optimize conditions relating to media, time periods, temperature, and IPTG induction concentration.

**Table 5:** Plasmids and producing strains for BrcA and BrcB.

<i>Plasmid and producer strain</i>	<i>Relevant properties<sup>a</sup></i>	<i>Ref. or source</i>
Plasmids		
pMAL <sup>TM</sup> -c2X	Amp <sup>r</sup> , 6648-bp, lacI, lacZ $\alpha$ and malE expression vector	[143-147]
pSG6189	Plasmid containing the brcA gene	[169]
pSG1551	PCR fragment containing the brcB gene	This study
Strains		
Origami <sup>TM</sup> B(DE3)	F <sup>+</sup> ompT hsdS <sub>B</sub> (r <sub>B</sub> <sup>-</sup> m <sub>B</sub> <sup>-</sup> ) gal dcm lacY1 ahpC gor522::Tn10(Tc <sup>R</sup> ) trx::kan (DE3)	

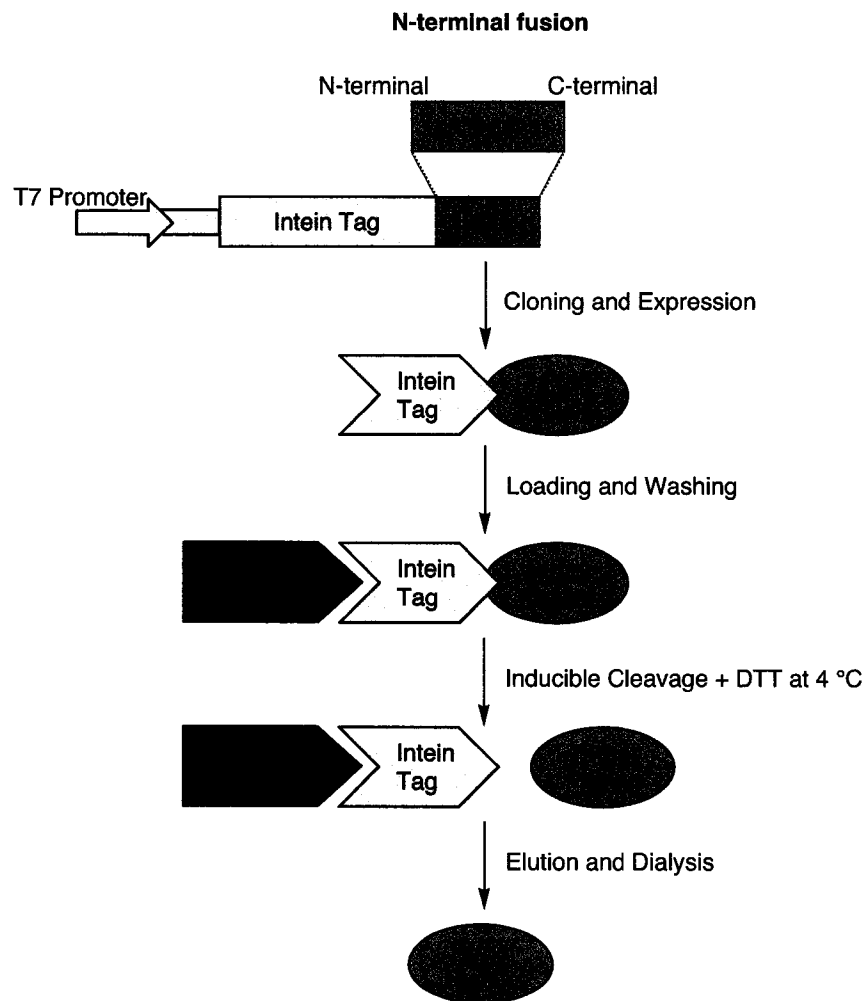
<sup>a</sup> Amp<sup>r</sup>, ampicillin resistant

SDS-PAGE gel electrophoresis (12%) is used to monitor the expression results. The gels indicate that BrcA in TB1 and BL21(DE3) *E. coli* hosts is not produced with LB, SOC or Rich media at 16, 25, 30 or 37 °C, as is also noted for BrcB in TBY1. This suggests that either the peptides are toxic to the cells or that correct folding of the proteins does not occur. BrcA and BrcB MBP-fusion in Origami B(DE3) cells show production of peptide (following induction) with best results of growth at 37 °C and 200 rpm, induction at 0.5 OD<sub>600</sub>, and an IPTG induction concentration of 3 mM followed by 4 h of incubation at 30 °C and 200 rpm. The BrcB Intein fusion shows similar results.

The IMPACT-CN system (Figure 21) uses the self-cleavage activity of a protein-splicing element, the intein, to isolate the target peptide from the affinity tag. The method presents several advantages, including rapid and simple purification of the native peptide without extra vector-derived residues, high affinity of the chitin-binding domain (CBD) to reduce non-specific binding, and easy separation of the desired peptide from the

affinity tag by using inexpensive thiol reagents (*e.g.* 1,4-dithiothreitol,  $\beta$ -mercaptoethanol or cysteine).

**Figure 21.** Schematic representation of the IMPACT-CN system with N-terminus cleavable intein tag



BrcA and BrcB were expressed in *E. coli* as recombinant protein fusions composed of the maltose-binding protein encoded on pMAL-c2X and the 59 and 43 amino acids of mature BrcA and BrcB, respectively. The fusion proteins of both are expressed in, and purified from, the cytoplasm of Origami™ B(DE3) *E. coli* cells. After purification on an amylose column, 103 mg BrcA MBP-fusion and 87 mg BrcB MBP-fusion proteins are recovered per litre of fermentation culture. The MBP-fusion proteins are analyzed by SDS-PAGE gel electrophoresis (12%), indicating that all of the clones produced fusions of the expected sizes.

BrcB was also expressed in *E. coli* as an Intein fusion. Purification on a chitin column with an induction time of 36 h at room temperature yields only a few milligrams of a fragment of BrcB (see below) (Appendix: Figure A.3).

## **2.10: Mass Spectrometry by MALDI-TOF of BrcA and Brc B**

Mass spectrometry results using MALDI show that expressed BrcA and BrcB MBP-fusions lack homogeneity; four peaks are noted with mass values ranging from 43000 to 48000 Da (approximately). There are several possible causes. The choice of host cells may not be optimal and indiscriminant proteolysis at double Gly-Gly<sup>144</sup> sites may be occurring (BrcA: residues 24-25, 47-48, or 54-55; BrcB: residues 8-9, 13-14, 18-19, 22-23 or 28-29-30). Alternately, cell lysis and purification methods may cause cleavage.

MALDI-TOF mass spectra of the BrcB Intein fusion indicate that only a fragment of BrcB, with a mass of 1761.6 Da, is produced. There may be indiscriminant cleavage of the peptide, possibly due to high DTT concentrations.

### **2.11: Conclusions for CbnB2P, CbnB2, BrcA, and BrcB**

Two class IIa bacteriocins, CbnB2P and CbiB2, and one class IIb bacteriocin, BrcC were studied utilizing current strategies for optimization of their biosynthesis and isotopic labelling procedures with  $^{15}\text{N}$  and  $^{13}\text{C}$  in *E. coli*. The long-term objective is to provide material for NMR studies to determine their three-dimensional conformations. Labelling of bacteriocins can be done with wild-type LAB organisms using a multistage procedure.<sup>133</sup> The present methodology could in principle afford much easier access to substantial quantities of labelled peptides; generation of bacteriocins and their precursors is accomplished by utilizing minimal media containing  $^{13}\text{C}$  and/or  $^{15}\text{N}$  compounds or commercially prepared universally labelled media. The expression of CbnB2P, CbiB2, BrcA and BrcB as maltose-binding protein fusions or intein fusions provides mild facile procedures for “fishing out” the proteins of interest, which often cannot be realized in natural hosts. Additionally, variants of these bacteriocins attained by amino acid substitutions preventing their secretion or rendering them toxic to the producer could be expressed and purified as fusions in *E. coli*. In practice, undesired truncation of the target peptide occurs frequently. Loss of the two C-terminal residues from CbnB2P to give CbnB2(1-64) is unlikely to change its overall geometry in NMR studies. However,

formation of heterogeneous mixtures during BrcA and BrcB expression indicates that such systems can be problematic.

One of the most challenging issues in bacteriocin research is determining the structure-function relationship and the regulatory mechanisms involved. Three-dimensional structure elucidation of cognate precursor, mature and immunity bacteriocins may help to establish a relationship between them. NMR studies of CbnB2P(1-64) have shown that the leader peptide possesses an  $\alpha$ -helical secondary structural motif, in addition to the  $\alpha$ -helix present in the mature bacteriocin.<sup>110</sup> NMR studies of CbiB2 are still in progress and hopefully will add to the repertoire of data on immunity proteins of bacteriocins.<sup>80,82,147</sup> Structural comparisons of immunity proteins may help elucidate the mechanism of how immunity is imparted to the producer organism and the relationship, if any, to the mature peptides.

Even though the antimicrobial spectra of LAB bacteriocins is limited, they show considerable promise because they are nontoxic to mammals (many occur naturally on food) and are much more potent than conventional antibiotics. The hypothesis that the extracellular loop of the D-subunit of EII<sub>t</sub><sup>MAN</sup> is the target of type IIa bacteriocins may eventually allow design of new antimicrobial agents with improved activity for pharmaceutical and commercial food applications.

## CHAPTER 3: *Bacillus subtilis* & Subtilosin A

### RESULTS AND DISCUSSION

#### 3.1: Overview

##### 3.1.1: The Genus *Bacillus*

The genus *Bacillus* has long been of interest to researchers and can be traced back to Louis Pasteur, who used heat-attenuated *Bacillus anthracis* to generate the first antibacterial vaccine,<sup>148</sup> and Robert Koch who used anthrax as the test case for development of postulates relating infectious agents and specific diseases.<sup>148</sup> By the mid-20th century *Bacillus* was known more generally for its role in human, animal, and insect infections and was valued as a producer of important antibiotics, proteases, and other useful products.<sup>148,149</sup>

##### 3.1.2: *Bacillus subtilis*

*Bacillus subtilis* is a spore-forming, nonpathogenic soil bacterium that is capable of growth under aerobic and anaerobic<sup>150</sup> conditions on a variety of substrates and is a common component of traditional fermented foods, particularly in Asian and African foods.<sup>151,152</sup> *B. subtilis* has been intensively studied, second only to *E. coli*, and the cornucopia of information about this bacterium has made it the principal paradigm for analysis of Gram-positive bacteria.<sup>148</sup> Usage as an experimental system for studying mechanisms of gene regulation, metabolism, differentiation and useful application of bacterial products can be traced to three critical lines of investigation.<sup>148</sup> Burkholder and Giles<sup>153</sup> investigated a number of auxotrophic mutants, which became the cornerstone for

biochemical-genetic analysis of aromatic amino acid biosynthesis (as well as other pathways) and became tools for detailed mechanistic studies of recombination. Spizizen<sup>154</sup> and coworkers established conditions for optimizing the efficiency of transformation of *B. subtilis* by chromosomal DNA; their method is still used in virtually all *B. subtilis* labs. The groups of Schaeffer,<sup>155</sup> Mandelstam,<sup>148</sup> Ryter and Fitz-James<sup>156</sup> explored sporulation-related morphological changes and correlated particular mutations with blockages at specific stages in spore development.

The genome for *B. subtilis* has been fully sequenced and is carried on a single chromosome of 4215 kb.<sup>157-159</sup> The availability of the entire *B. subtilis* genome sequence has changed the approach to investigations, and as more bacterial genomes are completed, it has become easier to deduce the function of any given gene.<sup>148</sup> Once isolated, each gene function can be tentatively identified by determining its N-terminal sequence and comparing that sequence with those of all the gene products that the organism is predicted to encode. However more knowledge often begets more questions, such as, what are the mechanisms that regulate genes expression and protein activity.

### **3.1.3: An Antimicrobial Peptide Produced by *Bacillus subtilis*: Subtilosin A (1A)**

Subtilosin A (Sub A, **1A**) is a bacteriocin produced by the Gram-positive spore-forming bacterium *Bacillus subtilis* JH642 and is a highly post-translationally modified ribosomally-generated peptide. Sub A, from *B. subtilis* 168, was first isolated in Japan by Babasaki *et al.*<sup>160</sup> The antibiotic was obtained from a Chinese fermented soybean seasoning culture, but since production of the seasoning does not require the use of *B. subtilis*, the isolate was probably carried by soybean from the soil.<sup>161</sup> *B. subtilis* is well

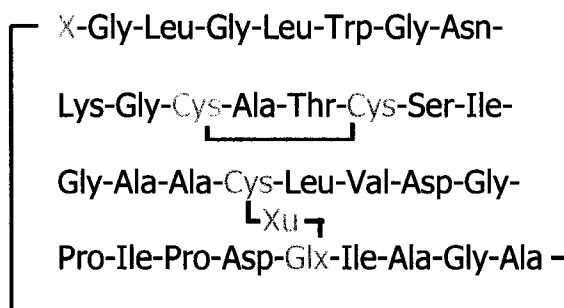
characterized, genetically and biochemically, and has been the subject of sporulation studies of bacterial cells.<sup>155,162-164</sup> Correlation between antibiotic production and sporulation in *B. subtilis* strains or other species of bacilli had also been studied.<sup>165</sup> Results indicated that in some cases there are antibiotics which favor sporulation, but in others a direct cause-and-effect relationship could not be demonstrated. It was determined that the antibiotic, Sub A (1A), has no effect on the sporulation of *B. subtilis* 168 (wild strain) or JH642 (standard genetic strain).<sup>160</sup> Sub A production time courses, with respect to cell growth and spore formation, demonstrate that antibiotic synthesis begins 1 h after vegetative growth ceases, increases linearly with time for 2 h and reaches a plateau, followed by a gradual decrease.<sup>160</sup> However, spores do not appear until 8 h after vegetative growth ceases at which time Sub A production has ended.<sup>160</sup> Maximal concentration of the antibiotic occurs at approximately 7 h subsequent to inoculation and yields 12-15 mg/L Sub A in nutrient sporulation media (NSM).<sup>166</sup>

Subtilosin A is synthesized as a precursor, comprised of 43 amino acids, including an unusually short<sup>152</sup> (with respect to other bacteriocins) eight-member leader peptide (Figure 22). The mature peptide is revealed upon cleavage between Asn 1 and Glu -1, unlike Class II bacteriocins where cleavage often occurs after a double Gly-Gly motif.

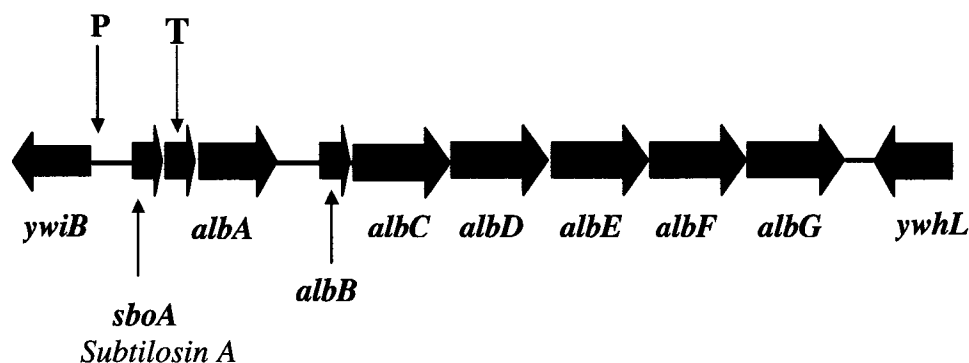
**Figure 22:** Amino Acid Sequence of Presubtilosin A and the Cleavage Position

Sub A is considered to be a bacteriocin and is active against *Listeria*, like class II bacteriocins. Unlike class IIa bacteriocins, Sub A has extensive post-translational modifications. These include an amide bond between the N-terminal Asn and the C-terminal Gly, in addition to three bridges involving the three cysteines. The mature peptide is highly resistant to enzymatic proteolysis (for example, pepsin) and is stable to moderate heat and mild acid conditions. Complete sequence analysis by Edman degradation or by mass spectral examination of Sub A or fragments generated by partial acid hydrolysis was unsuccessful.<sup>160</sup>

The first reported attempts to sequence the peptide and determine the nature of its post-translational modifications were unsuccessful in obtaining the correct amino acid sequence and structure.<sup>160</sup> Initially, Babasaki<sup>160</sup> and coworkers suggested that the amino- and carboxyl- termini were blocked and that cross-links were present within the molecule containing some non-amino acid constituents. They reported that only 32 amino acids were present (Figure 23).

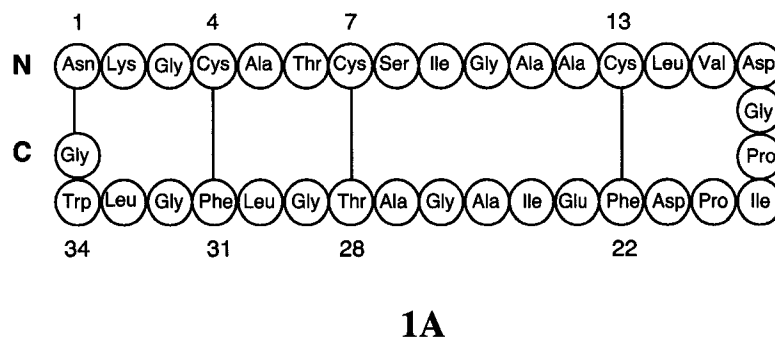
**Figure 23:** Cyclic and bridging connectivity proposed by Babasaki<sup>160</sup>

The flaws in this structural assignment became apparent when Zuber and coworkers analyzed the *sbo-alb* operon, in particular the *sbo* structural gene. This operon is composed of eight genes, *sboA* (the structural gene) and *albABCDEFG* which are responsible for production (*albA* and *albF*), immunity (*albB*) and post-translational modifications (Figure 24).<sup>176</sup> Zheng has shown that a mutation in *abrB* suppresses production of Sub A, which indicates that AbrB exerts negative control of antibiotic production and resistance.<sup>167</sup> Once biosynthesis is initiated positive regulation may occur from some gene products.<sup>167</sup> Identification of the genetic locus (Figure 24) for subtilosin production allowed for prediction of the correct amino acid sequence (Figure 25).<sup>161</sup> However, the monoisotopic mass (MALDI-TOF) of isolated subtilosin A (1A) is  $3401.2 \pm 0.5$  Da, and differs from the calculated mass, 3426 Da, by 24-25 units. This is consistent with the loss of water during cyclization of the N and C termini, plus the loss of six hydrogens.

**Figure 24:** Genetic locus for production of subtilosin A (1A)

Although two phenylalanine and two threonine residues are encoded by the genetic sequence, only one threonine and no phenylalanines were found by amino acid analysis of purified subtilosin.<sup>160</sup> Apprised of the correct genetic sequence, Marx *et al*,<sup>168</sup> proposed that linkages could exist between the cysteine residues at positions 4, 7 and 13 and Phe31, Thr28 and Phe22, respectively, which corresponds to the loss of hydrogen from each of these six residues. However, though they included these residue proximities in a NMR solution structure, the exact connectivity remained ambiguous, with bonds between sulfur and the aromatic rings or  $\beta$ -carbons of Phe22 and Phe31, as well as between sulfur and the  $\beta$ -carbon of Thr28 being proposed (Figure 25). Since the cross-links could not be determined, their proposed 3D structures<sup>168</sup> are inaccurate. In order to determine the precise positions of the cysteine sulfur-phenylalanine and sulfur-threonine bonds, NMR studies on <sup>13</sup>C, <sup>15</sup>N labelled subtilosin A **1B** were undertaken.

**Figure 25:** Amino acid sequence of subtilosin A (1A) The positions of the post-translationally formed linkages are indicated by solid lines.



**1A**

### 3.2: Isolation and Purification of Subtilosin A (1A)

#### 3.2.1: *Bacillus subtilis* JH642

Isolated colonies of *B. subtilis* JH642 produced by inoculation of Difco sporulation media (DSM) hard agar plates are ivory colored with slightly anomalous edges. The pale yellow yeast extract (YT) and Lauria Bertani (LB) tubes provide good growth. However, if over-incubation occurs a pinkish tinge is exhibited in the media, which signals over-growth, and is deleterious to maximal Sub A production. Subsequent to growth in NSM media, Sub A is isolated by extraction with *n*-butanol. This protocol for isolation is possible since the antibiotic is secreted across the cytoplasmic membrane to the supernatant, presumably via membrane associated ATP-dependent efflux protein complexes.<sup>73,169</sup> Following *n*-butanol removal *in vacuo* and resuspension in MeOH, Sub A is purified by RP-HPLC where elution of the peptide occurs at 28-30 min corresponding

to 56% CH<sub>3</sub>CN. Pursuant to lyophilization, Sub A affords a velvety ivory-white powder and yields 12-15 mg/L Sub A in NSM media.

### 3.2.2: *Bacillus subtilis* SMY

The same methodology for isolation and production is used for *B. subtilis* SMY strain as for JH642 strain. The essential differences exist in that the SMY strain is prototrophic versus auxotrophic and that a minimal media is employed versus a complex media, thereby providing decreased concentrations of Sub A with yields of 1-2 mg/L. Initially it was hoped that the SMY strain would be useful for production of labelled Sub A. The low production precluded its use for NMR investigation as the expense for <sup>13</sup>C, <sup>15</sup>N labelling would be prohibitive.

### 3.2.3: Antimicrobial Activity

Bacteriocin production is evaluated utilizing the spot-on-lawn test using the indicator organism, *Listeria monocytogenes* LI0502. BHI (Brain Heart Infusion) agar is employed for determining activity using absorbance units (AU). The zones of inhibition, clearing of the indicator organism, correspond to serial two-fold dilutions. The typical AU for Sub A are 400 to 500 AU corresponding to 12 to 15 mg/L of Sub A. Activity tests were also performed using uncyclized-Sub A (see below) at asparagine 1 and glycine 35, but with the sulfur bridges still intact, and show approximately one third less activity. Fully desulfurized Sub A gives no zones of inhibition. These results indicate that the post-translational modifications involving the sulfur linkages are of prime importance for antibacterial activity.

### 3.2.4: Mass Spectrum

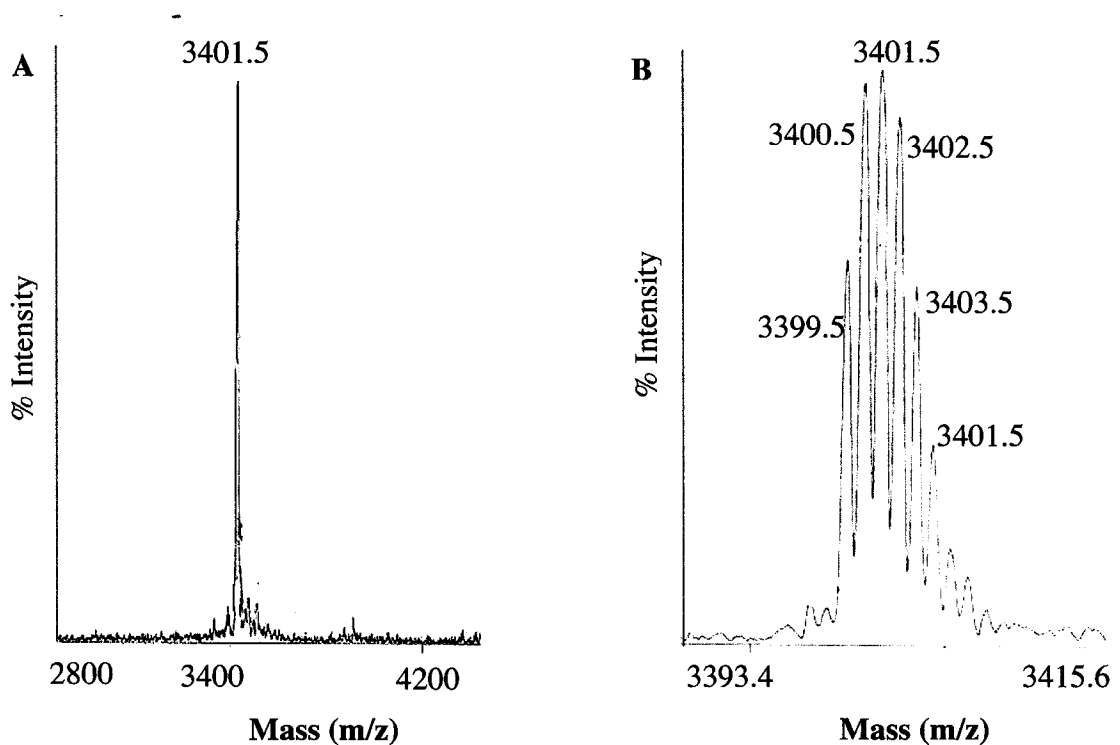
The average mass of  $3401.2 \pm 0.5$  Da was determined by MALDI-TOF mass spectrometry using sinapinic acid as a matrix (Figure 26 A). This differs from the calculated mass of 3426 Da by 24-25 units, which is consistent with the loss of water during cyclization of the N and C termini, in addition to the loss of six hydrogens. The two layers, methanolic-acidic Sub A and sinapinic acid, provide excellent conditions for mass spectral analysis of the peptide. Also shown is an expansion of the molecular ion region denoting the isotope pattern for the molecular ion seen within the pure sample (Figure 26 B).

### 3.3: $^{15}\text{N}$ and $^{13}\text{C}$ Labelling of Subtilosin A (1B)

The solution structure of peptides and proteins often rely on NMR studies of isotopically labelled material to overcome overlap problems of  $^1\text{H}$  resonances in 2D homonuclear experiments and allow spectral assignment by heteronuclear multidimensional correlation methodologies (e.g., HMQC, HMBC, HNCQ, HNCA, etc. see Table 6) However, the required universally  $^{15}\text{N}$  and  $^{13}\text{C}$  isotopically substituted proteins can be difficult and expensive to acquire. The expense of labelled  $^{15}\text{N}$ ,  $^{13}\text{C}$  amino acids and U- $^{13}\text{C}$  glucose commonly used as precursors in fermentations can be prohibitive. In addition, many biological systems fail to produce the desired metabolites on simple defined media, as for the *B. subtilis* SMY strain. Media generated from cyanobacteria (blue-green algae) provide a plausible solution to this problem because they are capable of *de novo* synthesis of all required amino acids from minimal media

utilizing inexpensive [ $^{13}\text{C}$ ] bicarbonate and sodium [ $^{15}\text{N}$ ] nitrate as sole carbon and nitrogen sources, respectively.<sup>133</sup>

**Figure 26:** MALDI-TOF mass spectrometry of unlabelled Sub A. **A:** The average mass of pure Sub A  $[\text{M}+\text{H}]^+$  ion. **B:** Expansion of the molecular ion region showing the isotope pattern for the molecular ion.



The algae specifically employed in these experiments was *Anabaena* ATCC 27899. Alternatively, cloning and overexpression of the structural and processing genes in *Escherichia coli*, which is capable of growth on  $^{15}\text{N}$  ammonium salts (sulfate or chloride) and/or U- $^{13}\text{C}$  glucose, could also provide universal labelling. This can be different if the

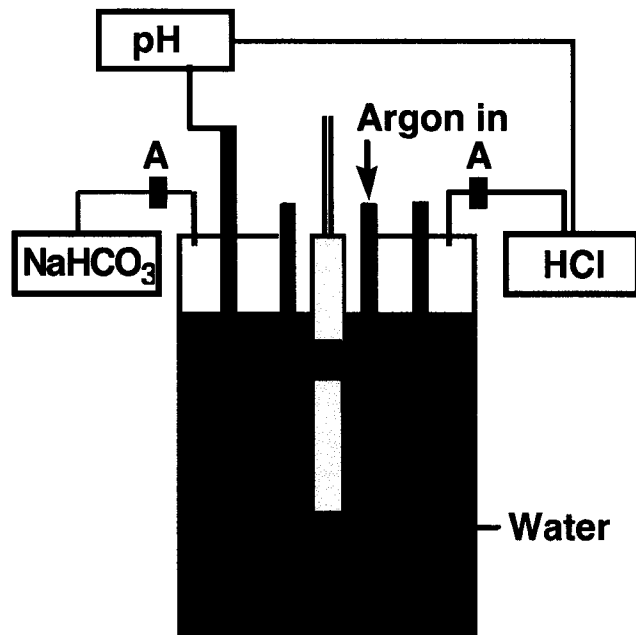
desired protein or peptide structure undergoes extensive post-translational modifications (amidation, glycosylation, isoprenylation, etc.) as a great deal of genetic manipulation becomes necessary. Therefore complex labelled media derived from hydrolysates (peptones) of yeasts or cyanobacterial cells grown on simple isotope-bearing precursors provides an attractive alternative. When this project was initiated, commercially available hydrolysates were available, but these often failed to support growth of organisms or production of specific metabolites, perhaps due to a loss of essential components such as labile amino acids and vitamins during acid hydrolysis. The approach developed earlier in our laboratory relies on milder enzymatic hydrolysis to generate the peptone.<sup>133</sup>

### 3.3.1: Production and Analysis of Labelled Peptone<sup>133</sup>

Production of peptone from *Anabaena* sp. is relatively easily achieved, but attention to fermentation conditions and careful monitoring during the growth period enhances the yield of cells and the level of isotopic incorporation (Figure 27). The typical growth period for the entire process is approximately one month, with the large-scale fermentation lasting 12 days (Figure 28).<sup>133</sup> Typical yields of dry *Anabaena* cells are 0.8-1.1 g/L of fermentation medium. The cells are extracted with ethyl acetate, utilizing a Soxhlet extractor, which removes lipids and pigments, thereby improving final peptone product quality. Following enzymatic digestion with commercially available pepsin and chymopapain, the typical yield is approximately 0.65 g soluble peptone from 1.0 g of dry cells prior to extraction. Utilization of the peptone as a feasible nutrient source depends on the nitrogen to carbon weight ratio. Elemental analyses of the peptone gave C, 36.7;

N, 10.2; H, 5.0 providing a N:C ratio of 0.28 which is comparable to other complex media commonly employed as amino acid sources for bacterial growth

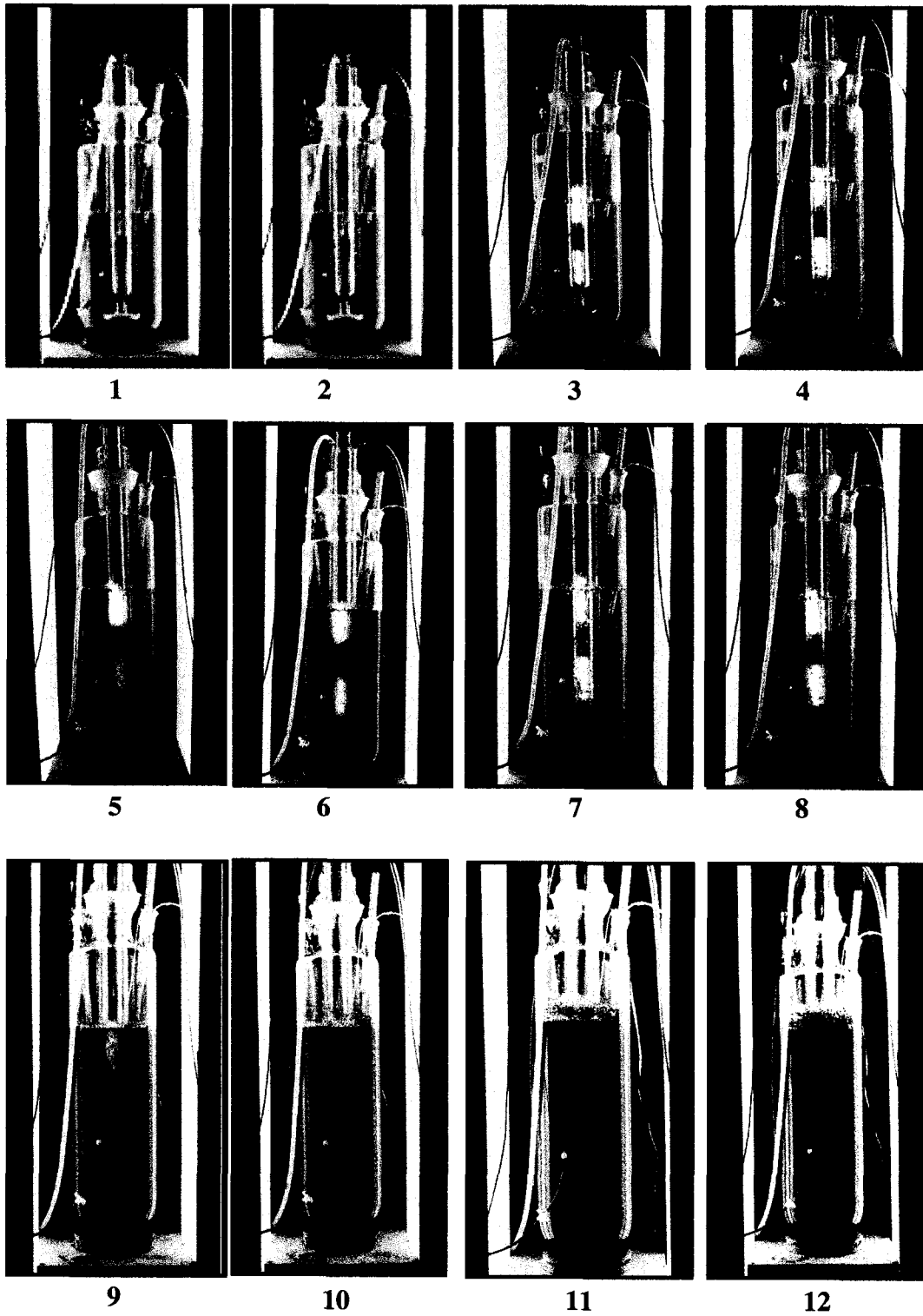
**Figure 27:** Apparatus for *Anabaena* sp. fermentation. A. Sterile filters for inlets of solutions and gases; B. pH probe; C. Filament light tubes to provide light for photosynthesis in addition to banks of fluorescent lights surrounding the vessel (not shown); D. 2 N HCl addition by a peristaltic pump.



(e.g. meat extract N:C 0.32; bactopeptone N:C 0.35; yeast extract N:C 0.27).<sup>133</sup> Sulfur content <sup>133</sup> (0.9–1.2 %) is approximately twice that of commercial peptones, which is an advantage when culturing peptides or proteins with high sulfur content, such as lantibiotics. Sailer *et al*, following complete acid hydrolysis, also determined the amino

acid composition of the *Anabaena* peptone.<sup>133</sup> Isotopic labelling levels were determined by combustion of small samples of peptone employing elemental (CHN) analysis equipment coupled with atomic emission determination of  $^{12}\text{C}/^{13}\text{C}$  and  $^{14}\text{N}/^{15}\text{N}$  ratios in the resulting gaseous products. Typical isotopic labelling using the protocol described below were 85-98%  $^{13}\text{C}$  and 77-95%  $^{15}\text{N}$ . Variation of labelling levels is a result of different quantities of precultures utilized in initiating the *Anabaena* fermentation. Isotopic purities of peptone close to that of the administered precursors,  $\text{NaH}^{13}\text{CO}_3$  (99%) and  $\text{Na}^{15}\text{NO}_3$  (99%), can be achieved if precultures are centrifuged and only the algal mass is added to the fermentation vessel.

Figure 28: The twelve days of *Anabaena*



### 3.3.2: Production of Universally Labelled Subtilosin A (1B)

A total of 21 g of labelled peptone media generated from 32 L (4 x 8 L) of blue-green algae (*Anabaena* sp. ATCC 27899) was used to prepare universally [<sup>13</sup>C, <sup>15</sup>N]-labelled Sub A. Magnesium and potassium ions are added in the form of MgSO<sub>4</sub>•H<sub>2</sub>O and KCl, respectively. Since the media requires autoclaving, and many vitamins are destroyed by heating, one half of a Quest™ “Once-A-Day” vitamin was added. From 800 mL of labelled media a yield of 5 mg of labelled subtilosin A **1B** can be attained. The molecular mass as determined by MALDI-TOF mass spectrometry (as above) is 3567 ± 0.5 Da, which is consistent with greater than 85% [<sup>13</sup>C, <sup>15</sup>N] labelling efficiency (See Appendix: Figure A.2).

### 3.4: Chemical and Enzymatic Studies of Subtilosin A (1A)

#### 3.4.1: Mild Acid Hydrolysis of Subtilosin A to Uncyclized-Subtilosin A

Sub A was submitted to mild acid hydrolysis<sup>170,171</sup> utilizing 0.25 N acetic acid. Mass spectrometry analysis using MALDI-TOF gave a mass of 3420.2 Da, which corresponds to addition of the elements of H<sub>2</sub>O to afford the uncyclized- Sub A, but with the bridges still intact. Activity tests were performed on the uncyclized-Sub A (see 3.2.3).

#### 3.4.2: Solubility

Investigation of subtilosin A's (**1A**) solubility confirmed previous studies.<sup>160</sup> It is a hydrophobic peptide as noted by its elution at 56-58% acetonitrile in 0.1% TFA on a RP-HPLC (C<sub>18</sub> column). Sub A is soluble in MeOH, glacial CH<sub>3</sub>COOH, EtOH, *i*-PrOH, 1 N HCl and DMSO. It is partially soluble in acetonitrile but insoluble in non-polar organic

solvents such as ether and hexane. Although it is soluble in alkaline solutions, it gradually decomposes even in mild base, for example 0.1 M  $\text{NH}_4\text{HCO}_3$  containing 10 mM  $\text{CaCl}_2$ .

### 3.4.3: Crystallization Studies

Several attempts at crystallization of Sub employing various methodologies were undertaken. Water was added to dissolved samples of Sub A dissolved in EtOH, MeOH, IPA, and IPA-MeOH. Since Sub A is hydrophobic and insoluble in water, it was hoped that crystals of Sub A would form during the slow evaporation of the volatile organic solvent. Tubes containing Sub A solubilized in MeOH, EtOH and MeOH/ $\text{CH}_3\text{CN}$  were placed inside jars containing  $\text{H}_2\text{O}$  or  $\text{H}_2\text{O}/\text{CH}_3\text{CN}$ . As this *slowly* increases the concentration of water in the organic phase, it was hoped that crystals of peptide would form. Constricted sealed Pasteur pipettes containing water in the bottom portion and Sub A in the upper portion dissolved in MeOH, EtOH and IPA were also tried. This method relies on the *slow* exchange of solvents at the water-organic interface, thereby potentially causing crystals to form at the interface. NMR tubes containing Sub A and MeOH, EtOH and IPA were overlaid with double the volume of  $\text{CH}_3\text{CN}$ . Since Sub A is not fully soluble in  $\text{CH}_3\text{CN}$  this method could cause crystal formation. However, no attempts resulted in the desired crystal formation. All crystallization attempts gave a fine powdery residue of Sub A on the glass surfaces, which was not suitable for x-ray crystallography. No crystal structures of bacteriocins have been reported in the literature.

### 3.4.4: Digestion of Sub A with Immobilized Pepsin

Sub A was subjected to a 40% methanol-water solution to try and produce Sub A fragments that would be suitable for desulfurization and derivatization (see below) or for sequencing by Edman degradation. All attempts at enzymatic digestion were unsuccessful as indicated by MALDI-TOF mass spectral data. Each sample gave mass values of approximately 3402 Da, which corresponds to intact Sub A. Pepsin cleaves proteins preferentially at carboxylic groups of aromatic amino acids such as phenylalanine and tyrosine. This suggests that the phenylalanines are inaccessible to the pepsin.

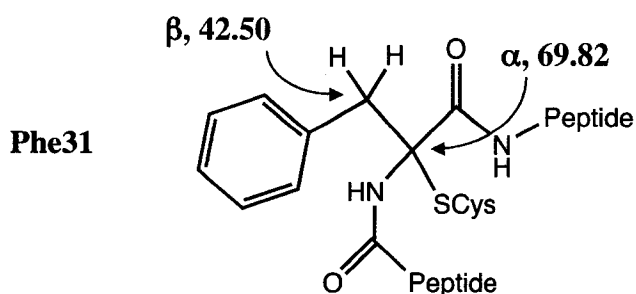
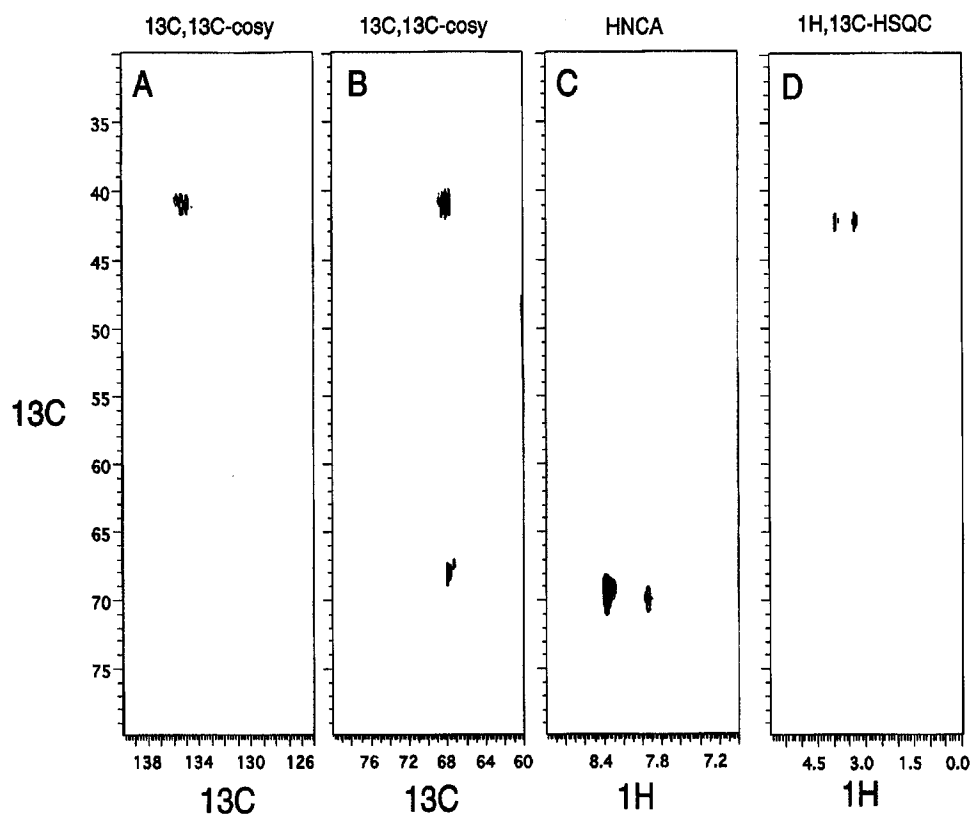
## 3.5: Stereochemical Investigation of Sub A

### 3.5.1: Analysis of the Cysteine-phenylalanine and Cysteine-threonine Bonds

Initial NMR investigation of Sub A indicated that labeling with  $^{13}\text{C}$  and  $^{15}\text{N}$  was essential due to extensive resonance overlap, which precluded unambiguous assignment of all signals. Backbone carbon, nitrogen and proton assignments for the 35 amino acid cyclic peptide were determined using a standard panel of NMR experiments, including HNCACB and CBCACONH (see Table 6, section 3.6). Interestingly, the chemical shifts for the  $\alpha$ -carbons of Phe22, Thr28 and Phe31 are downfield of compilation values<sup>141</sup> by approximately 10 ppm, which is consistent with the influence of an electronegative atom such as sulfur being directly attached. Experiments were conducted to confirm these shift values. Model compounds **4**, **6** and **8** were prepared by Dr. Chris Diaper (see 3.5.5 Scheme 1), and their  $\alpha$ -carbon chemical shifts agree with those observed for the modified

residues in subtilosin A **1B**. Complete assignment of all carbon, nitrogen and proton chemical shifts (including side chains) indicated that these  $\alpha$ -carbons are fully substituted. To confirm that the amino acid assignments are correct, universally labeled [ $^{13}\text{C}$ ,  $^{15}\text{N}$ ]-L-phenylalanine and [ $^{13}\text{C}$ ,  $^{15}\text{N}$ ]-L-threonine were added to separate fermentations of *B. subtilis* in unlabeled media.  $^{13}\text{C}$ -COSY experiments on the selectively labeled Sub A preparations verified that the resonances at 69.4, 69.8 and 72.8 ppm correspond to the  $\alpha$ -carbons of Phe22, Phe31 and Thr28, respectively (Figure 29). The absence of crosspeaks at these chemical shifts in  $^1\text{H}$ ,  $^{13}\text{C}$ -HSQC spectra further illustrates that the thioether linkage consists of an unusual sulfur- $\alpha$ -carbon bond. Inter-residue correlations of the three  $\alpha$ -modified amino acids identified the attached cysteines as Cys13, Cys7 and Cys4, respectively.

**Figure 29:** NMR spectra of Sub A U- $^{13}\text{C}$ ,  $^{15}\text{N}$ ]Phe A **1B**: A.  $^{13}\text{C}$ -COSY at 125 MHz showing Phe C $\beta$  (y-axis) correlations to aromatic carbon (x-axis) correlations; B.  $^{13}\text{C}$ -COSY of the Phe C $\beta$  (y-axis) to C $\alpha$  (x-axis) correlations; C.  $^1\text{H}$  $^{13}\text{C}$ -plane from HNCA displaying intraresidue Phe C $\alpha$  (y-axis) to  $^1\text{H}$  (x-axis),  $^{15}\text{N}$  correlations.  $^1\text{H}$ ,  $^{13}\text{C}$ -HSQC demonstrating that only the C $\beta$  (y-axis) have protons (x-axis) directly attached protons. The C $\alpha$  and C $\beta$  resonances of Phe22 and Phe31 are nearly overlapped (indistinguishable in panes A and B), but the two C $\alpha$  to NH correlations are clearly separated in panel C.



A literature search shows that this type of post-translational modification, namely oxidative linkage of cysteine sulfur to the  $\alpha$ -carbon of another amino acid residue, has not been previously observed in any other *ribosomally-synthesized* peptides. Cyclothiazomycin (Figure 30), a *nonribosomal* peptide from *Streptomyces* with renin inhibitory activity, is a rare example that has cysteine sulfur linked to the  $\alpha$ -carbon of an alanine with inversion of configuration at that center.<sup>172</sup> Another close analogy to these modifications occurs in fungal diketopiperazines (Figure 31), such as gliotoxins, aranotins and sporidesmins.<sup>173</sup> However, in these eukaryotic secondary metabolites the presence of disulfide and trisulfide bridges, as well as thiomethyl adducts, suggests that sulfur donor(s) other than cysteine as well as different mechanisms may be involved.

**Figure 30:** Structure of Cyclothiazomycin, a *nonribosomal* peptide from *Streptomyces*.

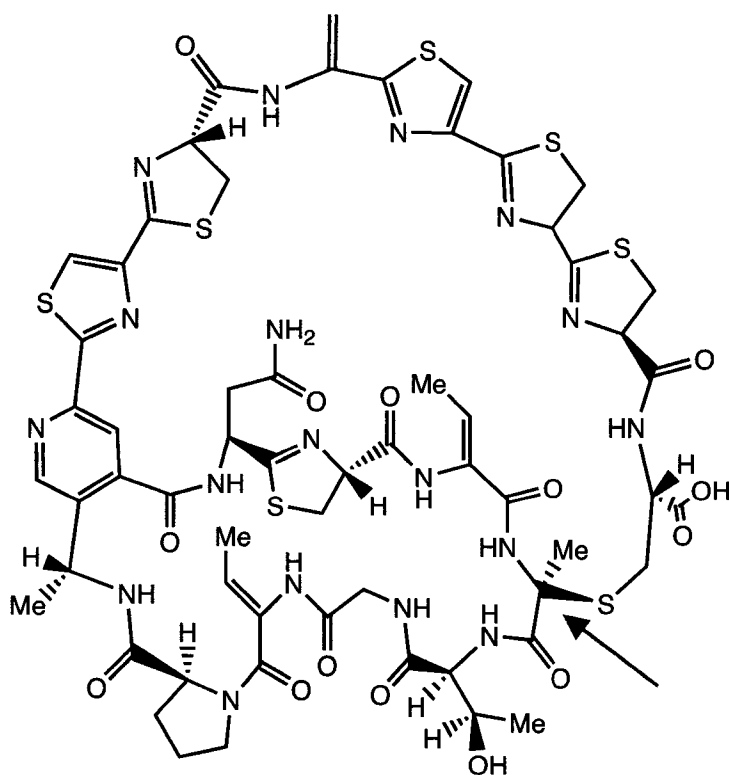
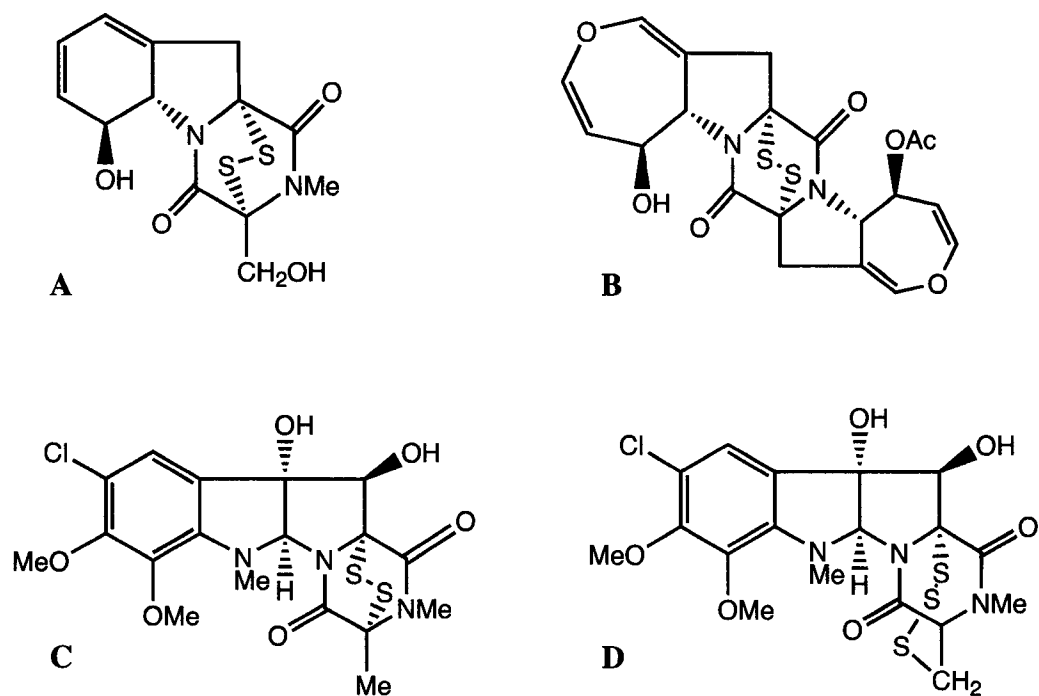


**Figure 31:** Examples of fungal diketopiperazines. A. Gliotoxin; B. Aranotin; C. Sporidesmin; D. Sporidesmin C.



### 3.5.2: Desulfurization and Hydrolysis of Subtilosin A (1A).

It appeared that desulfurization of this highly modified peptide could assist hydrolytic cleavage of the peptide backbone for sequencing as well as analysis of stereochemistry of the presumably unmodified amino acid residues. As mentioned above, both hydrolysis and amino acid sequencing of subtilosin A (1A) was problematic.<sup>160,161</sup> Nickel boride desulfurization to **2** was successful in reductive cleavage of the thioether bridges, as shown by the MALDI-TOF mass determination of  $3311.5 \pm 0.5$  Da, with

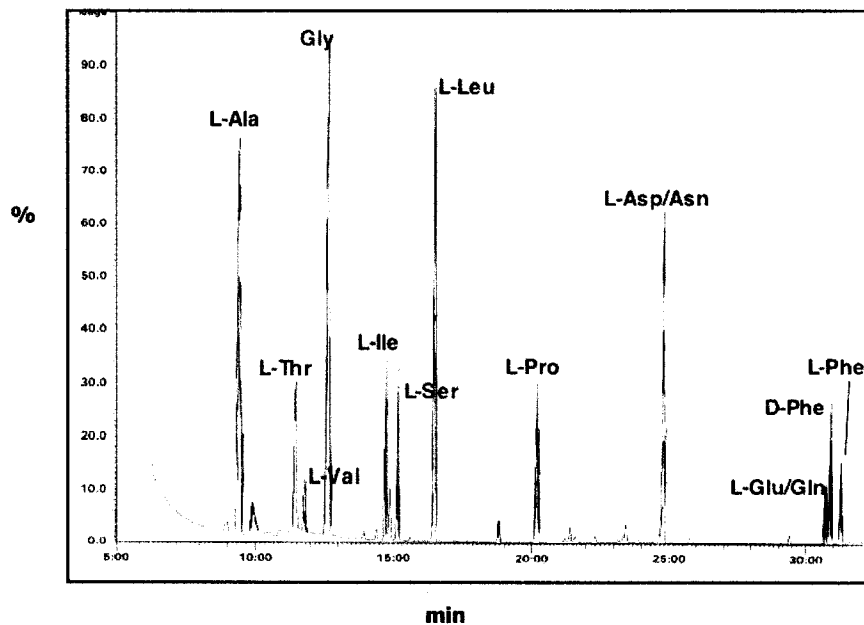
regeneration of the parent residues Phe22, Phe31 and Thr28, as well as conversion of Cys13, Cys7 and Cys4 to alanine residues (Figure 32).<sup>108,174,175</sup>

### 3.5.3: Chiral GC MS Analysis of Desulfurized Subtilosin A (2)

Following desulfurization, the resulting (2) was submitted to complete acid hydrolysis and conversion of the constituent amino acids to N-pentafluoropropanamide isopropyl esters for chiral GC MS analysis. GC MS of the crude derivatized mixture (Figure 33) detected L-Thr ( $t_R$  11.4 min), D-Phe ( $t_R$  30.8 min) and L-Phe ( $t_R$  31.4 min). Peak assignment was confirmed by co-injection of the mixture with authentic amino acid standards. Insulin chain B was also hydrolyzed and derivatized in trial runs to gauge the accuracy and reproducibility of the derivatization and separation procedures. The insulin chain B and Sub A are of similar size and possess many identical amino acids. The stereochemistry of all the unmodified residues was determined to be L. Threonine was detected as the L stereoisomer only, and a mixture of D and L stereochemistries was observed for phenylalanine. Since there is an unmodified threonine residue at position 6 and a modified threonine at position 28 in 1A, the desulfurization and subsequent hydrolysis experiments show that desulfurization of Thr28 proceeds with complete stereochemical selectivity. Detailed NMR analysis of subtilosin A (1A) (see 3.13) shows that prior to reductive desulfurization the modified Thr28 is D (*S* configuration due to priority change). The results demonstrate that the desulfurization of this residue proceeds with net *inversion* of configuration, presumably by formation of the corresponding N-

acyl imine under the basic conditions followed by hydride delivery from the less hindered exterior face of the cyclic peptide.

**Figure 32:** GC MS of crude derivatization mixture from desulfurized subtilosin A (2).

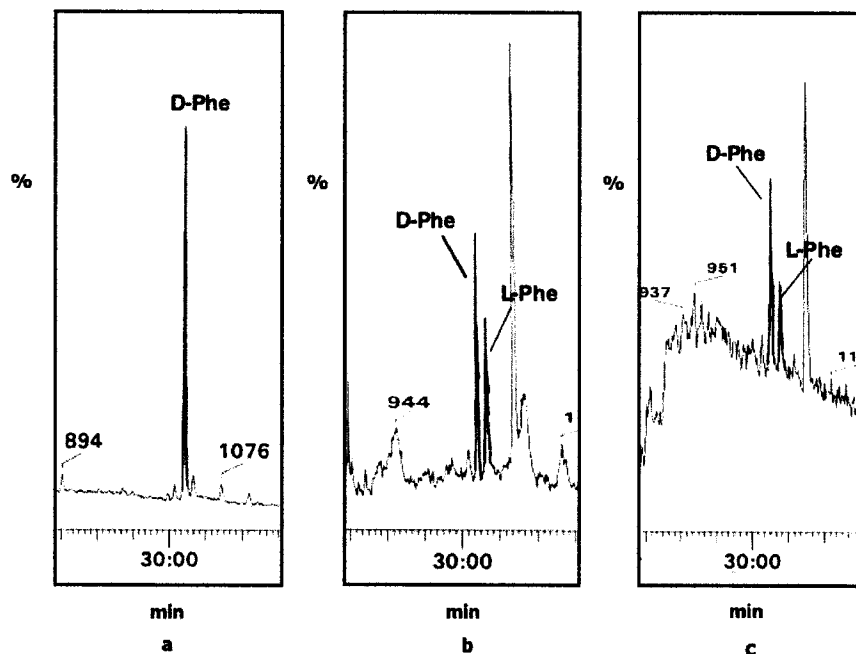


### 3.5.4: Derivatization and GC MS Analysis of Partial Hydrolysis Fragments from (2)

To determine the stereochemical outcome of reduction of the two modified phenylalanines, a limited hydrolysis with 0.1 N HCl was done on **2** to afford larger peptide fragments, which were separated by HPLC. A fragment with a mass of 1015.5 Da was isolated, corresponding to residues 17-26, (Gly-Pro-Ile-Pro-Asp-Phe-Glu-Ile-Ala-Gly), which contains Phe<sub>22</sub>. Two fragments containing Phe<sub>31</sub> were also separated: one with a mass of 692.4 Da, corresponding to residues 29-34 (Gly-Leu-Phe-Gly-Leu-Trp);<sup>176</sup> and another with mass of 635.4 Da, corresponding to residues 30-34 (Leu-Phe-Gly-Leu-

Trp). Each of these peptides was separately hydrolyzed to constituent amino acids, which were then converted to N-pentafluoropropanamide isopropyl esters for chiral GC MS analysis as before. The results show that in desulfurized compound **2**, within experimental error, Phe22 has exclusively D configuration, whereas Phe31 exists as a 4:1 mixture of D:L (Figure 33). NMR studies of subtilosin A **1B** (see 3.13) show that the modified Phe22 is L (*R* configuration due to priority change) and that modified Phe31 is D (*S*). Hence, nickel boride reduction of **1A** proceeds with *inversion* of configuration at Phe22 (a stereochemical outcome in agreement with the reduction of modified Thr28)<sup>177</sup> and with 4:1 *retention* at Phe31.

**Figure 33:** GC MS analysis of partial hydrolysis fragments from:  
 Fragment 1: Residues 17-26. D-Phe detected. L-Phe was absent from the mixture; 27a  
 Fragment 2: Residues 29-34. Both D-Phe and L-Phe detected; 27b  
 Fragment 3: Residues 30-34. Both D-Phe and L-Phe detected; 27c

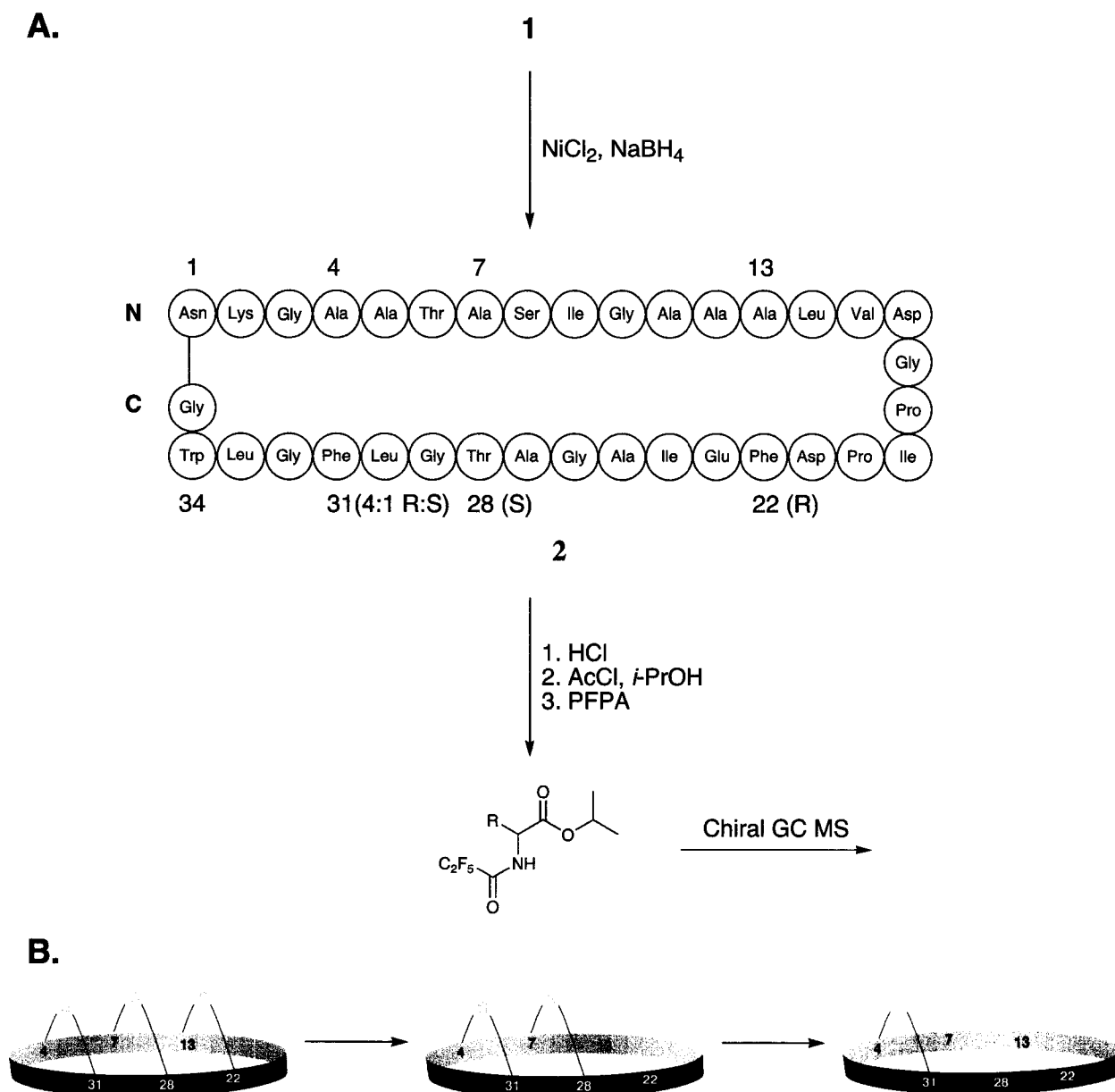


During desulfurization it was noted that two sulfurs are relatively easy to remove, (Cys7-Thr28; Cys13-Phe22) but the last sulfur (Cys4-Phe31) requires much longer reaction times and extra additions of NiCl<sub>2</sub>/NaBH<sub>4</sub>. This suggests that the desulfurization process ‘unzips’ the bowl-like molecule **1** (Figure 34) from the Cys13-Phe22 end, with the first two reductions occurring from the ‘exterior’ surface, and the last reduction proceeding predominantly from what was the ‘interior’ of the now opened bowl (Figure 34).

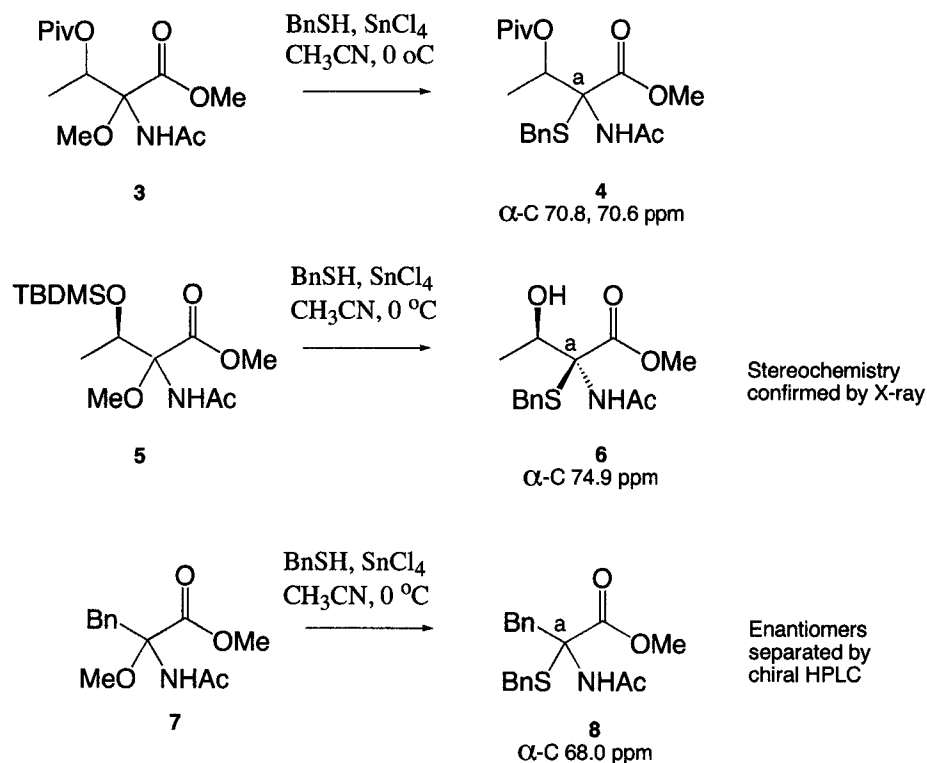
### 3.5.5: Synthesis and Desulfurization of Model Compounds

Model compounds **4**, **6** and **8** were synthesized by Dr. Chris Diaper<sup>177</sup> as shown in Scheme 1 to examine the chemical shifts at the  $\alpha$ -carbons as described above. In each case the key step was the generation of the highly reactive N-acyl imines from the  $\alpha$ -methoxy derivatives. The imines then undergo rapid nucleophilic attack by sulfur to give the  $\alpha$ -thiol.<sup>178</sup> Reaction of these imines was originally developed as a biomimetic approach, as the proposed enzymatic transformation involved in constructing the thiol linkages of subtilosin A (**1A**) may to proceed via these N-acyl intermediates.

**Figure 34:** A. Reductive cleavage of thioether bridges of subtilisin A (1A) to form 2 followed by complete hydrolysis and derivatization to determine residue stereochemistry. B. Proposed sequence of reductive desulfurizations.

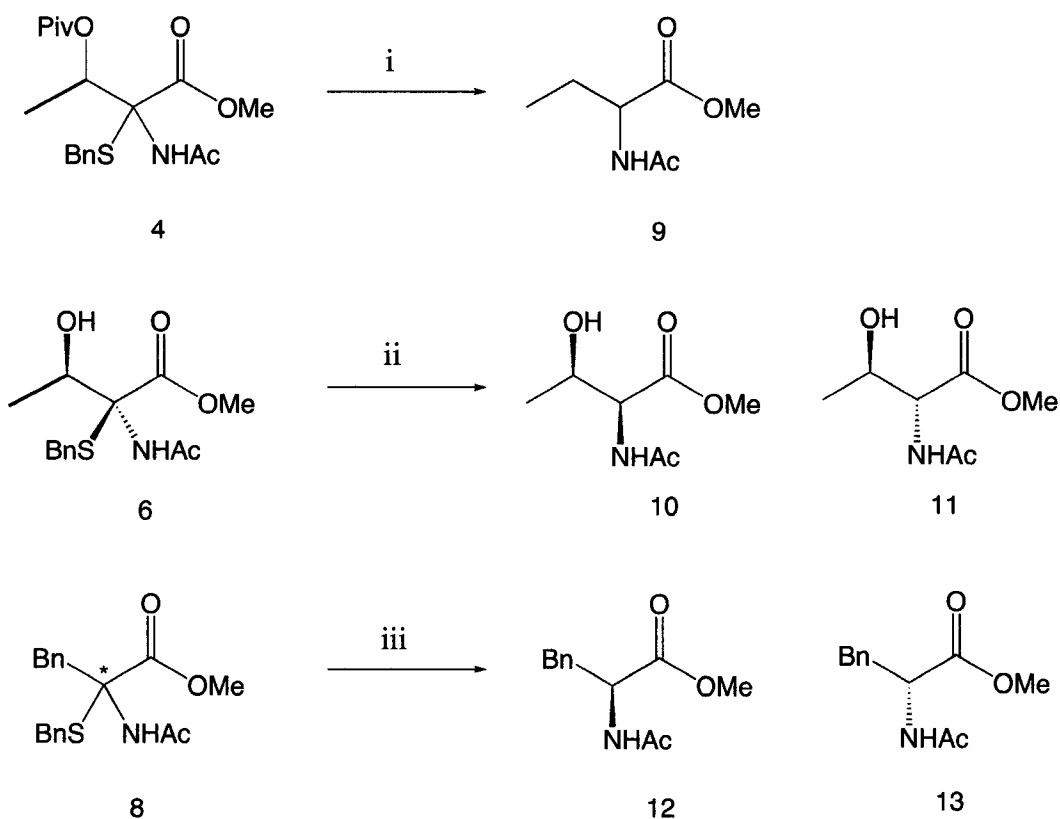


**Scheme 1:** Synthesis of phenylalanine- and threonine-derived model compounds and  $^{13}\text{C}$  chemical shift values for their  $\alpha$ -carbons.



Studies on nickel boride desulfurization, specifically of steroidal sulfides, have demonstrated that replacement of sulfur by hydrogen generally proceeds with retention of configuration.<sup>174</sup> Therefore it initially appeared that this reaction might be an effective probe for the stereochemistry of the sulfur to  $\alpha$ -carbon linkages in subtilosin A (**1A**). However, desulfurization results with Sub A (**1A**) (see above) show both inversion (Thr28, Phe22) and retention (Phe31). The outcome of the nickel boride desulfurization reactions with models **4**, **6** and **8** (Scheme 2) were examined by Dr. Chris Diaper to determine their stereochemistry.

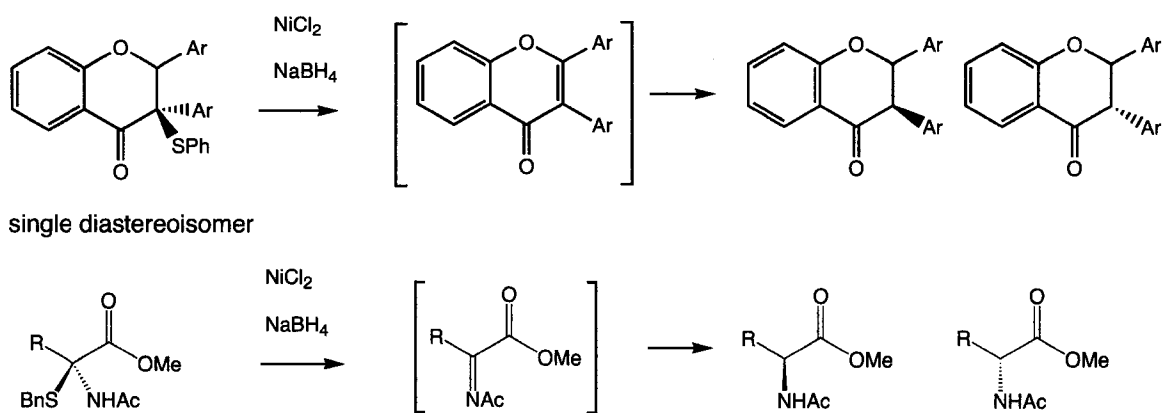
**Scheme 2:** Nickel boride reductions of **4**, **6** and **8**. *Reagents and conditions:* i, NaBH<sub>4</sub>, NiCl<sub>2</sub>, MeOH, rt, 5 min, quant.; ii, NaBH<sub>4</sub>, NiCl<sub>2</sub>, MeOH, 0 °C, 15 min, quant.; iii, NaBH<sub>4</sub>, NiCl<sub>2</sub>, MeOH, 50 °C, 3 h, quant.



Desulfurization of both the threonine and phenylalanine derivatives proceeds with epimerization at the  $\alpha$ -carbon (Scheme 2).<sup>177</sup> Examples from the literature indicate that desulfurizations of 3-aryl-3-phenylthioflavanones also result in loss of stereochemical integrity (Scheme 3).<sup>22</sup> Apparently, in this case the reaction proceeds by elimination of thiol followed by reduction of the planar achiral  $\alpha,\beta$ -unsaturated ketone. It is proposed that the amino acid model systems are analogous, and that the thiol is eliminated to form

a reactive planar N-acyl imine, which is then reduced to an amine in a non-stereospecific fashion.

**Scheme 3:** Proposed elimination-reduction mechanism for epimerisation during  $\text{NiB}_2$  desulfurizations of 3-aryl-3-phenylthioflavanones and  $\alpha$ -thiol-N-acyl amino acids.



### 3.5.6: Stereochemical Inferences from Desulfurization Investigations

In conjunction with the desulfurization of the model compounds, which proceeds with complete racemization, it is presumed that desulfurization of Sub A  $\alpha$ -thiol amino acid residues first eliminate thiolate under the basic nickel boride conditions followed by the reduction of the N-acyl imine with stereochemical preference being controlled by the geometry of the peptide. Although the nickel boride desulfurization results in epimerization for the model compounds **6** and **8** (in contrast to the normally observed retention of configuration for simple sulfides), in subtilosin A (**1A**) the chiral scaffold of the peptide could make one face of the intermediate N-acyl imine more accessible to reduction.

### 3.6: NMR solution structure

A panel (Table 6) of NMR experiments was used in determining the chemical shift assignments (see 4.11.13; Tables 6 and 7) and elucidating the three dimensional structure of Sub A. Since the stereochemistry of the three modified residues in Sub A could not be directly established by chemical degradation experiments, NMR structure determination was used to analyze the configuration at each of these stereocenters.  $^{13}\text{C}$ -HSQC-NOESY,  $^{15}\text{N}$ -HSQC-NOESY and HNHA experiments were recorded for universally  $^{13}\text{C}$ ,  $^{15}\text{N}$ -labeled subtilosin A **1B**. The structure calculations were done with the assistance of Dr. Tara Sprules of our group. Each of the eight possible stereoisomers of subtilosin A **1B** were submitted to eight rounds of ARIA calculations, starting with the same peak files and assignments. The stereoisomer with the L configuration at Phe22 and D stereochemistries at Thr28 and Phe31 (LDD) fit the NMR data the best, giving the lowest energy family of structures with the best r.m.s.d. The DDD isomer, the next best, does not match the NOE data as well, whereas the LLL isomer (i.e. hydrogen replacement by sulfur with retention of configuration for all 3 residues) has the worst fit. The structure for the LDD stereoisomer of subtilosin A **1B** was further refined, using a total of 301 unique NOEs and 20 dihedral angle restraints (See Appendix: Figure A.1).<sup>177</sup> A family of eight structures of subtilosin A **1B** was chosen to represent its conformation in MeOH. Subtilosin A **1B** forms a twisted, bowl-like structure, with most side chains pointing towards the solvent (Figure 35). The center of the molecule, bordered by the Cys4-Phe31 and Cys13-Phe22 crosslinks, is the most well-defined, with a backbone r.m.s.d. of 1.2 Å. The loops exhibit more variation in backbone and sidechain position.

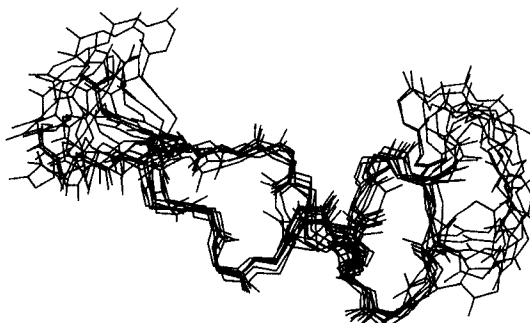
This is due in part to a lack of long-range NOEs within the loops, as the sidechains point to the exterior and there is a high proportion of glycines in the sequence. The amide protons of residues 21-23 exchange more rapidly with solvent, and residues 17 and 19 have low heteronuclear HN NOEs compared to the rest of the molecule, indicating that this portion of the structure is more mobile than the rest.

The conformation of subtilosin A **1B** in methanol differs significantly from that reported earlier in DMSO,<sup>168</sup> but the correct sulfur linkages in that structure were not established. In that case, residues 13-24 were found to be the most structured, and the two end loops were placed much closer together. The sulfide bridges are necessary for the antimicrobial activity of subtilosin A **1B**, and constrain the central portion of the structure, while allowing a degree of motional freedom to the sidechains and end loops. In contrast to many bacteriocins, which have an overall positive charge at physiological pH, Sub A has only one lysine and a total of three aspartate and glutamate residues. This suggests that it may not interact directly with the cell membrane, and must first bind to a surface receptor. The sulfide bridges may hold it in a conformation that easily adapts to its target molecule.

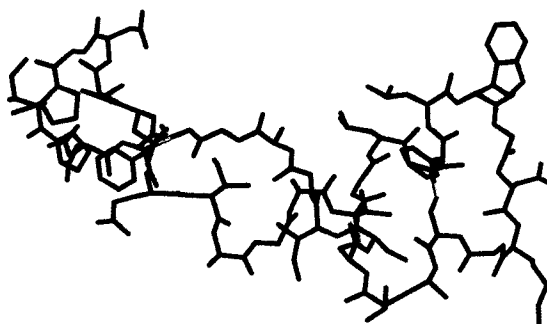
**Figure 35:** **A:** Superposition on the backbone of residues 4-13 and 22-31 of the eight lowest energy structures of subtilosin A **1B**. **B:** Representative conformer of

subtilosin A **1B** in the same orientation, illustrating the outward pointing sidechains. The positions and stereochemistry of the crosslinks are indicated. **C**: Backbone representation of **1B**.

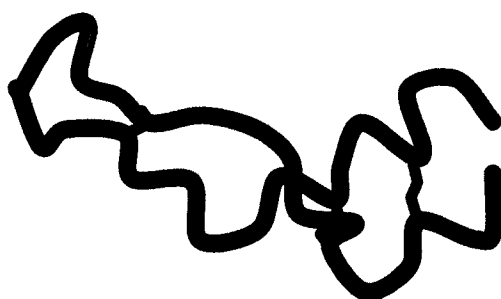
**A.**



**B.**



**C.**



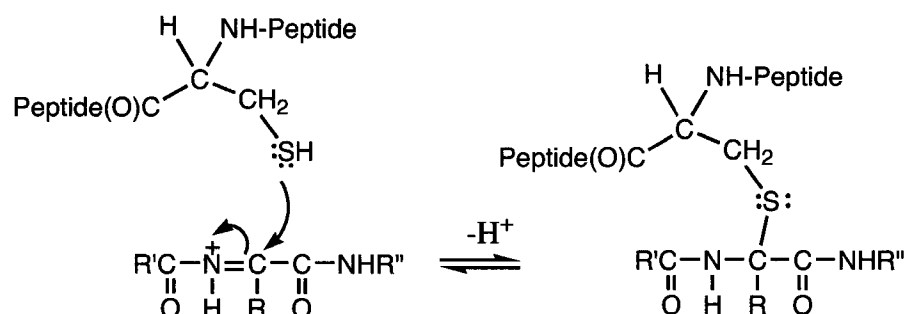
**3.6.1: NMR Experiments Used in the Structure Elucidation of Subtilosin A 1B****Table 6:** NMR experiments acquired

Experiment Name	Nuclei	Reference
$^{13}\text{C}$ -HSQC <sup>195</sup>	$^1\text{H}$ , $^{13}\text{C}$	[203,204]
$^{15}\text{N}$ -HSQC <sup>195</sup>	$^1\text{H}$ , $^{15}\text{N}$	[203,204]
HNHA	$^1\text{H}$ , $^1\text{H}_\alpha$ , $^{15}\text{N}$	[205]
CBCA(CO)NNH	$^1\text{H}$ , $^{13}\text{C}$ , $^{15}\text{N}$	[203]
HCCH-TOCSY	$^1\text{H}$ , $^1\text{H}$ , $^{13}\text{C}$	[206]
HNCO	$^1\text{H}$ , $^{13}\text{C}(\text{O})$ , $^{15}\text{N}$	[203]
HNCA	$^1\text{H}$ , $^{13}\text{C}_\alpha$ , $^{15}\text{N}$	[207]
HNCACB	$^1\text{H}$ , $^{13}\text{C}$ , $^{15}\text{N}$	[203]
$^{13}\text{C}$ -NOESYHSQC	$^1\text{H}$ , $^1\text{H}$ , $^{13}\text{C}$	[208]
$^{15}\text{N}$ -NOESYHSQC	$^1\text{H}$ , $^1\text{H}$ , $^{15}\text{N}$	[209]
$^{15}\text{N}$ -TOCSYHSQC	$^1\text{H}$ , $^1\text{H}$ , $^{15}\text{N}$	[209]
$^{13}\text{C}$ , $^{15}\text{N}$ -NOESY <sup>195</sup>	$^1\text{H}$ , $^1\text{H}$ , $^{13}\text{C}/^{15}\text{N}$	[210]

### 3.7: Possible Mechanisms for Formation of the Sulfur Bridges

As seen in model experiments described earlier, a possible process for Sub A (1A) formation involves enzymatic generation of N-acyl imines at Phe22, Thr28 and Phe31 followed by thiol attack (Scheme 4).

**Scheme 4:** Nucleophilic attack of cysteine sulfur on the C<sub>α</sub> position of an amino acid

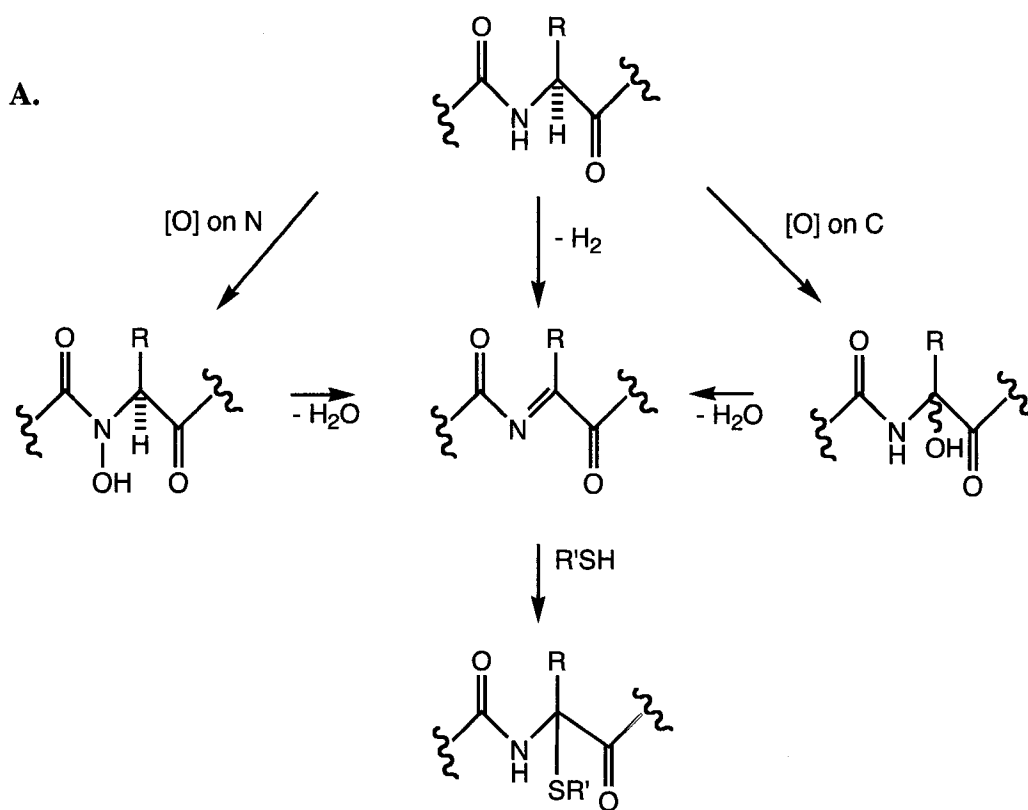


In principle such imines could be generated by direct oxidative dehydrogenation, by hydroxylation on nitrogen followed by dehydration, or (less likely) by hydroxylation on the  $\alpha$ -carbon followed by dehydration (Scheme 5A).

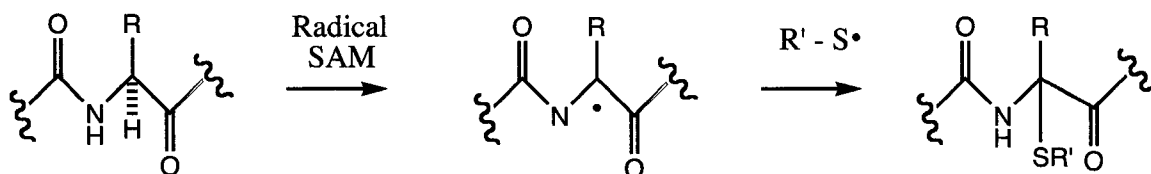
An alternative process would involve hydrogen abstraction at the  $\alpha$ -carbon to give a stabilized radical followed by coupling of a sulfur radical generated from the cysteine thiol. Two of the genes in the *sbo-alb* locus of *B. subtilis*, *albA* and *albF*, are critical for production of mature subtilosin A. Homology between the *albA* gene product and members of the Moa/NifB/PqqE family, which contain Cys clusters that bind Fe-S complexes,<sup>179,180</sup> suggests that this enzyme or one(s) which it generates may catalyze the oxidation reactions during the post-translational modification of the presubtilosin. AlbA

is homologous to radical SAM enzymes. Hence an adenosyl radical could form the Cys-Phe linkage (Scheme 5B).<sup>181,182</sup> The N-terminal half of AlbF demonstrates sequence similarity to mitochondrial metalloproteases associated with the cytochrome  $bc_1$  complex.<sup>183-185</sup>

**Scheme 5:** **A.** Hydroxylation at the nitrogen or  $\alpha$ -carbon or dehydrogenation followed by dehydration, and then nucleophilic attack by the cysteine sulfur. **B.** Radical reaction using *S*-adenosylmethionine (SAM).



B.



Identification of the products of these genes should yield insights into the mechanism of this novel post-translation modification, and could lead to discovery of other previously unknown thioether linkages in bacteriocins. Such mechanisms remain speculative until the detailed function of *albA* and *albF*, the putative oxidative enzymes in the operon, are elucidated.

### 3.8: Conclusions for Sub A

Structural and chemical investigations of Sub A were undertaken using labelled and unlabelled peptide and a panel of multi-dimensional NMR techniques. Labelling of the peptide required peptone media generated from fermentations of a blue-green algae, *Anabaena* sp. Initial proposals for Sub A by the groups of Babasaki<sup>160</sup> and Marx<sup>168</sup> did not succeed in producing a complete and correct structure. Our work shows that subtilosin A (**1A**) possesses highly unusual post-translational modifications, specifically sulfur to  $\alpha$ -carbon crosslinks. These crosslinks are necessary for its antimicrobial activity, and hold the peptide in a twisted, bowl-like conformation, with most of the side-chains

pointing towards the solvent. The configurations of the unmodified amino acids are all L, as determined by chiral GC MS by hydrolysis of desulfurized **1A** with subsequent derivatization of constituent amino acids to N-pentafluoropropanamide isopropyl esters. However, those of the modified residues are L-Phe22, D-Thr28, and D-Phe31, which was deduced by extensive NMR analysis. This means that the biochemical formation of the sulfur to  $\alpha$ -carbon crosslinks proceeds with net retention of configuration at Phe22, and with net inversion at Thr28 and Phe31. Evaluation of the NMR structures shows that there is a twist in the structure making the opposite face of the Cys13-Phe22 bond accessible in comparison to the Cys7-Thr28 and Cys4-Phe31 bonds. During the maturation of subtilosin A (**1A**) this orientation may be favored, resulting in the different chiralities at the modified amino acids.

The nickel boride reductive desulfurization of subtilosin A (**1A**), as well as of the model compounds **4**, **6** and **8**, shows that base-induced elimination of sulfur occurs to form an N-acyl imine followed by reduction to the amide. The model compounds exhibit racemization during desulfurization, but the stereochemical outcome with **1A** is governed by accessibility of the polymeric reducing agent to the relatively rigid peptide scaffold. Usually retention of configuration is observed in systems without acidic hydrogens on the atom adjacent to the carbon bearing sulfur, or that have the ability to stabilize an intermediate cation, as in the 3-aryl-3-thiaflavanone. The combination of nickel boride reduction of a sulfur-containing peptide, Edman degradation sequence analysis, and chiral GC MS is an excellent approach for structure elucidation of post-translationally modified peptides.

## CHAPTER 4: EXPERIMENTAL PROCEDURES

### GENERAL METHODOLOGIES

#### 4.1: Bacterial Strains, Plasmids, Culture Media

The plasmids and producer strains utilized in this study are listed in Tables 3 (see 2.2.1) and 5 (see 2.9). Plasmid pSG6189, fragment SG1551, and primers SG1352 and SG1343 were previously constructed by S. Garneau.<sup>144</sup> Bacterial strains, stored in LB broth (Luria-Bertani) supplemented with 20% (v/v) glycerol, were maintained as frozen stock cultures at -80 °C. Celtone<sup>®</sup>-U complete medium (5013L0) was purchased from Spectra Stable Isotopes (Columbia, MD, USA) and used as supplied. Transformants of *E. coli* were isolated on LB agar containing a selective concentration of ampicillin (100 µg/mL). Solid and soft agar media were prepared by addition of granulated agar 1.5% and 0.75% (w/v), respectively, to the broth media.

#### 4.2: Purchased Strains, Reagents, Solutions

**Genetics:** All genetic manipulations and biological experiments were performed under sterile conditions (material and solutions autoclaved at 121 °C for 10-15 min). Bacterial strains were obtained from the following suppliers: DH5α *E. coli* cells, Invitrogen; BL21(DE3) *E. coli* cells, Stratagene; and Origami<sup>™</sup> B(DE3) *E. coli* cells, Novagen. Restriction enzymes *Sst*I and *Sal*I were obtained from Invitrogen and *Xmn*I from New England Biolabs Inc. Restriction enzyme digestions were performed according to the manufacturer's instructions. T4 DNA ligase was purchased from Invitrogen, New England Biolabs Inc. or Promega. Ligations and *E. coli* transformations were performed

according to current protocols in molecular biology.<sup>117,118</sup> QIAquick™ Gel Extraction Kit, QIAGEN™ Mini Prep Spin Kit, and QIAGEN™ Maxi Prep Spin Kit were all purchased from QIAGEN Inc. (Mississauga, Ontario). The Miniplasmid preparation Kit (GenElute PLN-350 Kit) was purchased from Sigma. Agarose 1000 and ultrapure agarose were purchased from Invitrogen. Agarose gel (1.0 and 2.5% in Tris-borate-EDTA (TBE) containing 5 µL EtBr/100 mL) electrophoresis was conducted with TBE buffer (Sigma) at 110 V. The construction of MBP fusion protein of BrcA in *E. coli* was done using the Protein Fusion & Purification (pMAL™) System #E8000S (New England Biolabs Inc.). Chitin beads were obtained from New England Biolabs Inc.

**MBP-fusion:** Factor Xa was obtained from Protein Engineering Technology ApS, PET (Gustav Wieds Vej 10, Science Park Aarhus, DK-8000 Aarhus C, Denmark, pet@petdk.com]. Protease Inhibitor Cocktail Tablets (complete™ EDTA-free) were purchased from Roche (Roche Diagnostics Canada, Laval Quebec). Lysozyme was supplied by Sigma and IPTG from Rose Scientific Ltd. LB (Lauria Bertani), YT (Yeast Extract), Peptone, and Agar were provided by Difco (Aldrich) and prepared according to manufacturer's directions.

### 4.3: Preparation of Competent Cells

The desired *E. coli* cells were inoculated on LB agar plates without antibiotic and incubated overnight at 37 °C in order to attain isolated colonies. Individual colonies were 'picked' and grown in sterile LB broth (10 mL) without ampicillin and incubated overnight at 37 °C with shaking at 200 rpm. LB broth (2 mL) was inoculated with 100 µL of the bacterial culture and grown until turbid (~3 h) at 37 °C and 200 rpm. The cells

were isolated from the culture broth by centrifugation (1000 rpm, 10 min, 4 °C), then the cell pellets were resuspended (vortex for 5 s) in 1 mL ice-cold Buffer 1 (100 mM CaCl<sub>2</sub>, 10 mM MgCl<sub>2</sub>, 5 mM RbCl) and incubated on ice at 4 °C for 30 min. The cells were isolated by centrifugation (1000 rpm, 30 min, 4 °C), resuspended (gently turned back and forth) in 200 µL of ice-cold Buffer 2 (100 mM CaCl<sub>2</sub>, 10 mM MgCl<sub>2</sub>, 5 mM RbCl, 10% glycerol), and divided into aliquots (20-30 µL) that were stored at -80 °C.

#### **4.4: Transformation of Competent Cells**

Both the desired competent *E. coli* cells and purified plasmids, stored at -70 °C, were thawed on ice (~5 min). 1-2 µL of the desired pure plasmid was added to the thawed competent cells and gently mixed to ensure dispersion and incubated on ice for 30 min. After a heat-shock treatment at 42 °C for 90 s, LB broth (100 µL) was added and the resulting mixture was incubated at 37 °C for 1 h. The *E. coli* transformants were then grown on LB agar, containing a selective concentration of ampicillin (100 µg/mL), (Plate 1: 50 µL/plate; Plate 2: spin down the residual, discard supernatant add 10 µL LB broth and plate the residue) at 37 °C for 20 h.

#### **4.5: Pilot Experiments**

Pilot experiments were conducted according to protocols detailed in the pMAL™ Protein Fusion and Purification and IMPACT™-CN Protein Purification Systems utilizing the media that was appropriate to each individual transformant. The pertinent steps were monitored by SDS-PAGE gel electrophoresis.

## 4.6: Affinity Chromatography

### 4.6.1 Amylose Resin for the Purification of MBP Cytoplasmic (Soluble) Fusion Proteins

Induced cells from a large scale purification (1 L of culture) were harvested by centrifugation, (pre-cooled 500 mL centrifuge bottles; pre-cooled centrifuge; 8000 rpm, 15 min, 4 °C) and resuspended in ice-cold column buffer [15-20 mL, containing 20 mM Tris-HCl, 200 mM NaCl, 1 mM EDTA•Na<sub>2</sub>, 10 mM β-mercaptoethanol or 1 mM DTT (preferred), 1 mM NaN<sub>3</sub>, pH 7.4 (adjusted with 6 N HCl)]. All further manipulations were done at 4 °C. The cell suspension was placed in pre-cooled 30 mL sterile centrifuge tubes containing a complete™, EDTA-free Protease Inhibitor Cocktail tablet (in 1 mL column buffer), which were either stored overnight at -20 °C or immediately processed. Lysozyme (10-15 mg) was added to each tube (thawed or never frozen; *gentle mixing by inversion*) followed by three freeze-thaw cycles [20 min EtOH/Dry ice; 45-60 min cold water (achieve complete thawing each time)] The viscous cell mass was sonicated (utilizing a medium tip) 3 x for 20 s each and centrifuged at 20 000 rpm for 30 min at 4°C. The lysates were diluted with column buffer to 100 mL and loaded on a pre-washed (10 volumes of column buffer) 25-50 mL amylose resin column at 0.5 mL/min, then the column was washed with 12 to 15 volumes of column buffer. Elution of the MBP-fusion protein employs the same buffer containing 10 mM maltose. 10 mL fractions were collected on a Bio-Rad fraction collector with UV monitoring capability. Fractions containing the fusion protein were dialyzed against degassed milliQ water (4 °C; 3x, 1 h, 3 h. 5 h), lyophilized and stored under Ar at -20 °C.

#### **4.6.2 Amylose Resin for the Purification of MBP Periplasmic (Insoluble) Fusion Proteins**

All manipulations were performed at 4 °C. Induced cells from a large-scale purification (1 L of culture) were resuspended in 400 mL of buffer (30 mM Tris-HCl, 20% sucrose, pH 8.0; ~80 mL/gram of cells wet weight). EDTA was added to 1 mM and incubated for 5-10 minutes at 25 °C with shaking or stirring. The cell suspension was centrifuged, 8000 rpm for 20 min at 4 °C, and all the supernatant was removed. The cell pellet was resuspended in 400 mL of ice-cold 5 mM MgSO<sub>4</sub> and shaken for 10 min in an ice bath followed by centrifugation at 800 rpm for 20 min at 4 °C. Tris-HCl, 8 mL of 1 M, pH 7.4, was added to the supernatant (the cold osmotic shock fluid) and was loaded onto an amylose column as previously described (see General Methodologies, 6.1). After loading the column, the washing, elution, fraction collection and dialysis procedures were continued as for the cytoplasmic MBP-fusions.

#### **4.6.3: Chitin Beads for the Purification of Cytoplasmic (Soluble) Fusion Proteins**

Induced cells from a large-scale purification (1 L of culture) were harvested by centrifugation, (pre-cooled 500 mL centrifuge bottles; pre-cooled centrifuge; 8000 rpm, 15 min, 4 °C) and resuspended in 50 mL Cel Lysis Buffer (20 mM Tris-HCl, 500 mM NaCl, 1 mM EDTA•Na<sub>2</sub>, 20 μM PMSF, 1 mM TCEP) in a pre-cooled 200 mL sterile centrifuge bottle. All further manipulations were done at 4 °C. A low level of lysozyme (10-20 μg) was added and incubated at 4 °C for 1 h and the glutinous cell mass was sonicated (medium tip, 2 x 20 s), followed by centrifugation at 20 000 rpm for 30 min at 4°C. The clarified cell extract was loaded onto a pre-prepared (10 volumes of column

buffer; 20 mM Tris-HCl, 500 mM NaCl, 1 mM EDTA•Na<sub>2</sub>) Chitin bead column at 0.5 mL/min. On-column cleavage was achieved by quickly flushing the column with cleavage buffer [3 column volumes, 20 mM Tris-HCl, 500 mM NaCl, 1 mM EDTA•Na<sub>2</sub>, 30 mM DTT or a cysteine (50 mM)/DTT(1 mM) mixture]. The flow was stopped and the column left at rt for 36 h. During the induction the target protein was released from the intein tag and was eluted with column buffer. Fractions, 5 mL, were collected on a Bio-Rad fraction collector with UV monitoring capability and traces were recorded using LP Data View software. Fractions containing the fusion protein were dialyzed against degassed milliQ water (4 °C; 3x, 1 h, 3 h. 5 h), lyophilized and stored under Ar at -20 °C.

#### 4.7: Mass Spectrometry

Mass spectrometric analyses were performed with a linear matrix-assisted laser desorption-ionization time-of-flight (MALDI-TOF) mass spectrometer (Applied Biosystems Voyager Elite). All spectra were recorded in positive ion mode with an acceleration voltage of 20 kV in the presence of a nitrogen laser ( $\lambda = 337$  nm) used for desorption/ionization of the samples. Samples were prepared using  $\alpha$ -cyano-4-hydroxycinnamic acid (Aldrich) or sinapinic acid (Aldrich) as a matrix, and fixed to a gold or stainless steel target before analysis. Calibration of the instrument was performed daily prior to each experiment using Apomyoglobin [ $MH^+ = 16\ 952.56$ ] and Trypsinogen [ $MH^+ = 23\ 981.9$ ] for fusions and insulin [ $MH^+ = 5734.59$ ] and Ins Ch B [ $MH^+ = 3496.96$ ] for small proteins.

## 4.8: CD

Circular dichroism measurements on purified CbnB2P were performed (cell length 0.02 cm) in the absence and the presence of varying concentrations of TFE (10-70%) and MeOH (10-70%) between 250-185 nm at 25 °C using a JACSO J720 spectropolarimeter equipped with JASCO J700 software (done by R. Luty, Department of Biochemistry, University of Alberta).

## BIOLOGICAL EXPERIMENTS

### 4.9: CbnB2P and CbiB2

#### 4.9.1: Plasmid Isolation and Transformation

Tubes containing 10 mL LB with ampicillin (50 mg/mL) were inoculated with JM107 *E. coli* cells containing DNA plasmids pLQP and pLQ300i and incubated at 37 °C overnight with shaking at 200 rpm. The plasmids were harvested using a Qiagen™ Mini Prep Spin Kit and were then purified by agarose gel electrophoresis. The gels were then stained with ethidium bromide, visualized on a UV light box and the DNA was excised with a razor blade. The excised DNA fragments were purified from the agarose according to the QIAquick™ Gel Extraction Kit protocol using 50 µL elution buffer and were used (2 µL of each plasmid) to transform subcloning efficiency DH5α *E. coli* cells (100 µL). Single transformants were grown on LB agar containing 100 µg/mL ampicillin at 37 °C overnight. Several isolated colonies were picked, inoculated into 4 mL LB with 100 µg/mL ampicillin, and incubated at 37 °C overnight with shaking (200 rpm). The cells were harvested by centrifugation and the plasmid purified using alkaline lysis

methodology as described in the Qiagen MaxiPrep Kit. Clones were selected for DNA cycle sequencing (Amersham's DYEnamic ET terminator cycle sequencing kit) and analyzed using the oligonucleotide, 5' < GGT CGT CAG ACT GTC GAT GAA GCC > 3'. The DNA was purified using Sigma Spin Post-Reaction Purification Columns, dried, and analyzed by acrylamide gel electrophoresis on an ABI 373 sequencer (Applied Biosystems) at the Alberta Peptide Institute (Department of Biochemistry, University of Alberta).

#### **4.9.2: Production of CbnB2P and CbiB2**

##### **4.9.2.1: Unlabelled Fusion Proteins**

LB agar with ampicillin were inoculated from frozen stock cultures or freshly transformed competent cells (CbnB2P BL21(DE3) *E. coli* and CbiB2 BL21(DE3) *E. coli*) and incubated at 37 °C overnight to obtain isolated colonies. Tubes (10 mL) of the appropriate media (see below) were inoculated with individual colonies and incubated at 37 °C for 16-18 h at 200 rpm and subsequently added to 500 mL of culture media. For production of fusion proteins, *E. coli* strains were grown in Rich broth [10 g of tryptone, 5 g of yeast extract, 5 g of NaCl; and after autoclaving, addition of filter sterilized solutions: 10 mL of 20% glucose, 2 mL of ampicillin solution (50 mg/mL) per litre] or in complete minimal media (CMM) [6 g of Na<sub>2</sub>HPO<sub>4</sub>, 3 g of KH<sub>2</sub>PO<sub>4</sub>, 0.5 g of NaCl, 1 g of NH<sub>4</sub>Cl or 1.3 g (NH<sub>4</sub>)SO<sub>4</sub> (preferred), 2 mL of 1 M MgSO<sub>4</sub>; and after autoclaving, addition of filter sterilized solutions: 20 mL of 20% glucose, 1 mL of 1 M Thiamine•HCl, 1 mL 1 mM FeSO<sub>4</sub>•7H<sub>2</sub>O, 2 mL ampicillin solution (50 mg/mL) per litre]. The cultures were incubated at 37 °C with shaking (200 rpm) and when the cultures

reached an  $OD_{600}$  of 0.5, production of recombinant proteins was induced with isopropyl-1-thio- $\beta$ -galactopyranoside (IPTG, 0.3 mM). After induction the cultures were incubated (under the same conditions) for 3 h before the cells were harvested by centrifugation. The presence of overexpressed MBP-fusion proteins in *E. coli* was monitored by SDS-PAGE gel electrophoresis (12%).

#### **4.9.2.2: Isotopically Labelled [ $^{15}\text{N}$ ] Fusion Proteins**

CMM was used to produce the labelled proteins of interest following the same experimental procedures as above except for the replacement of unlabelled  $(\text{NH}_4)_2\text{SO}_4$  with labelled  $(^{15}\text{NH}_4)_2\text{SO}_4$ . Celtone<sup>®</sup>-U complete medium (5013L0) was used as supplied in 250 mL aliquots (1 L Erlenmeyer flasks) according to the above procedures.

#### **4.9.3: Purification of MBP-fusions CbnB2P and CbiB2**

Purification of the CbnB2P and CbiB2 MBP cytoplasmic fusions was accomplished as detailed in General Methodologies.

#### **4.9.4: Cleavage of CbnB2P and CbiB2 Fusion Proteins and Purification**

CbnB2P fusion protein was mixed with Factor Xa buffer (20 mM Tris•HCl, 100 mM NaCl, 2 mM  $\text{CaCl}_2$ ) in a 4:1 (w/v) ratio. The cleavage reaction was done at a w/w ratio of 2% with respect to the mass of the fusion protein (e.g., 1 mg Factor Xa/50 mg fusion protein) with gentle mixing at room temperature for 12 h. Cleavage of CbiB2 MBP-fusion follows the same procedure, except that a 5% ratio of Factor Xa to fusion protein and incubation at 25 °C for 16 h was required.

### 4.9.5: HPLC

The precursor and immunity peptides were purified by reversed-phase HPLC using a C<sub>8</sub> Vydac column (10 x 250 mm, 10- $\mu$ m particle size, 300-Å pore size; #208TP1010) and/or a C<sub>18</sub> Waters Nova-Pak cartridge (reversed-phase Pre-Pak C18, 300-Å pore size, 15- $\mu$ m particle size) with gradient elution (flow rates: 2.5 and 10 mL/min, respectively; monitored at 218 nm). Solvent A was 0.1% TFA in H<sub>2</sub>O, and solvent B was CH<sub>3</sub>CN with 0.1% TFA. Gradients were 30 to 60 % CH<sub>3</sub>CN in 30 min and 60 to 90% CH<sub>3</sub>CN in 5 min. The retention times of the CbnB2P-maltose-binding protein, undigested fusion protein and CbnB2P are 27, 25, and 17 min., respectively. The retention times for CbiB2-maltose-binding protein, undigested fusion protein and CbiB2 are 26, 23, and 19 min., respectively

### 4.9.6: NMR

NMR spectroscopy and structure elucidation of CbnB2P and CbiB2 were performed by Dr. T. Sprules. Fractions containing CbnB2P were combined, lyophilized and dissolved in 70:30 TFE-*d*<sub>3</sub> (99.9%):H<sub>2</sub>O or 70:30 TFE-*d*<sub>3</sub> (99.9%):D<sub>2</sub>O (100%) to a concentration of ca. 1 mM. High quality Shigemi NMR tubes were used, the TFE (trifluoroethanol) was not degassed but the H<sub>2</sub>O was, and the samples were kept under argon. NMR experiments were recorded on a Varian INOVA-600 spectrometer. <sup>15</sup>N HSQC,<sup>186</sup> <sup>15</sup>N HSQC-TOCSY,<sup>187</sup> <sup>15</sup>N HSQC-NOESY,<sup>187</sup> and HNHA<sup>188</sup> experiments were recorded in TFE/H<sub>2</sub>O at 35 °C. A <sup>15</sup>N HSQC, <sup>15</sup>N HSQC-NOESY, and HNHA were recorded in TFE/H<sub>2</sub>O at 20 °C. <sup>13</sup>C HSQC,<sup>186</sup> <sup>13</sup>C HSQC-NOESY<sup>189</sup> and a 2D NOESY spectra were recorded at 35 °C in TFE/D<sub>2</sub>O. <sup>13</sup>C HSQC and <sup>13</sup>C HSQC-NOESY spectra

were recorded at 20 °C in TFE/D<sub>2</sub>O. <sup>15</sup>N HSQC-NOESY mixing times were 200 ms; the <sup>13</sup>C HSQC-NOESY was recorded with a 150 ms mixing time. The TOCSY experiment was recorded with a 60 ms spinlock. Chemical shifts were referenced to an internal standard of 3-(Trimethylsilyl)-1-propanesulfonic acid (DSS).<sup>141</sup> Data were processed with NMRpipe,<sup>190</sup> and data analysis was performed with NMRView.<sup>191</sup> NMR structures were calculated using CNS with approximately 550 NOEs and 60 dihedral angles. Linear prediction was used in indirect dimensions, and indirect dimensions were multiplied by a 90 shifted sine-bell-squared function. The direct dimension was multiplied by a 60 degree shifted sine-bell function.

#### **4.10: BrcA and BrcB**

##### **4.10.1: Subcloning of BrcA and Brc B to Produce Cytoplasmic MBP-fusion**

###### **4.10.1.1: BrcA: Formation of Plasmid pKEK1A**

The plasmid pSG6189 and pMAL-c2X vector were digested with the restriction enzymes *Sst*I and *Sal*I. In separate microcentrifuge tubes pSG6189 (4 µg) and pMAL-c2x (1 µg) were resuspended in 1x React 2 buffer (final volume, 20 µL) with *Sst*I (10 units) and incubated for 2 h at 37 °C. NaCl was added to a final concentration of 150 mM with 1 M NaCl; then *Sal*I (10 units) was added and the mixture incubated overnight at 37 °C. Purification of both was accomplished by agarose gel electrophoresis; the pSG6189 fragment containing the *brcA* gene (2.5% agarose-1000), and pMAL-c2X fragment (1% Ultrapure agarose) in TAE buffer. The gels were then stained with ethidium bromide, visualized on a UV light box and the DNA excised with a razor blade.

The excised DNA fragments were purified from the agarose according to the QIAquick™ Gel Extraction Kit protocol using 30 µL elution buffer. Ligation of the pSG6189 fragment (22 ng) into the pMAL-c2X vector (66 ng) occurred at rt with T4 DNA ligase (1 unit) in 1x T4DNA ligase buffer (final volume 10 µL) yielding pKEK1A. 1.5 µL of the ligation reaction was used to transform subcloning efficiency DH5α *E. coli* cells (50 µL). Single transformants were grown on LB agar containing 100 µg/mL ampicillin at 37 °C overnight. Colonies were picked, inoculated into 4 mL LB with 100 µg/mL ampicillin, and incubated at 37 °C overnight with shaking (200 rpm). The cells were harvested by centrifugation and the plasmid purified using the alkaline lysis methodology as detailed in the Miniplasmid Preparation Kit (GenElute PLN-350 Kit). An analytical digest utilizing *SstI* and *SalI* was performed to confirm *BrcA* insertion into pMAL-c2X. The products were analyzed by agarose gel electrophoresis.

#### 4.10.1.2: **BrcB: Formation of Plasmid pKEK2B**

The PCR fragment SG1551 containing the *brcB* gene had been previously digested with *SalI*. The vector, pMAL-c2X, was digested with *XmnI* (generates blunt ends) and *SalI*. 1 µg of pMAL-c2X was suspended in 1x Neb2 buffer (final volume 20 µL), and 20 units of *XmnI*, and incubated at 37 °C for 2 h. NaCl was adjusted to 150 mM NaCl with 1 M NaCl and 10 units *SalI* was added. The reaction was incubated overnight at 37 °C. Plasmid pKEK2B was produced following the same procedure as for *BrcA* steps (purification, ligation, transformation of DH5α *E. coli* cells) except that incubation of the ligase reaction transpired at 16 °C. Clones were selected for DNA cycle sequencing (Amersham's DYEnamic ET terminator cycle sequencing kit) using primers

SG1342 (5'-CCCAGGTTGTTGTACAGAACAAAATAAATTGGGGAAATGTTG-3'; forward primer) and SG1343 (5'-ATATGTCGACTTACCATTGATCCCAAATACT-3'; reverse primer). The DNA is purified using Sigma Spin Post-Reaction Purification Columns, dried, and analyzed by acrylamide gel electrophoresis on an ABI 373 sequencer (Applied Biosystems) at the Molecular Biology Services Unit (Biological Sciences, University of Alberta).

#### **4.10.2: Production of BrcA and BrcB**

##### **4.10.2.1: BrcA and BrcB as MBP-fusion Proteins in SOC Media**

LB agar with ampicillin were inoculated from frozen stock cultures or freshly transformed competent cells (BrcA Origami™ B(DE3) *E. coli* and BrcB Origami™ B(DE3) *E. coli*) and incubated at 37 °C overnight to obtain isolated colonies. Tubes, 10 mL, of the appropriate media (see below) were inoculated with individual colonies and incubated at 37 °C for 16-18 h at 200 rpm) with subsequent addition to 500 mL of culture media contained in 2 L Erlenmeyer flasks. For production of fusion proteins, *E. coli* strains were grown in SOC media [20 g of tryptone, 5 g of yeast extract, 0.5 g of NaCl, 10 mL 250 mM KCl; and after autoclaving, addition of filter sterilized solutions: 5 mL 2 M MgCl<sub>2</sub>, 20 mL 20% glucose, 2 mL of ampicillin solution (50 mg/mL) per litre]. The cultures were incubated at 37 °C with shaking (200 rpm) and when the cultures reached an optical density of 0.5 at 600 nm, production of recombinant proteins was induced with IPTG, 0.3 mM. After induction the cultures were incubated at 30 °C for 4 h before the

cells were harvested by centrifugation. The presence of overexpressed MBP-fusion proteins in *E. coli* was monitored by SDS-PAGE gel electrophoresis (12%).

#### **4.10.2.2: BrcA and BrcB as MBP Cytoplasmic Fusion Proteins, BrcB Intein-fusion in Celtone™-U Complete Medium**

BrcA Origami™ B(DE3) *E. coli*, BrcB Origami™ B(DE3) *E. coli* and BrcB ER2566 *E. coli* were grown in Celtone®-U complete medium (5013L0), which was used as supplied (with the addition of ampicillin) in 250 mL aliquots (1 L Erlenmeyer flasks) according to the above procedures (Section 4.10.2.1).

#### **4.10.2.3: BrcA as MBP Periplasmic Fusion in *E. coli* in LB**

LB agar with ampicillin were inoculated from frozen stock cultures of BrcB ER2566 *E. coli* incubated at 37 °C overnight to obtain isolated colonies. Tubes, 10 mL, of LB broth with ampicillin, 100 µg/mL, were inoculated with individual colonies and incubated at 37 °C for 16-18 h at 200 rpm with subsequent addition to 500 mL of LB broth (x2), containing 100 µg/mL ampicillin, contained in 2 L Erlenmeyer flasks. The cultures were incubated at 37 °C with shaking (200 rpm) and when the cultures reached an optical density of 0.5 at 600 nm, production of recombinant proteins was induced with IPTG, 0.3 mM. After induction the cultures were incubated at 30 °C for 3 h before the cells were harvested by centrifugation. The presence of overexpressed MBP-fusion proteins in *E. coli* was monitored by SDS-PAGE gel electrophoresis (12%).

**4.10.2.4: BrcA and BrcB MBP Fusion Proteins in LB and Rich Broth in BL21(DE3) *E. coli* Cells**

Production of fusion proteins followed the same procedures outlined in part 2.2.1 above. The presence of overexpressed MBP-fusion proteins in *E. coli* was monitored by SDS-PAGE gel electrophoresis (12%).

**4.10.2.5: BrcB Intein Fusion ER2566 *E. coli* in LB**

LB agar with ampicillin was inoculated from frozen stock cultures of BrcB ER2566 *E. coli* (pSG6196 in ER2566 *E. coli* utilizing IMPACT™ -CN, #E6900S; New England Biolabs Inc.) incubated at 37 °C overnight to obtain isolated colonies. 10 mL tubes of LB broth with ampicillin, 100 µg/mL, were inoculated with individual colonies and incubated at 37 °C for 16-18 h at 200 rpm and subsequently added to 500 mL of LB broth (in 2 L Erlenmeyer flasks) containing 100 µg/mL ampicillin. The cultures were incubated at 37 °C with shaking (200 rpm) and when the cultures reached an optical density of 0.5 at 600 nm, production of recombinant proteins was induced with isopropyl-1-thio-β-galactopyranoside (IPTG, 0.3 mM). After induction the cultures were incubated at 15-20 °C for 3 h before the cells were harvested by centrifugation. The presence of overexpressed proteins was monitored by SDS-PAGE gel electrophoresis (12%).

### **4.10.3: Purification of MBP-fusions BrcA, BrcB (cytoplasmic) BrcA (periplasmic) and BrcB Intein Fusion**

Purification of the BrcA and BrcB MBP cytoplasmic fusions was accomplished as delineated in General Methodologies, Section 6, part 6.1. Purification of the BrcB Intein fusion followed the procedure in General Methodologies, Section 6, part 6.3. Purification of BrcB MBP periplasmic fusion was accomplished as delineated in General Methodologies, Section 6, part 6.2.

### **4.10.4: Cleavage of the BrcA and BrcB MBP Fusion Proteins and Purification**

Both BrcA and BrcB MBP-fusions were mixed with Factor Xa buffer (20 mM Tris•HCl, 100 mM NaCl, 2 mM CaCl<sub>2</sub>) in a 3:1 (w/v) ratio. The cleavage reaction was done at a w/w ratio of 2.5% with respect to the mass of the fusion protein (e.g., 1.25 mg Factor Xa/50 mg fusion protein) with gentle mixing at room temperature for 12 h.

## **4.11: SUBTILOSIN A**

### **4.11.1: General.**

High pressure liquid chromatography (HPLC) was performed on either of two instruments, a Beckman System Gold instrument equipped with a model 166 variable wavelength UV detector set at 218 nm and an Altex 210A injector with a 5 mL sample loop or a Rainin instrument equipped with a Rainin UV-1 detector set at 218 nm with 1 mL and 20  $\mu$ L loops. Columns included a Waters Nova-Pak cartridge (reversed-phase Pre-Pak C18, 300-Å pore size, 5- $\mu$ m particle size column), a Vydac reverse phase

#208TP1010, C8, 300-Å pore size, 10-µm particle size column and a Vydac reverse phase #208TP54, C8, 300-Å pore size with a 5-µm particle size. All HPLC solvents were prepared fresh daily and filtered under vacuum before use. All aqueous solutions used milli-Q water. Cambridge Isotope Laboratories (Andover MA) supplied labelled sodium [<sup>13</sup>C]bicarbonate and sodium [<sup>15</sup>N]nitrate. All reactions were performed under dry Ar. All solvents were purified and distilled according to Perrin *et al.*<sup>192</sup> UV fluorescence, ninhydrin, molybdic acid or potassium permanganate for visualization. NMR spectra were recorded on Inova Varian 300, 400, 500 and 800 MHz instruments. IR spectra were determined with a Nicolet Magna 750 FT-IR spectrometer. Mass spectra (MS) were recorded with a Micromass ZabSpec Hybrid Sector-TOF instrument (electrospray ionization (ES)) and on an Applied Biosystems Voyager Elite MALDI system equipped with delayed extraction and an ion mirror (reflectron). Microanalyses were completed at the University of Alberta Microanalytical Laboratory. All literature compounds had IR, <sup>1</sup>H NMR, <sup>13</sup>C NMR and MS consistent with assigned structures.

#### **4.11.2: Production and Purification of Subtilisin A**

##### **4.11.2.1: *Bacillus subtilis* JH642**

Isolated colonies of *Bacillus subtilis* 168 derivative JH642 were obtained by inoculation of DSM agar plates utilizing a stock frozen culture and overnight incubation at 37 °C. DSM consists of: 8 g Difco Nutrient broth, 10 mL 1.2% MgSO<sub>4</sub>•7H<sub>2</sub>O, 10 mL 10% KCl, 0.6 mL 1 N NaOH, 13 g agar dissolved in 1 L milli-Q H<sub>2</sub>O and autoclaved at 121 °C for 15 min. Each of the following filter sterilized solutions are added to 1 L cooled media; 1 mL each of Ca(NO<sub>3</sub>)<sub>2</sub>•4H<sub>2</sub>O, 0.01 M MnCl<sub>2</sub>•4H<sub>2</sub>O and 1 mM

FeSO<sub>4</sub>•7H<sub>2</sub>O.<sup>193</sup> YT tubes were inoculated with single colonies and grown overnight at 37 °C, with shaking at 260 rpm.<sup>167</sup> YT media consists of (per 500 mL): 0.5% Difco Yeast Extract, 2.0% glucose and 0.1% trace elements solution (2.2 g ZnSO<sub>4</sub>•7H<sub>2</sub>O, 1.1 g H<sub>3</sub>BO<sub>4</sub>, 0.5 g MnCl<sub>2</sub>•4H<sub>2</sub>O, 0.5 g FeSO<sub>4</sub>•7H<sub>2</sub>O, 0.16 g CoCl<sub>2</sub>•5H<sub>2</sub>O, 0.16 g CuSO<sub>4</sub>•5H<sub>2</sub>O, 5.0 g Na<sub>2</sub>EDTA, 0.11 g (NH<sub>4</sub>)<sub>6</sub>Mo<sub>7</sub>O<sub>24</sub>•4H<sub>2</sub>O in 100 mL sterile milli-Q water). 1% (v/v) of the YT media was added into 7.5 mL LB tubes and incubated for 7 h at 37 °C. 1.5 mL of the LB culture was then added to 500 mL of pre-warmed (35-37 °C) NSM media<sup>194</sup> and incubated at for 7 h (x2). The supernatant was extracted by adding on quarter the volume of *n*-BuOH and shaking for 1 h, then poured into a separatory funnel and allowed to stand overnight.<sup>160</sup> The organic layer was concentrated *in vacuo* and the residue resuspended in MeOH (10 mL L<sup>-1</sup> of cell culture). Subtilosin A was further purified by HPLC using a reversed phase C18 column (5 mL injection volume, 10 mL/min) and a gradient from 24 % to 76 % CH<sub>3</sub>CN/0.1 % TFA (aq) and a *t<sub>r</sub>* of 28-30 min. A mixture of crude subtilosin A in MeOH/0.1 % TFA (aq) 8:2 was prepared approximately 5 min before injection onto the column. Fractions containing subtilosin A were combined, concentrated *in vacuo* and lyophilized to afford a velvety ivory-white powder.

#### 4.11.2.2: *Bacillus subtilis* SMY

Production of Sub A utilizing the SMY strain was achieved in the same manner as JH642 strain but is grown in defined media. The phosphate media, based upon Spizizen's medium, consists of: 2 g (NH<sub>4</sub>)<sub>2</sub>SO<sub>4</sub>, 14 g Na<sub>2</sub>HPO<sub>4</sub>, 6 g KH<sub>2</sub>PO<sub>4</sub>, 1 g citrate, 0.2 g MgSO<sub>4</sub>•7H<sub>2</sub> in 1 L mill-Q water. The solution is autoclaved at 121 °C for 15 min.

and cooled. Additions include 1 mL trace elements solution (as above) plus 1 mL of the following filter sterilized solutions: 1% glucose, 0.2% glutamic acid, 0.01% tryptophan and 0.01% phenylalanine. HPLC was performed as above with the same elution conditions and CH<sub>3</sub>CN percentage, and utilized a Vydac reverse phase C8 column.

#### **4.11.3: Mass Spectrometry**

MALDI-TOF mass spectrometry employed a 1:2 mixture of approximately 1 to 10 µg/µL subtilisin A in MeOH/0.1% TFA (aq) 7:3 and a saturated solution of sinapinic acid (MeOH/0.1% TFA (aq) 1:3). The samples were analyzed on an Applied Biosystems Voyager Elite MALDI system equipped with delayed extraction and an ion mirror (reflectron) for improving resolution and mass accuracy. External calibration is performed using Insulin [ $MH^+ = 5734.59$ ] and Ins Ch B [ $MH^+ = 3496.96$ ].

#### **4.11.4: Antimicrobial Activity**

Bacteriocin production was determined by the spot-on-lawn test. The indicator organism, *Listeria Monocytogenes* LI0502, was grown overnight in 7.5 mL of TSBY or BHI broth without shaking at 30 °C. Serial twofold dilutions (in LB broth) were spotted (20 µL) onto a BHI hard agar plate, allowed to dry, and overlaid with 7.5 mL of a 1 % LI0502 inoculated BHI soft agar. Zones of inhibition were measured following 16 h incubation at 37 °C. Serial twofold dilutions were also performed on uncyclized-Sub A (see below).

#### **4.11.5: Mild Acid Hydrolysis of Sub A to Uncyclized Sub A**

Acetic acid, 0.25 N, 5 mL, is added to 5mg Sub A in a 15 mL pressure tube and brought to 110 °C for 10 h. MALDI-TOF is performed as described in 4.11.3

providing a mass value of 3420.2 Da and HPLC is performed as for 4.11.1. The retention time for uncyclized-Sub A is 23 min.

#### **4.11.6: Solubility Studies on Subtilosin A**

Sub A, 0.1 mg, was placed in each well of a nine well 3 x 3 glass plate and various solvents: H<sub>2</sub>O, CH<sub>3</sub>CN, MeOH, EtOH, propanol, 1 N HCl, ether, DMSO and hexane are added. Each well was examined with a magnifying glass to observe solubility.

#### **4.11.7: Crystallization Studies on Subtilosin A**

(a) Sub A (5 mg) was placed in each of five small 0.5 mL screw cap conical vials. Minimum amounts of EtOH, MeOH, IPA and IPA-MeOH are added to five vials; 1, 2, 3-4 and 5, respectively, to dissolve the subtilosin. Water was added to all vials until cloudiness was just discernible and each was warmed until clarity was restored. All vials were loosely capped, left in the dark undisturbed.

(b) Six 100 mL jars were employed containing, respectively, 20 mL each of H<sub>2</sub>O, H<sub>2</sub>O/MeOH (50:50); H<sub>2</sub>O, H<sub>2</sub>O/EtOH; and H<sub>2</sub>O, H<sub>2</sub>O/CH<sub>3</sub>CN. Sub A, 5 mg, was placed in six small test tubes and dissolved in 1 mL of MeOH (tubes 1-2), 1 mL EtOH (tubes 3-4), 1 mL MeOH/CH<sub>3</sub>CN (tubes 5-6). The tubes were suspended inside the jar, which was then capped and left undisturbed in the dark. The jars were examined over a period of six months.

(c) Three Pasteur pipettes were sealed at the junction of the tapered portion utilizing a Bunsen burner (the narrow bottom was discarded). The top portion was heated until a very narrow constriction was formed; a height ratio of 2:1 is established with respect to

bottom to top. The bottom portions were filled with milli-Q H<sub>2</sub>O to the middle of the constriction. Each top portion contained 5 mg of Sub A previously dissolved in MeOH, EtOH and IPA, respectively. The tubes were capped, left in the dark undisturbed and observed over a three-month period.

(d) Three NMR tubes containing 5 mg Sub A and 200  $\mu$ L of MeOH, EtOH and IPA, respectively, were overlaid with 400  $\mu$ L of CH<sub>3</sub>CN. The tubes were then capped, left in the dark undisturbed and were inspected at regular intervals.

#### 4.11.8: Pepsin Digest of Sub A

0.1% TFA/H<sub>2</sub>O to 0.4 mL immobilized pepsin (Pierce Products) was added to three 5 mL glass test tubes, mixed, and centrifuged 5 min at 1000 rpm (the supernatant was discarded). MeOH/H<sub>2</sub>O, 4.0 mL 40%, was added to each tube, mixed, and centrifuged 5 min at 1000 rpm (discard the supernatant). MeOH/H<sub>2</sub>O, 0.5 mL 40%, was added to tubes 1 and 3, 0.5 mL 70% MeOH/H<sub>2</sub>O to tube 2 and mixed. Cyt C, 0.33 mg, in 0.5 mL 40% MeOH/H<sub>2</sub>O was added to tube 1, and 0.33 mg Cyt C in 0.5 mL 70% MeOH/H<sub>2</sub>O was added to tube 2, 0.5 mg Sub A and 0.5 mL 50% MeOH/H<sub>2</sub>O was added to tube 3. The tubes were incubated in a water bath at 37 °C with stirring. Samples, 10  $\mu$ L, were removed from each tube at 0.5, 1, 1.5, 2, 2.5, 3 and 24 h and evaluated by MALDI-TOF as above.

#### 4.11.9: Preparation of Labelled Peptone<sup>133</sup>

A culture of the cyanobacterium *Anabaena* sp. ATCC 27899 served as a producer for the peptone in a modified BG-11 medium containing (per liter of solution): MgSO<sub>4</sub>•7H<sub>2</sub>O, 75 mg; CaCl<sub>2</sub>•2H<sub>2</sub>O, 50 mg; K<sub>2</sub>HPO<sub>4</sub>•3H<sub>2</sub>O, 40 mg; Sea Water Mix (Bio-

Crystals Marine-mix, Marine Enterprises, Baltimore, MD), 125 mg; ASTM Micro Elements Solution, 1 mL ( $\text{FeCl}_3 \cdot 6\text{H}_2\text{O}$ , 0.54 mg;  $\text{Na}_2\text{-EDTA}$ , 3 mg,  $\text{H}_3\text{BO}_3$ , 0.62 mg;  $\text{MnCl}_2 \cdot 4\text{H}_2\text{O}$ , 1.4 mg;  $\text{ZnCl}_2$ , 0.1 mg;  $\text{MoO}_3$ , 12  $\mu\text{g}$ ;  $\text{CoCl}_2 \cdot 2\text{H}_2\text{O}$ , 34 ng). The pH of the medium was adjusted to 7.6 prior to autoclaving at 121 °C for 20 min. The *Anabaena* sp. was maintained in 20 mL screw cap culture tubes (partially open to allow gas exchange) containing 10 mL of medium, gently swirled everyday, and reinoculated in fresh medium every 3 weeks. About 20 mL of the growing culture was transferred to a 2 L Erlenmeyer flask containing 500 mL of BG-11 medium. The standing cultures were propagated at rt under cool white fluorescent tubes for 12 days with gentle swirling twice per day. 1 L of cyanobacterium *Anabaena* sp. was centrifuged (15 min, 8000 rpm), the supernatant was removed, and the algae were used as an inoculum for an 8 L fermentation. This large-scale fermentation was performed in a 10-liter glass vessel equipped with a magnetic stirrer, a temperature controller, a light source, a pH controller, and a fritted gas inlet. The pH of the gently stirred culture was maintained at 7.7 by the addition of 1 N HCl using a pH controller, and the temperature was kept at 28 °C. The oxygen produced by *Anabaena* sp. photosynthesis was removed with a continuous flow of argon. The argon was purified using  $\text{CO}_2$ -absorbing Ascarite, and was bubbled through the culture such that concentration of oxygen did not exceed 5-10% in the gas leaving the system. Solutions of  $\text{NaH}^{13}\text{CO}_3$  in  $\text{H}_2\text{O}$  were continually added to the culture with a peristaltic pump (~0.9 mL/min) by passing through a sterile syringe filter (0.2  $\mu\text{m}$ ). The concentration of  $\text{NaH}^{13}\text{CO}_3$  was increased during the growth process (1 g/60 mL for days 1-2, 2 g/60 mL for days 3-4, and 3 g/60 mL for days 5-11).  $\text{Na}^{15}\text{NO}_3$  (1.5 g/10 mL  $\text{H}_2\text{O}$ )

and was added to the culture on day 1, 4, and 7 using a peristaltic pump (~0.9 mL/min) by passing through a sterile syringe filter (0.2  $\mu\text{m}$ ). Good growth was established by supplying light from 4 cool white fluorescent tubes surrounding the vessel and one filament tube located in the interior. After 12 days the cells were collected by centrifugation (8000 rpm, 20 min, 4 °C) and lyophilized, yielding ~0.8-1 g of dry cells per liter of fermentation. The dry cells were extracted with EtOAc in a Soxhlet extractor for 1 day to remove lipids, chlorophyll and other pigments. The resulting blue residue was resuspended in H<sub>2</sub>O (1.5 g/100 mL) and digested at 37 °C with pepsin (Sigma, 3300 units/mg) at a concentration of 70 units/mL for 12 h at pH 2.0 (adjusted with concentrated HCl). Subsequently the pH was adjusted to 6.7 using 2 N NaOH, and the mixture was incubated with chymopapain (Sigma, 4.5 units/mg) at a concentration of 1 unit/mL for 36 h at 37 °C. The mixture was autoclaved (20 min, 121 °C) and the insoluble components were removed by centrifugation (8000 rpm, 15 min, 4 °C). The pellets were extracted with H<sub>2</sub>O (2 x 300 mL) and centrifuged (8000 rpm, 15 min, 4 °C). All supernatant fluids were combined and lyophilized to yield 0.65-0.7 g per 1 g of dry *Anabaena* cells (8.3-10.4 g/16 L) of an off green colored peptone representing approximately 65-70% peptone yield with respect to the dry cells. 4 x 8 L fermentations were grown in order to attain enough peptone for NMR studies on Sub A. **A + B:** 12.5 g, 100% <sup>13</sup>C, 83% <sup>15</sup>N; **C:** 17.9 g, 100% <sup>13</sup>C, 77% <sup>15</sup>N; **D:** 13.2 g, 100% <sup>13</sup>C, 81% <sup>15</sup>N. The respective percentage ratios of H:C:N were (5-6%):(34-37%):(9-10%).

**4.11.8.1: Determination of  $^{13}\text{C}$  and  $^{15}\text{N}$  Enrichment of Peptone**

A Carlo Erba EA1108 CHN Analyzer was coupled to a Hewlett Packard (HP) Gas Chromatograph (GC) (5890 series II) with a HP 5MS column (30 m x 0.25 mm x 0.25  $\mu\text{m}$  film) and a HP Atomic Emission Detector (AED) (5921A). Samples of peptone (1-3 mg) were subjected to normal combustion analysis on the CHN instrument and the vapor stream from these samples was fed directly into the GC-AED system. The GC-AED was set to monitor  $^{12}\text{C}$  at 342.574 nm,  $^{13}\text{C}$  at 334.712 nm,  $^{14}\text{N}$  at 421.465 nm and  $^{15}\text{N}$  at 420.168 nm. Quantification for  $^{12}\text{C}$  and  $^{13}\text{C}$  isotopes was achieved using standards of *p*-chlorobenzoic acid and unlabeled and [ $^{13}\text{C}$ ]-labeled succinic acid. Benzamide samples ( $^{15}\text{N}$ -labeled and unlabeled) were used as standards for  $^{14}\text{N}$  and  $^{15}\text{N}$  isotope analysis. All data were corrected for background and detector response. The amount of labeled peptone and percentages of  $^{13}\text{C}$  and  $^{15}\text{N}$  incorporated were as follows: fermentations A + B: 12.5 g, 100 %  $^{13}\text{C}$ , 83 %  $^{15}\text{N}$ ; C: 17.9 g, 100 %  $^{13}\text{C}$ , 77 %  $^{15}\text{N}$ ; D: 13.2 g, 100 %  $^{13}\text{C}$ , 81 %  $^{15}\text{N}$ . The percentage ratios of H:C:N were (5-6):(34-37):(9-10).

**4.11.9: Production of Labelled Subtilosin A**

A combined sample of labeled peptone (21 g) and 400 mL of milli-Q  $\text{H}_2\text{O}$  were added to each of two 2 L Erlenmeyer flasks and autoclaved at 121 °C for 15 min. One-half of a Quest™ “Once-a-day” vitamin (crushed with mortar and pestle) plus filter sterilized solutions of 0.5 g  $\text{MgSO}_4 \cdot \text{H}_2\text{O}$  and 2 g KCl were then added. Subtilosin A was grown and purified as above, with the following alteration. The solution was centrifuged, the BuOH layer was carefully pipetted to a flask for evaporation and the residual emulsion re-extracted with BuOH.

#### 4.11.10: Labelling of Subtilosin A with [U-<sup>13</sup>C, <sup>15</sup>N]-Phenylalanine and [U-<sup>13</sup>C, <sup>15</sup>N]-Threonine

Subtilosin A was produced as above with the following adjustments. A culture (1.5 mL) of logarithmically growing cells of *B. subtilis* JH642 were transferred to 500 mL of NSM media (with no added glucose). [U-<sup>13</sup>C, <sup>15</sup>N]-L-Phenylalanine (1 g, 98 % <sup>13</sup>C; 96-99 % <sup>15</sup>N) was added at 0.5 g per 500 mL of NSM media. In a separate experiment, [U-<sup>13</sup>C, <sup>15</sup>N]-L-threonine (1 g, 98 % <sup>13</sup>C; 96-99 % <sup>15</sup>N) was added to 500 mL of NSM media. The cultures were shaken, incubated and processed as above.

#### 4.11.11: Desulfurization of Subtilosin A

NaBH<sub>4</sub> (7.5 mg) was added to a suspension of subtilosin A (**11**) (5 mg) and NiCl<sub>2</sub> (7.5 mg) in MeOH (3.75 mL) and mill-Q H<sub>2</sub>O (2.5 mL) in a 15 mL pressure sealed tube, which was then immediately capped. The reaction was heated to 50 °C for 5 minutes, then a further aliquot of NaBH<sub>4</sub> was added and the reaction continued for another 5 min. A 100 μL aliquot was removed and acidified by adding 3 μL of TFA, then microcentrifuged for 1 min at 12,000 rpm. The extent of desulfurization was evaluated by MALDI-TOF and further aliquots of NaBH<sub>4</sub> and NiCl<sub>2</sub> were added as necessary to bring the reaction to completion. The mixture was then centrifuged for 10 min at 8000 rpm and purified by HPLC using a Waters Nova-Pak cartridge column with a 24 to 76 % CH<sub>3</sub>CN gradient over 20 min, t<sub>R</sub> **1**, 17 min. Fractions containing **1** were concentrated *in vacuo* and lyophilized. Mass spectral analysis using an Applied Biosystems Voyager Elite MALDI-TOF system with delayed extraction and ion mirror (reflectron) gave M = 3311.1, corresponding to addition of six hydrogens and the loss of three sulfurs.

#### 4.11.11.1: Hydrolysis of SubA and Formation of N-Pentfluoropropanoyl Isopropyl Ester derivatives of Constituent Amino Acids for GCMS Analysis

Following desulfurization, the dry peptide was derivatized according to Alltech GC reagent instructions included in the PFP-IPA Amino Acid Derivatization Kit (Cat. No. 18093). Desulfurized (**2**) (20 mg) was acid hydrolyzed by heating for 5 min at 100 °C with 3 mL 0.2 M HCl and reduced to dryness *in vacuo*. The dried, acid hydrolyzed amino acids were esterified by heating for 45 min at 100 °C using 5 mL of a mixture of acetyl chloride and *i*-PrOH and dried over Ar. The esterified amino acids underwent addition of the pentafluoropropyl group by heating for 15 min at 100 °C using 2 mL of pentafluoropropionic anhydride. Upon cooling excess reagent was evaporated under argon and redissolved in CH<sub>2</sub>Cl<sub>2</sub> in preparation for chiral GC analysis with an Alltech Heliflex® Chirasil-Val® capillary column for the separation of optical isomers was utilized. Each injection was 1 µL with a concentration of 1 µg µL<sup>-1</sup>. Standards were prepared separately in the same fashion using 20 mg each of L-Phe, D-Phe, L-Thr and D-Thr. A mixture of L-amino acids (5 mg each of Ala, Ile, Lys, Trp, Gly, Phe and Val) was also derivatized to evaluate efficiency of separation of the column and to prepare a library.

#### 4.11.11.2: Partial Acid Hydrolysis of Desulfurized Sub A (2)

A solution (1 mM) of desulfurized subtilisin A (**2**) (20 mg) in 0.1 N HCl was added to a 15 mL pressure sealed tube, which was then heated at 100 °C for 10 h. The sample was then concentrated *in vacuo* over NaOH. The peptide mixture was redissolved

in MeOH (8 mL) and subjected to RP-HPLC using a Waters Nova-Pak cartridge column, gradient of 20 to 80 % CH<sub>3</sub>CN over 60 min. Fractions were combined and reduced to a volume of 1 mL in a vacuum centrifuge. Each fraction was evaluated using LC MS (Agilent 1100) and PAWS (Protein Analysis WorkSheet for the analysis of proteins using mass spectra) software. The chosen fractions were then lyophilized, derivatized and analyzed employing chiral GC MS (injection volume 3  $\mu$ L).

#### 4.11.11.3: Insulin chain B: Trial Hydrolysis and Derivatization

Insulin chain B (25 mg) was added to degassed 6 M HCl (5 mL) and heated to 110 °C for 20 h in a sealed tube. The mixture was then concentrated *in vacuo* over NaOH, rinsed with milli-Q H<sub>2</sub>O (3 mL) and concentrated *in vacuo*. Water was then added and the sample was lyophilized. The component amino acids were derivatized and analyzed following the identical protocol for that detailed for subtilisin A.

#### 4.11.12: NMR Spectroscopy

All samples for NMR used 500  $\mu$ L of degassed CD<sub>3</sub>OH (Sigma) and 5 mm high quality Wilmad NMR tubes, and all solvents and solutions were kept under argon. A suite (see Table 6) of two and three-dimensional homo- and heteronuclear experiments were conducted at 15 °C on either a Varian Inova-500 or Inova-800 MHz spectrometer, and were referenced to DSS.<sup>141</sup> All experiments were processed using the software package NMRPipe<sup>190</sup> and analyzed using the program NMRView<sup>191</sup> with substantial in-house modifications available upon request (<http://www.nanuc.ca>). Linear prediction was used to increase the number of points in the indirectly detected dimensions by up to half

the number of acquired points, and zero filling was used to extend both the directly and indirectly detected dimensions to twice the number of acquired plus predicted points. Spectra were apodized using a  $\pi/2$  or  $\pi/3$  shifted sine bell before Fourier transformation.

**Table 7:**  $^1\text{H}$  Chemical shift assignments of subtilisin A (1B).

	<b>HN</b>	<b>H<math>\alpha</math></b>	<b>H<math>\beta</math></b>	<b>others</b>
<b>Asn 1</b>	7.45	4.71	3.88,2.49	$\gamma\text{NH}_2$ 7.97,7.09
<b>Lys 2</b>	9.26	3.93	1.73,1.84	$\gamma\text{CH}_2$ 1.58,1.47, $\delta\text{CH}_2$ 1.62, $\epsilon\text{CH}_2$ 2.89
<b>Gly 3</b>	9.13	3.83,3.75		
<b>Cys 4</b>	7.77	3.97	3.45,3.14	
<b>Ala 5</b>	7.85	4.10	1.47	
<b>Thr 6</b>	7.78	3.90	4.13	$\gamma\text{CH}_3$ 1.24
<b>Cys 7</b>	7.15	4.02	2.84,3.61	
<b>Ser 8</b>	8.00	4.04	3.94	
<b>Ile 9</b>	7.47	4.05	1.91	$\gamma\text{CH}_2$ 1.45, $\gamma\text{CH}_3$ 0.94, $\delta\text{CH}_3$ 0.88
<b>Gly 10</b>	7.95	4.01,3.46		
<b>Ala 11</b>	7.99	3.98	1.42	
<b>Ala 12</b>	8.02	4.00	1.47	
<b>Cys 13</b>	7.52	4.18	3.49,3.28	
<b>Leu 14</b>	8.07	4.22	1.50,1.90	$\gamma\text{CH}$ 1.691, $\delta\text{CH}_3$ 0.90,0.86
<b>Val 15</b>	7.52	3.82	2.22	$\gamma\text{CH}_3$ 0.95,1.02

<b>15</b>				
<b>Asp 16</b>	6.76	4.80	3.20,2.42	
<b>Gly 17</b>	7.90	4.40,3.73		
<b>Pro 18</b>	#	4.50	2.09,1.94	$\gamma\text{CH}_2$ 1.92,1.75, $\delta\text{CH}_2$ 3.76,3.50
<b>Ile 19</b>	7.07	4.04	1.56	$\gamma\text{CH}_2$ 1.05,1.54, $\gamma\text{CH}_3$ 0.73, $\delta\text{CH}_3$ 0.86
<b>Pro 20</b>	#	4.12	1.95,1.89	$\gamma\text{CH}_2$ 1.95,2.28, $\delta\text{CH}_2$ 3.87,3.54
<b>Asp 21</b>	8.93	4.45	2.76,2.24	
<b>Phe 22</b>	7.98	none	3.21,3.75	2,6H 7.12
<b>Glu 23</b>	10.48	3.85	1.88,1.73	$\gamma\text{CH}_2$ 2.51, 2.12
<b>Ile 24</b>	7.77	3.79	1.91	$\gamma\text{CH}_2$ 1.50,1.32, $\gamma\text{CH}_3$ 0.90, $\delta\text{CH}_3$ 0.95
<b>Ala 25</b>	8.02	4.12	1.44	
<b>Gly 26</b>	8.14	4.23,3.78		
<b>Ala 27</b>	7.75	3.95	1.43	
<b>Thr 28</b>	8.10	none	4.23	$\gamma\text{CH}_3$ 1.00
<b>Gly 29</b>	8.12	3.81,3.89		
<b>Leu 30</b>	7.62	3.94	1.49	$\gamma\text{CH}$ 1.84, $\delta\text{CH}_3$ 0.86,0.94
<b>Phe 31</b>	8.43	none	3.32,3.90	2,6H 7.00, 3,5H 7.10

<b>Gly 32</b>	8.15	4.01,3.81		
<b>Leu 33</b>	7.89	3.98	1.77,1.19	$\gamma$ CH 1.63, $\delta$ CH <sub>3</sub> 0.75,0.88
<b>Trp 34</b>	7.12	4.72	2.98,3.70	1NH 10.41, 2H 7.24, 4H 7.05, 5H 7.46, 6H 6.90, 7H 7.05
<b>Gly 35</b>	7.81	4.04,3.66		

**Table 8:** Nitrogen and carbon chemical shifts for subtilisin A **1B**.

	<b>N</b>	<b>C<math>\alpha</math></b>	<b>C<math>\beta</math></b>	<b>Others</b>
<b>Asn 1</b>	116.22	52.38	39.33	N $\delta$ 107.76
<b>Lys 2</b>	127.22	59.07	32.26	C $\gamma$ 25.69, C $\delta$ 29.44, C $\epsilon$ 41.91
<b>Gly 3</b>	105.74	46.57		
<b>Cys 4</b>	118.63	57.70	33.34	
<b>Ala 5</b>	120.18	54.72	17.88	
<b>Thr 6</b>	111.27	65.21	68.74	C $\gamma$ 21.61
<b>Cys 7</b>	117.13	56.91	31.84	
<b>Ser 8</b>	116.23	61.89	62.61	
<b>Ile 9</b>	119.57	62.83	38.44	C $\gamma$ 27.66, C $\gamma'$ 17.44, C $\delta$ 13.41
<b>Gly 10</b>	106.89	47.13		
<b>Ala 11</b>	121.47	54.69	17.70	
<b>Ala 12</b>	118.72	54.66	17.43	
<b>Cys 13</b>	110.22	56.14	32.11	
<b>Leu 14</b>	125.16	56.67	40.94	C $\gamma$ 27.60, C $\delta$ 24.82, 22.35
<b>Val 15</b>	118.02	65.06	31.52	C $\gamma$ 20.12, 20.87
<b>Asp 16</b>	114.42	50.47	38.40	

<b>Gly 17</b>	104.27	44.13		
<b>Pro 18</b>	#	63.58	30.96	C $\gamma$ 26.39, C $\delta$ 49.74
<b>Ile 19</b>	121.99	60.08	38.23	C $\gamma$ 28.19, C $\gamma'$ 16.16, C $\delta$ 12.89
<b>Pro 20</b>	#	63.05	30.60	C $\gamma$ 27.70, C $\delta$ 51.55
<b>Asp 21</b>	122.25	54.22	38.19	
<b>Phe 22</b>	124.89	69.38	40.74	
<b>Glu 23</b>	120.46	61.50	28.74	C $\gamma$ 36.88
<b>Ile 24</b>	117.79	63.86	38.09	C $\gamma$ 28.63, C $\gamma'$ 20.03, C $\delta$ 17.09
<b>Ala 25</b>	120.82	53.95	17.95	
<b>Gly 26</b>	102.81	45.99		
<b>Ala 27</b>	123.66	54.88	17.85	
<b>Thr 28</b>	120.25	72.80	70.89	C $\gamma$ 18.43
<b>Gly 29</b>	108.69	46.83		
<b>Leu 30</b>	120.84	57.84	42.40	C $\gamma$ 27.06, C $\delta$ 25.48, 24.98
<b>Phe 31</b>	122.36	69.82	42.50	
<b>Gly 32</b>	107.68	47.16		
<b>Leu 33</b>	120.19	57.03	40.87	C $\gamma$ 27.19, C $\delta$ 22.22, 25.20
<b>Trp 34</b>	114.29	56.04	29.92	N $\epsilon$ 127.11
<b>Gly 35</b>	105.34	45.84		

## General Conclusion

This research focused on the isolation and NMR characterization of five bacteriocins or related peptides: 1. CbnB2P, a class IIa bacteriocin, 2. CbiB2, the immunity protein of CbnB2, 3. BrcC, a two-peptide bacteriocin comprised of BrcA and BrcB and 4. subtilosin A, an as yet unclassified bacteriocin. These were studied utilizing current strategies for optimization of their biosynthesis and isotopic labelling procedures with  $^{15}\text{N}$  and  $^{13}\text{C}$  to facilitate NMR studies. The objective was to provide material for NMR studies to determine their three-dimensional conformations. One of the most challenging issues in bacteriocin research is determining the structure-function relationship and the regulatory mechanisms involved. Three-dimensional structure elucidation of cognate precursor, mature and immunity bacteriocins may also help to illuminate a relationship between them.

Overexpression of CbnB2P and CbiB2 as maltose-binding protein fusion proteins provided mild facile procedures for isolating the proteins of interest. Undesired truncation of the CbnB2P resulted in the loss of the two C-terminal residues to give CbnB2P(1-64), but the precursor's overall geometry probably remains unaffected, in NMR studies, since the C-terminal portion is unstructured. The precursor was shown to be approximately 125 times less active than the mature bacteriocin (CbnB2), which initiated structural studies in order to illuminate this interesting characteristic. Multi-dimensional NMR studies allowed for the comparison of the precursor and mature bacteriocin 3D structures. This permitted an evaluation of their commonalities, the determination of possible covalent or through-space connections between the leader and mature portions, and may also lead to

understanding the function of the leader peptide, which is currently unclear. The leader peptide possesses an  $\alpha$ -helical secondary structural motif, in addition to the  $\alpha$ -helix present in the mature bacteriocin and no connections were detected between the leader and mature portions of the peptide.<sup>110</sup> The  $\alpha$ -helix of the mature bacteriocin is an amphipathic helix where one side of the helix is non-polar and the other side is polar. In contrast the helical portion of the leader is predominantly non-polar on one side but contains primarily charged residues on the other, which may be required for recognition by the secretion machinery. The leader peptide may also be required to neutralize biological activity within the cell. NMR studies of CbiB2 are still in progress (preliminary data indicates  $\alpha$ -helical content) and will hopefully contribute to the understanding of immunity proteins of bacteriocins.<sup>80,82,147</sup> Structural comparisons of immunity proteins may help elucidate the mechanism of how immunity is imparted to the producer organism and the relationship, if any, to the mature peptides. Future studies may involve variants of CbnB2P and CbiB2 that are attained by amino acid substitutions (also expressed and purified as fusions in *E. coli*), to probe their stability or toxicity within the cell, their secretion mechanism, and their mode of action. Probing for a receptor may result in the design of new antimicrobial agents, with improved activity for pharmaceutical and commercial food applications.

Very low yields of BrcA and BrcB from the native *Brocothrix campestris* and the occurrence of activity without the presence of the complementary peptide prompted the cloning and overexpression of BrcA and BrcB as maltose fusion proteins. BrcB was also cloned and expressed as an intein fusion protein. The issues under investigation included

how the two peptides associate, their order and ratio of association, and their mode of action. Pilot experiments, monitored by SDS-PAGE gel electrophoresis, established conditions for the choice of host cell, media choice, temperature, and concentration of the inducing agent, IPTG. Unfortunately the MBP-fusion protein was shown to be non-homogeneous indicating that fragmentation was occurring. Proteases in *E. coli* strains are most likely causing proteolytic cleavage at some, or all, of the several double glycine sites that are present. Future studies include cloning using a different over-expression system or utilizing a different plasmid in a host cell that is more closely related to *B. campestris*, or using different hosts such as *Streptomyces* or *B. subtilis* strains. Another approach would be to explore the production of BrcA and BrcB utilizing a cell-free lysate.

Structural and chemical investigations of Subtilosin A were undertaken using labelled and unlabelled peptide and a panel of multi-dimensional NMR techniques. A multistage procedure involving the enzymatic hydrolysis of an algal mass produced by a cyanobacterium, *Anabaena* sp.,<sup>133</sup> was utilized to isotopically label subtilosin A. This methodology affords easy access to substantial quantities of labelled peptides which are produced by fermentation in complex media.. Isotopic labelling of CbnB2P and CbiB2 was accomplished by utilizing minimal media containing <sup>13</sup>C and/or <sup>15</sup>N compounds. Initial proposals for Subtilosin A by the groups of Babasaki<sup>160</sup> and Marx<sup>168</sup> did not succeed in producing a complete and correct structure. Our work showed that subtilosin A (**1A**) possesses highly unusual post-translational modifications, specifically sulfur to  $\alpha$ -carbon cross-links. These cross-links are necessary for its antimicrobial activity, and hold

the peptide in a twisted, bowl-like conformation, with most of the side-chains pointing towards the solvent. Desulfurization of subtilisin A was undertaken in order to determine the stereochemistry of the cross-links. The configurations of the unmodified amino acids are all L, as determined by chiral GC MS by hydrolysis of desulfurized **1A** with subsequent derivatization of constituent amino acids to N-pentafluoropropanamide isopropyl esters. However, the modified residues are L-Phe22, D-Thr28, and D-Phe31 and were deduced by extensive NMR analysis. The nickel boride reductive desulfurization of subtilisin A (**1A**), as well as of the model compounds **4**, **6** and **8**, shows that base-induced elimination of sulfur occurs to form an N-acyl imine followed by reduction to the amide. The model compounds exhibit racemization during desulfurization, but the stereochemical outcome with **1A** is governed by accessibility of the polymeric reducing agent to the relatively rigid peptide scaffold. This means that the biochemical formation of the sulfur to  $\alpha$ -carbon cross-links proceeds with net retention of configuration at Phe22, and with net inversion at Thr28 and Phe31. Evaluation of the NMR structures shows that there is a twist in the structure making the opposite face of the Cys13-Phe22 bond accessible in comparison to the Cys7-Thr28 and Cys4-Phe31 bonds. During the maturation of subtilisin A (**1A**) this orientation may be favored, resulting in the different chiralities at the modified amino acids.

The combination of nickel boride reduction of a sulfur-containing peptide, Edman degradation sequence analysis, and chiral GC MS is an excellent approach for structure elucidation of post-translationally modified peptides. Future investigations of subtilisin might involve purification of the enzymes that are thought to be responsible for the post-

translational modifications and could be evaluated through the use of the subtilisin A precursor (via cloning or peptide synthesis).

Bacteriocins have received considerable attention in the last twenty years. However, the studies on these antimicrobial peptides were largely directed towards their activity spectra and genetics. These, and continuing, structural studies will assist in a more complete understanding of bacteriocins, especially with respect to their mode of action. Additionally, as for subtilisin A, other distinctive connectivities may be discovered further exemplifying the kaleidoscope of bacteriocins.

**REFERENCES**

- (1) Davidson, P. M.; Brannen, A. L. *Antimicrobials in Foods*; ASM Press: New York, 1993.
- (2) Dillon, V. M.; Board, R. G. *Natural Antimicrobial Systems and Food Preservation*; CAB International: Wallington, Oxon, 1994.
- (3) van Belkum, M. J.; Stiles, M. E. *Nat. Prod. Rep.* **2000**, *17*, 323-335.
- (4) Oscariz, J. C.; Pisabarro, A. G. *Int. Microbiol.* **2001**, *4*, 13-19.
- (5) Riley, M. A.; Wertz, J. E. *Biochimie* **2002**, *84*, 357-364.
- (6) Jack, R. W.; Tagg, J. R.; Ray, B. *Microbiol. Rev.* **1995**, 171-200.
- (7) Vandamme, P.; Pot, B.; Gillis, M.; De Vos, P.; Kersters, K.; Swings, J. *Microbiol. Rev.* **1996**, *60*, 407-438.
- (8) Chung, K.; Dickson, J.; Crouse, J. *Appl. Environ. Microbiol.* **1989**, *55*, 1329-1333.
- (9) Abee, T. *FEMS Microbiol. Lett.* **1995**, *129*, 1-10.
- (10) Hirsch, A. J. *Gen. Microbiol.* **1950**, *4*, 70-78.
- (11) Hirsch, A.; Grinstes, J. J. *Dairy Res.* **1954**, *21*, 101-109.
- (12) Ramseier, H. R. *Arch. Mikrobiol.* **1960**, *37*, 57.
- (13) Carr, F. J.; Chill, D.; Maida, N. *Crit. Rev. Microbiol.* **2002**, *28*, 281-370.
- (14) Olasupo, N. A. *Folia Microbiol.* **1996**, *41*, 130-136.
- (15) Neu, H. C. *Science* **1992**, *257*, 1064-1073.
- (16) Roy, P. H. *Med. Sci.* **1997**, *13*, 927-933.
- (17) Walker, E. S.; Levy, F. *Evolution* **2001**, *55*, 1110-1122.

- (18) Lipsitch, M.; Bergstrom, C. T.; Levin, B. R. *Proc. Natl. Acad. Sci. USA* **2000**, *97*, 1938-1943.
- (19) Farber, J. M.; Peterkin, P. I. *Microbiol. Rev.* **1991**, *55*, 476-511.
- (20) Palumbo, S. J. *Proteins* **1986**, *49*, 1003-1009.
- (21) Nissen-Meyer, J.; Nes, I. F. *Arch. Microbiol.* **1997**, *167*, 67-77.
- (22) Degnan, A. J.; Yousef, A. E.; Luchansky, J. B. *J. Food Protection* **1992**, *55*, 98-103.
- (23) Nes, I. F.; Diep, D. B.; Havarstein, L. S.; Brurberg, M. B.; Eijsink, V. G.; Holo, H. *Antonie van Leeuwenhoek* **1996**, *70*, 113-128.
- (24) Ennahar, S.; Sashihara, T.; Sonomoto, K.; Ishizaki, A. *FEMS Microbiol. Rev.* **2000**, *24*, 85-106.
- (25) Jack, R. W.; Wan, J.; Gordon, J.; Harnark, K.; Davidson, B.; Hillier, A. J.; Wettenhall, R. E. H.; Hickey, M. W.; Coventry, M. J. *Appl. Environ. Microbiol.* **1996**, *Aug*, 2897-2903.
- (26) Baba, T.; Schneewind, O. *Trends Microbiol.* **1998**, *6*, 66-71.
- (27) Klaenhammer, T. R. *FEMS Microbiol. Rev.* **1993**, *12*, 39-86.
- (28) Taber, H. W. *Introduction to the Peptide Antibiotics*; 1<sup>st</sup> ed.; Marcel Dekker, Inc.: New York, 2002.
- (29) Eijsink, V. G. H.; Axelsson, L.; Diep, D. B.; Havarstein, L. S.; Holo, H.; F., N. I. *Antonie van Leeuwenhoek* **2002**, *81*, 639-654.
- (30) Guder, A.; Wiedemann, I.; Sahl, H. G. *Biopolymers* **2000**, *55*, 62-73.
- (31) McAuliffe, O.; Ross, R. P.; Hill, C. *FEMS Microbiol. Rev.* **2001**, *25*, 285-308.

- (32) van Kraaij, C.; de Vos, W. M.; Siezen, R. J.; Kuipers, O. P. *Nat. Prod. Rep.* **1999**, *16*, 575-587.
- (33) Sahl, H.-G.; Bierbaum, G. *Annu. Rev. Microbiol.* **1998**, *52*, 41-79.
- (34) Sahl, H.-G.; Jack, R. W.; Bierbaum, G. *Eur. J. Biochem.* **1995**, *230*, 827-853.
- (35) Jung, G.; Sahl, H.-G. In *Nisin and Novel Lantibiotics*; Jung, G., Sahl, H.-G., Eds.; Escom: Leiden, 1991, pp 1-34.
- (36) Garneau, S.; Martin, N. I.; Vederas, J. C. *Biochimie* **2002**, *84*, 577-592.
- (37) Ennahar, S.; Sonomoto, K.; Ishizaki, A. *J. Biosci. Bioeng.* **1999**, *87*, 705-716.
- (38) Eijsink, V. G. H.; Skeie, M.; Middelhoven, P. H.; Brurberg, M. B.; Nes, I. F. *Appl. Environ. Microbiol.* **1998**, *64*, 3275-3281.
- (39) Diep, D. B.; Nes, I. F. *Curr. Drug Targets* **2002**, *3*, 107-122.
- (40) Huhne, K.; Axelsson, L.; Holck, A.; Krockel, L. *Microbiology* **1996**, *142*, 3384.
- (41) Kleerebezem, M.; Quadri, L. E. N.; Kuipers, O. P.; de Vos, W. M. *Mol. Microbiol.* **1997**, *24*, 895-904.
- (42) Quadri, L. E.; Yan, L. Z.; Stiles, M. E.; Vederas, J. C. *J. Biol. Chem.* **1997**, *272*, 3384-3388.
- (43) Quadri, L. E.; Kleerebezem, M.; Kuipers, O. P.; de Vos, W. M.; Roy, K. L.; Vederas, J. C.; Stiles, M. E. *J. Bacteriol.* **1997**, *179*, 6163-6171.
- (44) Franz, C. M. A. P.; van Belkum, M. J.; Worobo, R. W.; Vederas, J. C.; Stiles, M. E. *Microbiology* **2000**, *146*, 621-631.
- (45) Worobo, R. W.; Van Belkum, M. J.; Sailer, M.; Roy, K. L.; Vederas, J. C.; Stiles, M. E. *J. Bacteriol.* **1995**, *177*, 3143-3149.

- (46) Tomita, H.; Fujimoto, S.; Tanimoto, K.; Ike, Y. *J. Bacteriol.* **1996**, *178*, 3585-3593.
- (47) Cintas, L. M.; Casaus, P.; Havarstein, L. S.; Hernandez, P. E.; Nes, I. F. *Appl. Environ. Microbiol.* **1997**, *63*, 4321-4330.
- (48) Economou, A. *Mol. Microbiol.* **1998**, *27*, 511-518.
- (49) van Belkum, M. J.; Worobo, R. W.; Stiles, M. E. *Mol. Microbiol.* **1997**, *23*, 1293-1301.
- (50) Fremaux, C.; Hechard, Y.; Cenatiempo, Y. *Microbiology* **1995**, *141*, 1637-1645.
- (51) McCormick, J. K.; Worobo, R. W.; Stiles, M. E. *Appl. Environ. Microbiol.* **1996**, *62*, 4095-4099.
- (52) Horn, N.; Martinez, J. M.; Hernandez, P. E.; Gasson, M. J.; Rodriguez, J. M.; Dodd, H. M. *J. Appl. Environ. Microbiol.* **1998**, *64*, 818-823.
- (53) Biet, F.; Berjeaud, J. M.; Worobo, R. W.; Cenatiempo, Y.; Fremaux, C. *Microbiology* **1998**, *144*, 2845-2854.
- (54) Allison, G. E.; Ahn, C.; Stiles, M. E.; Klaenhammer, T. R. *FEMS Microbiol. Lett.* **1995**, *131*, 87-93.
- (55) Allison, G. E.; Worobo, R. W.; Stiles, M. E.; Klaenhammer, T. R. *Appl. Environ. Microbiol.* **1995**, *61*, 1371-1377.
- (56) Nes, I. F.; Eisjink, V. G. H. In *Cell-Cell Signalling in Bacteria*; Dunny, G. M., Winans, S. C., Eds.; American Society for Microbiology: Washington, D. C., 1999, pp 175-192.

- (57) Kleerebezem, M.; Kuipers, O. P.; de Vos, W. M.; Stiles, M. E.; Quadri, L. E. *Peptides* **2001**, *22*, 1597-1601.
- (58) West, A. H.; Stock, A. M. *Trends Biochem. Sci.* **2001**, *26*, 369-376.
- (59) Diep, D. B.; Havarstein, L. S.; Nes, I. F. *Mol. Microbiol.* **1995**, *18*, 631-639.
- (60) Diep, D. B.; Havarstein, L. S.; Nes, I. F. *J. Bacteriol.* **1996**, *178*, 4472-4483.
- (61) Brurberg, M. B.; Nes, I. F.; Eijsink, V. G. H. *Mol. Microbiol.* **1997**, *26*, 347-360.
- (62) Risoen, P. A.; Brurberg, M. B.; Eijsink, V. G. H.; Nes, I. F. *Mol. Microbiol.* **2000**, *37*, 619-628.
- (63) Saucier, L.; Poon, A.; Stiles, M. E. *J. Appl. Bacteriol.* **1995**, *78*, 684-690.
- (64) Eijsink, V. G. H.; Brurberg, M. B.; Middlehoven, P. H.; F., N. I. *J. Bacteriol.* **1996**, 2232-2237.
- (65) Nilsen, T.; Nes, I. F.; Hole, H. *J. Bacteriol.* **1998**, *180*, 1848-1854.
- (66) Martin, B.; Prudhomme, M.; Alloing, G.; Granadel, C.; Claverys, J.-P. *Mol. Microbiol.* **2000**, *38*, 867-878.
- (67) Claverys, J. P.; Havarstein, L. S. *Fron. Biosci.* **2002**, *7*, 1798-1814.
- (68) Marugg, J. D.; Gonzalez, C. F.; Kunka, B. S.; Ledebøer, A. M.; Pucci, M. J.; Toonen, M. Y.; Walker, S. A.; Zoetmulder, L. C.; Vandenberg, P. A. *Appl. Environ. Microbiol.* **1992**, *58*, 2360-2367.
- (69) Bukhtiyarova, M.; Yang, R.; Ray, B. *Appl. Environ. Microbiol.* **1994**, *60*, 3405-3409.
- (70) van Belkum, M. J.; Stiles, M. E. *Appl. Environ. Microbiol.* **1995**, *61*, 3573-3579.
- (71) Axelsson, L.; Holck, A. *J. Bacteriol.* **1995**, *177*, 2125-2137.

- (72) Higgins, C. F. *Res. Microbiol.* **2001**, *152*, 205-210.
- (73) Havarstein, L. S.; Diep, D. B.; F., N. I. *Mol. Microbiol.* **1995**, *16*, 229-240.
- (74) Axelsson, L.; Katla, T.; Bjornslett, M.; Eijsink, V. G.; Holck, A. *FEMS Microbiol. Lett.* **1998**, *168*, 137-143.
- (75) McCormick, J. K.; Poon, A.; Sailer, M.; Gao, Y.; Roy, K. L.; McMullen, L. M.; Vederas, J. C.; Stiles, M. E.; Van Belkum, M. J. *Appl. Environ. Microbiol.* **1998**, *64*, 4757-4766.
- (76) Franke, C. M.; Tiemersma, J.; Venema, G.; Kok, J. *J. Biol. Chem.* **1999**, *274*, 8484-8490.
- (77) Fath, F. J.; Kotler, R. *Microbiol. Rev.* **1993**, *57*, 995-1017.
- (78) Motlagh, A. M.; Bukhitiyarova, M.; Ray, B. *Lett. Appl. Microbiol.* **1994**, *18*, 305-312.
- (79) Venema, K.; Kok, J.; Marugg, J. D.; Toonen, M. Y.; Ledebøer, A. M.; Venema, G.; Chikindas, M. L. *Mol. Microbiol.* **1995**, *17*.
- (80) Fimland, G. E., V.G.H.; Nissen-Meyer, J. *Microbiology* **2002**, *148*, 3661-3670.
- (81) Abdel-Dayem, M.; Fleury, Y.; Devilliers, G.; Chaboisseau, E.; Girard, R.; Nicolas, P.; Delfour, A. *FEMS Microbiol. Lett.* **1996**, *138*, 251-259.
- (82) Quadri, L. E.; Sailer, M.; Terebiznik, M. R.; Roy, K. L.; Vederas, J. C.; Stiles, M. *E. J. Bacteriol.* **1995**, *177*, 1144-1151.
- (83) Nes, I. F.; Holo, H. *Biopolymers* **2000**, *55*, 50-61.

- (84) Chikindas, M. L.; Garcia-Garcera, M. J.; Driessen, A. J.; Ledebøer, A. M.; Nissen-Meyer, J.; Nes, I. F.; Abee, T.; Konings, W. N.; Venema, G. *Appl. Environ. Microbiol.* **1993**, *59*, 3577-3584.
- (85) Nissen-Meyer, J.; Havarstein, L. S.; Holo, H.; Sletten, K.; Nes, I. F. *J. Gen. Microbiol.* **1993**, *139*, 1503-1509.
- (86) Venema, K.; Haverkort, R. E.; Abee, T.; Haandrikman, A. J.; Leenhouts, K. J.; de Leij, L.; Venema, G.; Kok, J. *Mol. Microbiol.* **1994**, *14*, 521-532.
- (87) Wu, M.; Maier, E.; Benz, R.; Hancock, R. E. *Biochemistry* **1999**, *38*, 7235-7242.
- (88) Hechard, Y.; Sahl, H. G. *Biochimie* **2002**, *84*, 545-557.
- (89) Fimland, G.; Blingsmo, O. R.; Sletten, K.; Jung, G.; Nes, I. F.; Nissen-Meyer, J. *Appl. Environ. Microbiol.* **1996**, *62*, 3313-3318.
- (90) Breukink, E.; Wiedemann, I.; van Kraaij, C.; Kuipers, O. P.; Sahl, H.; de Kruijff, B. *Science* **1999**, *286*, 2361-2364.
- (91) Brotz, H.; Sahl, H. G. *J. Antimicrob. Chemother.* **2000**, *46*, 1-6.
- (92) Wiedemann, I.; Breukink, E.; van Kraaij, C.; Kuipers, O. P.; Bierbaum, G.; de Kruijff, B.; Sahl, H. G. *J. Biol. Chem.* **2001**, *276*, 1772-1779.
- (93) Dalet, K.; Briand, C.; Cenatiempo, Y.; Hechard, Y. *Curr. Microbiol.* **2000**, *41*, 441-443.
- (94) Dalet, K.; Cenatiempo, Y.; Cossart, P.; Hechard, Y. *Microbiology* **2001**, *147*, 3263-3269.
- (95) Hechard, Y.; Pelletier, C.; Cenatiempo, Y.; Frere, J. *Microbiology* **2001**, *147*, 1575-1580.

- (96) Yan, L. Z.; Gibbs, A. C.; Stiles, M. E.; Wishart, D. S.; Vederas, J. C. *J. Med. Chem.* **2000**, *43*, 4579-4581.
- (97) Zheng, G. L.; Yan, L. Z.; Vederas, J. C.; Zuber, P. J. *Bacteriol.* **1999**, *181*, 7346-7355.
- (98) Ramnath, M.; Beukes, M.; Tamura, K.; Hastings, J. W. *Appl. Environ. Microbiol.* **2000**, *66*, 3098-3101.
- (99) Montville, T. J.; Chen, Y. *Appl. Microbiol.* **1998**, *50*, 511-519.
- (100) Brotz, H.; Bierbaum, G.; Leopold, K.; Reynolds, P. E.; Sahl, H. G. *Antimicrob. Agents Chemother.* **1998**, *42*, 154-160.
- (101) Breukink, E.; van Heusden, H. E.; Vollmerhaus, P. J.; Swiezewska, E.; Brunner, L.; Walker, S.; Heck, A. J.; de Kruijff, B. *J. Biol. Chem.* **2003**, *278*, 19898-19903.
- (102) Brotz, H.; Bierbaum, G.; Markus, A.; Molitor, E.; Sahl, H. G. *Antimicrob. Agents Chemother.* **1995**, *39*, 714-719.
- (103) Brotz, H.; Bierbaum, G.; Reynolds, P. E.; Sahl, H. G. *Eur. J. Biochem.* **1997**, *246*, 193-199.
- (104) Sahl, H. *Nisin and Novel Lantibiotics*; Escom: Lieden, 1991.
- (105) Rasch, M.; Knochel, S. *Lett. Appl. Microbiol.* **1998**, *27*, 275-278.
- (106) Voet, D.; Voet, J. G. *Biochemistry 2nd ed.*; John Wiley and Sons: New York, 1995.
- (107) Saier, M. H.; Reizer, J. *Mol. Microbiol.* **1994**, *13*, 755-764.
- (108) Yan, L. Z.; Dawson, P. E. *J. Am. Chem. Soc.* **2001**, *123*, 526-533.

- (109) Fregeau Gallagher, N. L.; Sailer, M.; Niemczura, W. P.; Nakashima, T. T.; Stiles, M. E.; Vederas, J. C. *Biochemistry* **1997**, *36*, 15062-15072.
- (110) Wang, Y.; Henz, M. E.; Gallagher, N. L.; Chai, S.; Gibbs, A. C.; Yan, L. Z.; Stiles, M. E.; Wishart, D. S.; Vederas, J. C. *Biochemistry* **1999**, *38*, 15438-15447.
- (111) Schillinger, U.; Lucke, F.-K. *Food Microbiol.* **1987**, *4*, 199-208.
- (112) Holzapfel, W. H.; Gerber, E. S. *Sys. Appl. Microbiol.* **1983**, *4*, 522-534.
- (113) Carolissen-Mackay, V.; Arends, G.; Hastings, J. W. *Int. J. Food Microbiol.* **1997**, *34*, 1-16.
- (114) Quadri, L. E.; Sailer, M.; Roy, K. L.; Vederas, J. C.; Stiles, M. E. *J. Biol. Chem.* **1994**, *269*, 12204-12211.
- (115) Ahn, C.; Stiles, M. E. *J. Appl. Bacteriol.* **1990**, *69*, 302-310.
- (116) Ahn, C.; Stiles, M. E. *Appl. Environ. Microbiol.* **1990**, *56*, 2503-2510.
- (117) Sambrook, J.; Russell, D. W. *Molecular Cloning, A Laboratory Manual*; 3<sup>rd</sup> ed.; Cold Spring Harbor Laboratory Press: Cold Spring Harbor, 2001.
- (118) Ausubel, F. M.; Brent, R.; Kingston, R. E.; Moore, D. D.; Seidman, J. G.; Smith, J. A.; Struhl, K. *Short Protocols in Molecular Biology 4th ed*; John Wiley & Sons, Inc.: New York, 1999.
- (119) Kapust, R. B.; Waugh, D. S. *Protein Sci.* **1999**, *8*, 1668-1674.
- (120) Maina, C. V.; Riggs, P. D.; Grandea, A. G.; Slatko, B. E.; Moran, L. S.; Tagliamonte, J. A.; McReynolds, L. A.; Guan, C. D. *Gene* **1988**, *74*, 365-373.
- (121) di Guan, C.; Li, P.; Riggs, P. D.; Inouye, H. *Gene* **1988**, *67*, 21-30.

- (122) Riggs, P. D. *Current Protocols in Molecular Biology*; Greene Associates/Wiley Interscience: New York, 1992.
- (123) Kellermann, O. K.; Ferenci, T. *Methods Enzymol.* **1982**, *90*, 459-463.
- (124) Madigan, M. T.; Martinko, J. M.; Parker, J. *Brock Biology of Microorganisms*; 9<sup>th</sup> ed.; Prentice-Hall Inc.: Upper Saddle River, 2000.
- (125) Nagai, K.; Thogersen, H. C. *Nature* **1984**, *309*, 810-812.
- (126) Nagai, K.; Thogersen, H. C. *Methods Enzymol.* **1987**, *153*, 461-481.
- (127) Kapust, R. B.; Routzahn, K. M.; Waugh, D. S. *Protein Expr. Purif.* **2002**, *24*, 61-70.
- (128) Hickman, A. B.; Dyda, F.; Craigie, R. *Protein Eng.* **1997**, *10*, 601-606.
- (129) Kane, J. F. *Curr. Opin. Biotech.* **1995**, *6*, 494-500.
- (130) Sprules, P. c. w. D. T.,
- (131) Watson, R. M.; Woody, R. W.; Lewis, R. V.; Bohle, D. S.; Andreotti, A. H.; Ray, B.; Miller, K. W. *Biochemistry* **2001**, *40*, 14037-14046.
- (132) Chen, Y.; Shapira, R.; Eisenstein, M.; Montville, T. J. *Appl. Environ. Microbiol.* **1997**, *63*, 524-531.
- (133) Sailer, M.; Helms, G. L.; Henkel, T.; Niemczura, W. P.; Stiles, M. E.; Vederas, J. C. *Biochemistry* **1993**, *32*, 310-318.
- (134) Cavanagh, J.; Fairbrother, W. J.; Palmer, A. G.; Skelton, N. J. *Protein NMR Spectroscopy*; Academic Press: New York, 1996.
- (135) Muller, L. *J. Am. Chem. Soc.* **1979**, *101*, 4481-4484.
- (136) Bodenhausen, G. *Chem. Phys. Lett.* **1980**, *69*, 185-189.

- (137) Bax, A.; Ikura, M.; Kay, L. E.; Torchira, D. A.; Tschudin, R. J., *Magn. Reson.* **1990**, *86*.
- (138) Norwood, T. J.; Boyd, J.; Heritage, J. E.; Soffe, N.; Campbell, I. D. *J. Magn. Reson.* **1990**, *87*, 488-501.
- (139) Wishart, D. S.; Sykes, B. D.; Richards, F. M. *J. Mol. Biol.* **1991**, *222*, 311-333.
- (140) Wishart, D. S.; Sykes, B. D.; Richards, F. M. *Biochemistry* **1992**, *31*, 1647-1651.
- (141) Wishart, D. S.; Bigam, C. G.; Holm, A.; Hodges, R. S.; Sykes, B. D. *J. Biomol. NMR* **1995**, *5*, 67-81.
- (142) Siragusa, G. R.; Cutter, C. N. *Appl. Environ. Microbiol.* **1993**, *59*, 2326-2328.
- (143) Gao, Y.; van Belkum, M. J.; Stiles, M. E. *Appl. Environ. Microbiol.* **1999**, *65*, 4329-4333.
- (144) Garneau, S. In *Ph.D. Thesis*; University of Alberta: Edmonton, 2003, pp 1-208.
- (145) Prinz, W. A.; Aslund, F.; Holmgren, A.; Beckwith, J. *J. Biol. Chem.* **1997**, *272*, 15661-15667.
- (146) Stewart, E. J.; Aslund, F.; Beckwith, J. *Embo J.* **1998**, *17*, 5543-5550.
- (147) Venema, K.; Venema, G.; Kok, J. *Trends Microbiol.* **1995**, *3*, 299-304.
- (148) Sonenshein, A. L.; Hoch, A. J.; Losick, R. *Bacillus subtilis and Its Closest Relatives: From Genes to Cells*; ASM Press: Washington, D.C., 2002.
- (149) Sonenshein, A. L.; Hoch, A. J.; Losick, R. *Bacillus subtilis and Other Gram-Positive Bacteria: Biochemistry, Physiology, and Molecular Genetics*; ASM Press: Washington, D.C., 1993.
- (150) Nakano, M. M.; Zheng, G. L.; Zuber, P. J. *Bacteriol.* **2000**, *182*, 3274-3277.

- (151) Beuchat, L. R. In *Food Microbiology: Fundamentals and Frontiers*; Doyle, L. R., Beuchat, L. R., Montville, T. J., Eds.; American Society for Microbiology: Washington, D. C., 1997, pp 629-648.
- (152) Zheng, G. L.; Hehn, R.; Zuber, P. *J. Bacteriol.* **2000**, *182*, 3266-3273.
- (153) Burkholder, P. R.; Giles, N. H. *Am. J. Botany* **1947**, *34*, 345-348.
- (154) Spizizen, J. *Proc. Natl. Acad. Sci. USA* **1958**, *44*, 1072-1078.
- (155) Schaeffer, P. *Bacteriol. Rev.* **1969**, *33*, 48-71.
- (156) Ryter, A.; Schaeffer, P.; Ionesco, H. *Ann. Inst. Pasteur (Paris)* **1966**, *110*, 305-315.
- (157) Kunst, F.; Vassarotti, A.; Danchin, A. *Microbiology* **1995**, *141*, 249-255.
- (158) Kunst, F.; Ogasawara, N.; Moszer, I.; Albertini, A. M.; Alloni, G.; Azevedo, V.; Bertero, M. G.; Bessieres, P.; Bolotin, A.; Borchert, S.; Borriss, R.; Boursier, L.; Brans, A.; Braun, M.; Brignell, S. C.; Bron, S.; Brouillet, S.; Bruschi, C. V.; Caldwell, B.; Capuano, V.; Carter, N. M.; Choi, S. K.; Codani, J. J.; Connerton, I. F.; Danchin, A.; et al. *Nature* **1997**, *390*, 249-256.
- (159) Kunst, F.; Devine, K. *Res. Microbiol.* **1991**, *142*, 905-912.
- (160) Babasaki, K.; Takao, T.; Shimonishi, Y.; Kurahashi, K. *J. Biochem. (Tokyo)* **1985**, *98*, 585-603.
- (161) Zheng, G.; Slavik, M. F. *Lett. Appl. Microbiol.* **1999**, *28*, 363-367.
- (162) Piggot, P. J.; Coote, J. G. *Bacteriol Rev* **1976**, *40*, 908-962.
- (163) Hoch, J. A. *Adv. Genet.* **1976**, *18*, 69-98.

- (164) Freese, E. *Sporulation and Germination*; American Society for Microbiology: Washington, 1981.
- (165) Katz, E.; Demain, A. L. *Bacteriol. Rev.* **1977**, *41*, 449-474.
- (166) Kawulka, K.; Sprules, T.; McKay, R. T.; Mercier, P.; Diaper, C. M.; Zuber, P.; Vederas, J. C. *J. Am. Chem. Soc.* **2003**, *125*, 4726-4727.
- (167) Zheng, G.; Yan, L. Z.; Vederas, J. C.; Zuber, P. *J. Bacteriol.* **1999**, *181*, 7346-7355.
- (168) Marx, R.; Stein, T.; Entian, K. D.; Glaser, S. J. *J. Protein Chem.* **2001**, *20*, 501-506.
- (169) Dijl, J. M.; Bolhuis, A.; Tjalsma, H.; Jongbloed, J. D. H.; De Jong, A.; Bron, S. *Protein Transport Pathways in Bacillus subtilis: a Genome-Based Road Map*; ASM Press, 2002.
- (170) Light, A. In *Methods in Enzymology*; Academic Press: New York, 1977; Vol. 46, pp 417-420.
- (171) Schultz, J. In *Methods in Enzymology*; Academic Press: New York, 1972; Vol. 28, pp 255-263.
- (172) Aoki, M.; Ohtsuka, T.; Yamada, M.; Ohba, Y.; Yoshizaki, H.; Yasuno, H.; Sano, T.; Watanabe, J.; Yokose, K.; Seto, H. *J. Antibiot. (Tokyo)* **1991**, *44*, 582-588.
- (173) Kirby, G. W.; Robins, D. J. *Biosynthesis of Mycotoxins*; Academic Press: New York, 1980.
- (174) Back, T. G.; Yang, K.; Krouse, H. R. *J. Org. Chem.* **1992**, *57*, 1986-1990.
- (175) Khurana, J. M.; Gogia, A. *Org. Prep. Proceed. Int.* **1997**, *29*, 1-32.

- (176) This fragment could also contain residues 30-35 (leu-Phe-Gly-Leu-Trp-Gly). The two possibilities were not distinguished because each contains only Phe31, whose isolation was the goal of this analysis.
- (177) Kawulka, K. E.; Sprules, T.; Diaper, C. M.; Whittall, R. M.; McKay, R. T.; Mercier, P.; Zuber, P.; Vederas, J. C. *J. Am. Chem. Soc.*, *Submitted*.
- (178) Schmidt, U.; Hausler, J.; Ohler, E.; Poisel, H. *Fortschr. Chem. Org. Naturst.* **1979**, *37*, 251-258.
- (179) Solomon, P. S.; Shaw, A. L.; Lane, I.; Hanson, G. R.; Palmer, T.; McEwan, A. G. *Microbiology* **1999**, *145*, 1421-1429.
- (180) Menendez, C.; Siebert, D.; Brandsch, R. *FEBS Lett.* **1996**, *391*, 101-103.
- (181) Frey, P. A.; Magnusson, O. T. *Chem. Rev.* **2003**, *103*, 2129-2148.
- (182) Sofia, H. J.; Chen, G.; Hetzler, B. G.; Reyes-Spindola, J. F.; Miller, N. E. *Nucleic Acids Res.* **2001**, *29*, 1097-1106.
- (183) Clary, D. O.; Wahleithner, J. A.; Wolstenholme, D. R. *Nucleic Acids Res.* **1984**, *12*, 3747-3762.
- (184) Paces, V.; Rosenberg, L. E.; Fenton, W. A.; Kalousek, F. *Proc. Natl. Acad. Sci. U S A* **1993**, *90*, 5355-5358.
- (185) Braun, H. P.; Schmitz, U. K. *Trends Biochem. Sci.* **1995**, *20*, 171-175.
- (186) Kay, L. E.; Keifer, P.; Saarinen, T. *J. Am. Chem. Soc.* **1992**, *114*, 10663-10665.
- (187) Zhang, O.; Kay, L. E.; Olivier, J. P.; Forman-Kay, J. D. *J. Biomol. NMR* **1994**, *4*, 845-858.

- (188) Vuister, G. W.; Yamazaki, T.; Torchia, D. A.; Bax, A. *J. Biomol. NMR* **1993**, *3*, 297-306.
- (189) Pascal, S. M.; Muhandiram, D. R.; Yamazaki, T.; Forman-Kay, J. D.; Kay, L. E. *J. Magn. Reson. B* **1994**, *103*, 197-201.
- (190) Delaglio, F.; Brzesick, S.; Vuister, G. W.; Zhu, G.; Pfeifer, J.; Bax, A. *J. Biomol. NMR* **1995**, *6*, 277-293.
- (191) Johnson, B. A.; Blevins, R. A. *J. Biomol. NMR* **1994**, *4*, 603-614.
- (192) Perrin, D. D. *Purification of Laboratory Chemicals*; 2 ed.; Pergamon Press: New York, 1980.
- (193) Harwood, C. R.; Cutting, S. M. *Molecular Biological Methods for Bacillus*; John Wiley and Sons: Chichester, U K, 1990.
- (194) Korch, C. T.; Doi, R. H. *J. Bacteriol.* **1971**, *105*, 1110-1118.
- (195) This experiment performed at 800 MHz, NANUC, University of Alberta.
- (196) Calculations are performed using EXPasy protparam tool.  
([www.us.EXOasy.org/](http://www.us.EXOasy.org/))

## APPENDIX

Table A.1: NOE Data for subtilisin A (1B)

Residue A	Atom A	Residue B	Atom B	Min.	Max.
1	HB#	1	HD2#	2	6
1	HA	1	HB#	2	5
1	HB#	31	HB#	2	4.8
1	HB#	34	HB#	0	6
2	HA	3	HN	1.9	4.5
2	HA	4	HN	2	4.6
2	HA	2	HB#	1.7	3.5
2	HA	2	HG#	1.9	4.3
2	HG#	2	HN	1.8	3.8
2	HD#	2	HE#	1.7	3.1
2	HE#	2	HG#	2	4.6
1	HA	2	HN	1.6	2.8
2	HB#	2	HN	1.8	4
2	HB#	2	HG#	1.9	4.3
2	HB#	3	HN	2	5.4
2	HA	2	HD#	2	5.8
2	HD#	2	HN	2	5.8
2	HG#	2	HN	2	4.6
2	HA	2	HN	1.8	3.6
3	HA#	3	HN	1.8	3.6
3	HA#	4	HN	1.9	4.7
3	HA#	4	HB#	0	6
3	HN	4	HN	1.9	3.7
4	HA	4	HB#	1.9	4.7
4	HA	4	HN	1.8	3.8
4	HB#	32	HN	1.8	3.4
4	HB#	4	HN	1.9	4.9
4	HB#	32	HA#	1.9	4.1
4	HA	5	HN	1.9	4.1
4	HB#	5	HN	2	5
5	HB%	5	HN	1.7	3.1
5	HA	5	HB%	1.6	2.6
5	HA	5	HN	1.8	3.4
5	HA	7	HN	2	5.2
6	HN	7	HN	1.8	3.4

6	HG2%	6	HN	1.7	3.5
6	HB	6	HG2%	1.7	2.9
6	HA	6	HG2%	0	6
6	HB	7	HN	2	6
6	HA	8	HN	1.9	4.7
6	HA	6	HN	1.8	3.4
6	HA	6	HB	1.6	2.8
5	HB%	6	HA	0	6
6	HA	7	HN	1.9	4.7
6	HB	6	HN	1.8	3.6
5	HB%	6	HN	1.9	4.3
7	HN	8	HN	1.8	3.8
7	HA	9	HG1#	0	6
7	HA	9	HG2%	0	6
7	HB#	28	HN	1.8	3.6
7	HB#	28	HB	1.9	4.7
7	HA	8	HN	1.9	4.7
7	HB#	29	HA#	2	6
7	HA	7	HB#	1.9	3.9
7	HA	9	HN	1.9	5.1
7	HB#	7	HN	1.9	4.3
7	HA	7	HN	1.8	3.6
8	HA	8	HN	1.8	3.8
8	HB#	8	HN	1.7	3.3
8	HN	9	HN	1.7	3.3
8	HB#	9	HN	1.7	3.3
9	HB	9	HN	1.7	3.3
9	HB	9	HG2%	0	6
9	HG1#	10	HN	2	5.4
9	HB	9	HG1#	1.8	3.6
9	HG1#	9	HG2%	1.9	4.1
9	HG2%	10	HN	1.9	4.1
9	HG2%	9	HN	0	6
9	HA	9	HG2%	0	6
9	HA	9	HD1%	1.9	4.1
9	HB	9	HD1%	1.9	4.1
9	HD1%	9	HG1#	1.7	3.1
9	HA	10	HN	1.9	3.9
9	HA	9	HN	1.8	3.4
9	HA	9	HB	1.6	3
9	HA	9	HG1#	1.7	3.1
10	HA#	29	HA#	1.9	4.5

9	HN	10	HN	1.9	4.3
10	HA#	10	HN	1.9	3.9
10	HA#	11	HN	2	4.8
10	HA#	11	HB%	0	6
11	HB%	11	HN	1.6	3
11	HA	11	HN	1.7	3.3
11	HA	11	HB%	0	6
11	HB%	30	HD##	1.8	3.4
12	HA	12	HN	1.8	3.4
12	HB%	12	HN	1.7	3.3
12	HB%	13	HN	1.9	4.7
12	HA	12	HB%	1.5	2.7
12	HA	13	HN	1.8	4
12	HN	13	HN	1.8	3.4
13	HB#	23	HN	1.7	3.5
13	HB#	16	HB#	0	6
13	HB#	13	HN	2	5.8
13	HB#	23	HG#	2	5.6
13	HB#	23	HA	2	5.8
13	HA	14	HN	2	4.8
13	HA	13	HN	1.8	3.6
13	HA	13	HB#	1.9	4.3
13	HA	14	HB#	2	5.8
13	HA	15	HG##	2	6
14	HN	15	HN	1.7	3.1
14	HB#	14	HG	1.6	2.8
14	HB#	14	HD##	1.8	3.4
14	HB#	14	HN	2	4.8
14	HA	14	HN	1.8	3.6
14	HG	14	HN	1.9	3.9
14	HA	17	HN	1.9	4.5
14	HA	14	HB#	1.8	3.6
14	HD##	14	HG	1.8	3.6
14	HA	14	HG	1.8	3.8
14	HA	14	HD##	0	6
14	HD##	14	HN	2	5.8
14	HG	12	HA	0	6
14	HG	11	HA		
14	HD##	12	HA	0	6
14	HD##	11	HA	0	0
14	HN	12	HA	2	4.8
14	HN	11	HA		

15	HB	15	HN	1.6	3
15	HG##	15	HN	1.9	4.5
15	HG##	19	HA	2	5.4
15	HB	15	HG##	1.6	2.6
15	HA	15	HG##	1.9	4.1
15	HB	15	HG##	1.6	2.6
15	HA	15	HN	1.7	3.1
15	HA	16	HN	1.9	4.5
15	HA	19	HA	1.5	2.5
15	HA	15	HB	1.5	2.7
14	HA	15	HN	1.9	4.3
16	HA	16	HB#	2	5.4
15	HN	16	HN	1.8	3.6
16	HN	17	HN	1.8	3.4
14	HA	16	HN	2	5
15	HG##	16	HN	2	5.6
16	HA	16	HN	1.9	4.1
16	HB#	16	HN	1.9	4.7
16	HA	17	HN	2	4.6
17	HA#	17	HN	1.9	4.3
18	HD#	19	HN	2	5.8
18	HD#	18	HG#	1.9	3.9
17	HA#	18	HD#	1.9	3.9
17	HA#	19	HD1%	2	5.6
17	HA#	14	HD##		
18	HA	19	HD1%	0	6
18	HA	14	HD##		
18	HB#	18	HG#	1.7	3.1
18	HB#	18	HD#	2	5.6
18	HA	18	HB#	1.8	3.6
18	HA	18	HG#	2	5.8
18	HA	19	HN	1.9	4.5
19	HG2%	19	HN	2	5.8
19	HB	19	HG1#	1.9	4.3
19	HB	19	HN	1.8	3.6
19	HB	19	HD1%	1.8	4.2
19	HG1#	19	HG2%	2	4.6
19	HA	19	HG1#	1.9	4.5
19	HG1#	20	HD#	2	5.4
19	HG1#	19	HN	2	5
19	HA	20	HD#	1.7	3.1
19	HG2%	19	HN	1.9	5.1

19	HG2%	21	HB#	0	6
19	HB	19	HG2%	1.8	3.4
19	HD1%	19	HG1#	1.7	3.1
19	HA	19	HN	1.8	3.6
19	HA	19	HB	1.7	2.9
19	HA	19	HD1%	1.9	4.3
19	HA	19	HG2%	1.7	3.5
20	HA	20	HB#	1.8	3.6
20	HB#	20	HG#	1.8	3.8
20	HB#	20	HD#	2	5
20	HG#	23	HB#	0	6
20	HA	20	HG#	2	5.8
20	HA	21	HN	1.8	3.4
20	HA	21	HA	0	6
20	HA	20	HB#	1.8	3.6
20	HA	23	HB#	0	6
20	HD#	20	HG#	1.9	4.1
19	HG2%	20	HD#	2	5.8
19	HG1#	20	HD#	2	6
20	HD#	14	HB#	1.9	4.3
21	HA	21	HN	2	4.6
21	HA	22	HD%	2	5.4
21	HA	21	HB#	1.9	4.7
22	HB#	22	HN	1.9	4.5
22	HB#	24	HD1%	2	5
22	HB#	22	HD%	1.8	3.6
22	HB#	24	HG1#	1.9	5.1
13	HB#	23	HN	1.9	4.9
23	HB#	23	HN	1.9	4.9
14	HD##	23	HG#	0	6
23	HA	23	HG#	2	4.8
23	HB#	23	HG#	1.8	4
14	HD##	23	HG#	0	6
13	HB#	23	HG#	0	6
23	HA	23	HG#	1.9	4.5
23	HB#	23	HG#	1.9	3.9
23	HA	23	HN	1.9	4.3
23	HA	24	HN	2	4.8
13	HB#	23	HA	2	5.4
23	HA	23	HB#	1.9	4.3
23	HN	24	HN	1.9	4.5
24	HB	25	HN	1.9	4.7

24	HB	24	HN	1.8	3.4
24	HG1#	24	HN	1.9	4.3
24	HB	24	HG1#	1.9	3.9
24	HG1#	24	HG2%	1.8	4.2
24	HD1%	24	HG1#	1.8	3.6
24	HG1#	24	HN	1.9	4.1
24	HG2%	25	HB%	0	6
24	HA	24	HD1%	0	6
23	HB#	24	HN	2	6
24	HD1%	24	HN	1.9	4.3
24	HG2%	24	HN	2	5.2
24	HA	24	HB	1.8	3.6
24	HA	24	HN	1.8	3.6
24	HA	24	HG1#	1.9	4.9
24	HA	24	HG2%	1.7	3.5
24	HN	25	HN	1.7	3.3
24	HA	25	HN	1.9	4.3
25	HB%	25	HN	1.8	3.6
24	HA	25	HB%	0	6
25	HA	26	HN	2	4.4
25	HA	25	HN	1.8	3.8
25	HA	25	HB%	0	6
24	HG2%	25	HA	0	6
24	HG2%	27	HA	1.9	4.3
26	HA#	26	HN	1.8	3.8
7	HB#	26	HA#	1.8	4
26	HA#	27	HN	2	5.2
26	HN	27	HN	1.7	3.1
27	HB%	27	HN	1.8	3.6
27	HA	27	HB%	1.4	2.4
27	HA	30	HN	2	5.2
27	HA	30	HG	1.9	4.5
27	HA	28	HN	1.9	4.1
27	HA	27	HN	1.8	3.6
27	HN	28	HN	1.8	3.6
28	HB	28	HN	1.9	4.7
27	HB%	28	HN	1.9	4.3
28	HB	31	HN	2	5.6
27	HB%	28	HB	0	6
28	HB	30	HN	2	5.2
28	HB	31	HE%	0	6
7	HB#	28	HB	1.9	4.5

28	HG2%	28	HN	0	6
7	HN	28	HG2%	0	6
28	HB	28	HG2%	1.7	3.3
7	HB#	29	HA#	2	6
29	HA#	30	HN	1.9	5.1
29	HA#	29	HN	1.7	3.1
9	HN	29	HA#	2	5
7	HB#	29	HN	2	5
29	HN	30	HN	1.7	3.5
30	HB#	30	HN	1.9	3.9
30	HB#	31	HE%	0	6
30	HB#	31	HD%	0	6
30	HB#	30	HG	1.7	3.3
29	HN	30	HA	2	5.8
30	HA	33	HN	1.9	4.5
30	HA	30	HG	1.9	4.1
30	HA	33	HG	1.8	4
30	HA	30	HB#	1.6	2.8
30	HA	30	HN	1.8	3.4
30	HD##	30	HN	2	5.6
30	HG	30	HN	1.7	3.1
30	HD##	30	HG	1.8	3.4
30	HB#	30	HD##	2	4.6
30	HA	30	HD##	2	4.4
31	HN	32	HN	1.8	3.6
30	HN	31	HN	1.8	3.4
30	HA	31	HN	1.8	4.2
4	HB#	31	HN	2	5.6
31	HB#	34	HB#	2	5
31	HB#	31	HD%	1.7	3.3
4	HB#	31	HN	1.7	3.1
31	HB#	31	HE%	2	5.6
31	HB#	31	HD%	1.8	3.6
31	HD%	31	HN	1.9	4.9
30	HB#	31	HN	2	4.8
32	HA#	33	HN	2	5.2
32	HA#	32	HN	1.7	3.3
4	HB#	32	HA#	2	5.6
32	HA#	32	HN	1.9	4.1
32	HN	33	HN	1.7	3.5
33	HN	34	HN	1.7	3.1
33	HB#	34	HN	1.9	4.9

33	HB#	33	HN	1.9	4.3
33	HB#	33	HD##	2	4.4
33	HB#	33	HG	1.8	3.6
33	HA	33	HB#	1.8	3.6
33	HA	33	HN	1.7	3.3
33	HG	33	HN	1.7	3.3
33	HA	33	HG	1.9	4.3
33	HD##	33	HG	1.9	4.7
33	HA	33	HD##	1.9	4.3
33	HD##	33	HN	2	6
34	HB#	34	HN	2	4.4
34	HA	34	HN	1.9	4.1
33	HA	34	HN	1.9	4.5
33	HB#	34	HN	2	5.4
35	HA#	35	HN	1.8	3.8
34	HN	35	HN	1.7	3.5
10	HA#	29	HN	2	5.6
10	HA#	28	HN		
19	HA	18	HB#	2	6
19	HA	20	HG#		
19	HA	20	HB#		
26	HN	25	HB%	2	5
26	HN	27	HB%		

Figure A.2: MALDI-TOF of  $^{15}\text{N}$  and  $^{13}\text{C}$  labelled subtilisin A (**1B**).

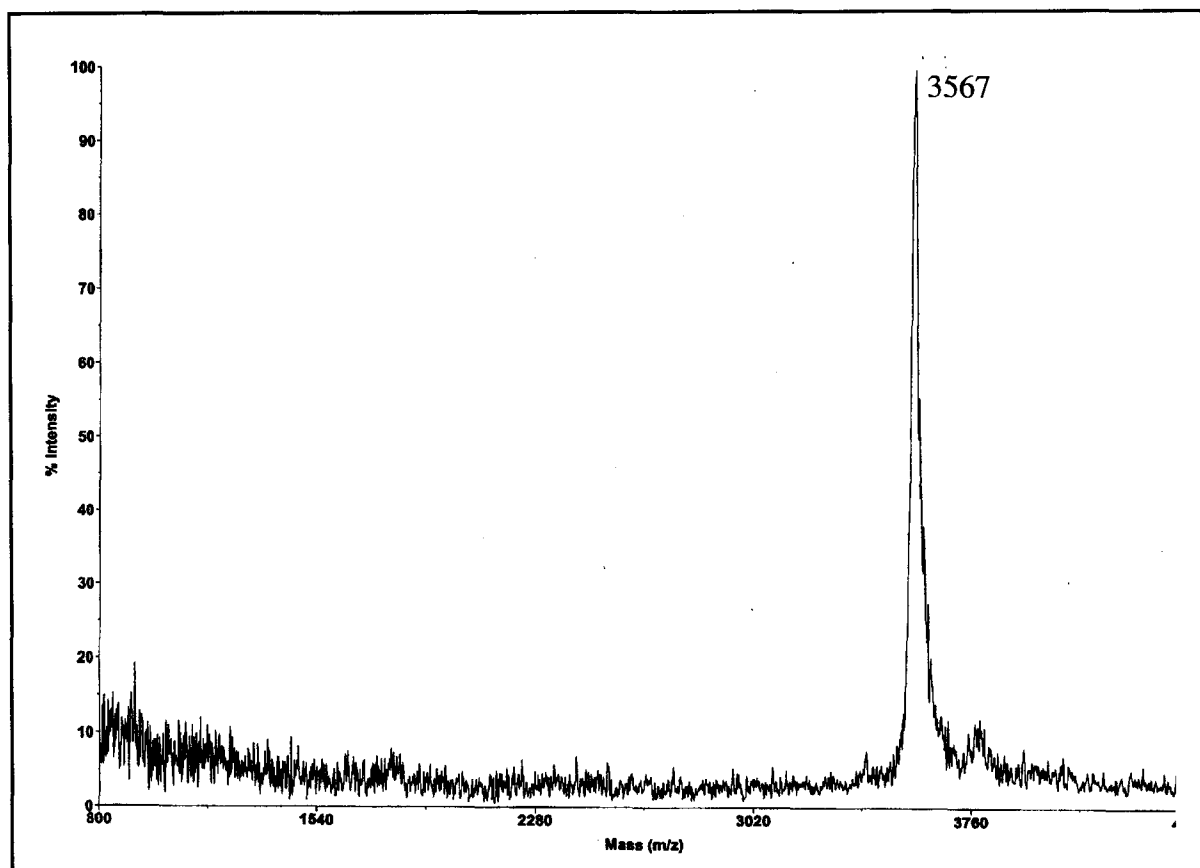


Figure A.3: Nonspecific cleavage of BrcB on the intein column.

